THE RELATION BETWEEN MASS TRANSFER COEFFICIENT AND FRICTION VELOCITY

A Thesis
Submitted to the College of Engineering of
Al-Nahrain University in Partial Fulfillment of the
Requirements for the Degree of Master of Science in
Chemical Engineering

by

Hala Muhammed Hussain
B.Sc. in Chemical Engineering 2009

Rabii Al-thani 1433
March 2012

Certification

I certify that thesis entitled **"THE RELATION BETWEEN MASS TRANSFER COEFFICIENT AND FRICTION VELOCITY"** was prepared by **Hala Muhammed Hussain** under my supervision at Al-Nahrain University/College of Engineering in partial fulfillment of the requirements for the degree of Master of Science in Chemical Engineering.

Signature:
Name: Prof. Dr. Qasim J. M. Slaiman
(Supervisor)
Date: 20 / 3 / 2012

Signature:
Name: **Asst. Prof. Dr. Basim O. Hasan**
(Head of Department)
Date: 20 / 3 /2012

Certificate

We certify, as an examining committee, that we have read this thesis entitled **"THE RELATION BETWEEN MASS TRANSFER COEFFICIENT AND FRICTION VELOCITY"** examined the student **Hala Muhammed Hussain** in it's content and found it meets the standard of thesis for the degree of master of science in Chemical Engineering.

Signature:
Name: Prof. Dr. Qasim J. M. Slaiman
(Supervisor)
Date: 20 / 3 / 2012

Signature:
Name:Asst. Prof. Dr. Sami I. Al-Rubaiey
(Member)
Date: 2 / 4 / 2012

Signature:
Name: Asst. Prof. Dr. Basim O. Hasan
(Member)
Date: 20 / 3 / 2012

Signature: A. Sulaymon
Name: Prof. Dr. Abbas H. Sulaymon
(Chairman)
Date: 20 / 3 / 2012

Approval of the college of engineering:

Signature: M. J. Jweeg
Name: Prof. Dr. Muhsin J. Jweeg
(Dean)
Date: 17 / 4 / 2012

Abstract

This work aims to study the effect of the relationship between the mass transfer coefficient and friction/shear velocity by the analysis of experimental results using Rotating Cylinder Electrode (RCE) to evaluate the limiting current density (LCD) under turbulent flow conditions at three different temperatures 40,50,60 ^{0}C. The experimental runs were carried out in NaCl salt solution of increasing concentration, i.e., 0.1, 0.3, and 0.5N to determine the limiting current density and therefore the mass transfer coefficient on two different metals (yellow admiralty brass and carbon steel), one of them is highly corroding (carbon steel) as function of friction/shear velocity.

Experiments showed that increasing the temperature for a given sodium chloride concentration leads to increase limiting current density and hence increased mass transfer coefficient on both metals. A similar trend is obtained for increasing NaCl salt concentration at a given temperature. As limiting current density is mass transfer controlled, slight or limited differences are noted on the two metals due to the fact the surface texture and morphology can not be reproduced equally the same. Temperature and increased NaCl salt concentration affect to different extent the dissolved oxygen concentration and the physical properties of the present system solutions. These variations are reflected on the limiting current and hence on mass transfer coefficient experimental results.

Mass transfer coefficient depends mainly on velocity, i.e., Reynolds Number, which are influenced by temperature and solution NaCl concentration.

The experimentally determined limiting current density and hence mass transfer coefficient, and friction velocity are related through experimentally found results to be related theoretically by the following equation:-

$$U* = Sc^{0.335}\sqrt{kU}$$

List of Contents

Chapter One

Rotating Cylinder Electrode

5.2.1. Effect of temperature

5.3. Mass Transfer Coefficient

5.3.1. Brass

5.3.2. Carbon Steel

Chapter Six

NOMECLATURE

a_{oxide}	Activities (concentration) of oxidized	mol/l
a_{red}	Activities (concentration) of reduction	mol/l
ΔC	Different concentration ($C_b - C_s$)	mol/cm^3
C_b	Bulk concentration	mol/cm^3
C_s	Surface concentration	mol/cm^3
d	Diameter of specimens	cm
d_{cyl}	Diameter of cylinder	cm
d_{pipe}	Diameter of pipe	cm
D	Diffusivity	cm^2/s
E_i, E	Electrode potential	V
E_0	Standard electrode potential	V
E_{eq}	Equilibrium potential	V
F	Faraday No. (96500)	
f	Friction factore	
i_{corr}	corrosion current density	A/cm^2
i_{ℓ}	Limiting current density	A/cm^2
i	Total current density	A/cm^2
i_0	Exchange current density at C_s	A/cm^2
I	Current	A
J	Flux of substance	$mol/cm^2.s$
k	Mass transfer coefficient	cm/s
K	Constant of equation 2.26.	
L	Length	cm
N_A, N	Rate of mass transfer coefficient	$mol/cm^2.s$
r	Radius of cylinder	cm

R	Gas constant (8.314)	
$R_{solution}$	Electric resistance of solution	Ωcm
R_f	Resistance produced by films	Ωcm
t	Exposure time	s
T	Temperature	^0C
U	Velocity	cm/s
U_{cyl}	Velocity of rotating cylinder	cm/s
U_{pipe}	Velocity of pipe	cm/s
U*	friction/shear velocity	cm/s
n, z	No. of electrons	

Greek Symbols

ν	Kinematics viscosity	cm^2/s
ω	angular velocity	rpm
ρ	density	g/cm^3
τ	shear stress	$g/cm.s^2$
τ_w	Wall shear stress	$g/cm.s^2$
μ	Viscocity	g/cm.s
δ_D	Nernst diffusion layer	µm
δ_H	Hydrodynamic thickness	µm
β_c	Tafel constant	
ε_D	Eddy diffusivity for mass transfer	cm^2/s
η_C	Concentration polarization	V
η_t	Total polarization	V
η_A	Activation polarization	V
η_{red}	Reduction polarization	V

η_R	Resistance over potential	V

Dimensionless Group:-

Sh	Sherwood No.	kd/D
Re	Reynolds No.	$\rho Ud/\mu$
Sc	Schmidt No.	ν/D
St	Stanton No.	k/U

Abbreviations:-

LCD	Limiting Current Density
RCE	Rotating Cylinder Electrode
RDE	Rotating Disk Electrode
BTAH	Benzotriazola

List of Tables

List of Figures

CHAPTER ONE

INTRODUCTION

1.1. Introduction

The transfer of mass, heat, or momentum between a solid phase boundary and a turbulent fluid is encountered in many chemical engineering processes, and the interrelationships between the three have received much study.

Fluid flow can affect electrochemical reaction rate, e.g., mass transfer controlled corrosion. The problem has been to determine when this effect occurs in equipment, especially before the equipment is designed. A new velocity sensitivity test using a Rotating Cylinder Electrode (RCE) is being used for this purpose. The strength of the apparatus is its defined hydrodynamics. The test procedure rests on the assumption that by operating the rotating cylinder electrode in the range of the wall shear stresses expected in the plant geometry, the mechanism by which fluid flow affects corrosion rates may be simulated in the laboratory. Once the mechanism is defined, the appropriate relationship between fluid flow rate and corrosion rate for the plant geometry can be used to predict the expected corrosion rate in the plant.

Fluid flow past a corroding surface often affects the way an alloy corrodes in an environment. Numerous studies have discussed this phenomena and processes have been examined included corrosion of mild steel in concentrated sulfuric acid [1], corrosion of mild steel in oxygenated water [2], and corrosion of copper-nickel alloys in sea water [3]. An acceleration of the corrosion rate caused by fluid moving past the alloy surface would make corrosion rate predictions based on stagnant tests inaccurate indeed, this inaccuracy was recognized long ago, and test methods have been developed which attempt to define qualitatively the effect of fluid velocity.

Corrosion can often take place in pipe lines or under equipment in which aqueous liquids are being transported (flow differential oxidation corrosion). This usually occurs at position where there is difference in velocity between different potions of the liquid, i.e. at bends, nozzles, constriction, etc. When liquid containing oxygen flows rapidly past a given section of pipe the oxygen can be supplied cathodically far more quickly to the surface than it can in parts where the liquid is comparatively stagnant, consequently the stagnant part of the pipe becomes the anode and corrodes [4].

1.2. Limiting Current Density (LCD)

The limiting current is defined as the maximum current that can be generated by a given electrochemical reaction, at a given reactant concentration, under well established hydrodynamic steady state conditions. This definition implies that the limiting rate is determined by the composition and transport properties of electrolytic solution and by the hydrodynamic conditions at the electrode surface[5].

1.3. Mass transfer coefficient (*k*)

Usually determined experimentally by the dissolving wall method, or the electrochemical method (limiting current density), or by the analogy with heat transfer. In the dissolving wall method, a specimen is made of or coated with a material that is soluble in the test environment. Results obtained by dissolving surfaces are of uncertain reliability because of surface roughness can develop while the dissolution progressing. Consequently, in recent year the electrochemical method (limiting current density) has been of greater favor, and has wide applications. So the limiting current density values obtained experimentally and theoretically for a RCE case will be analyzed in this study as related to shear velocity[1].

1.3. Influence of Velocity on Electrochemical Corrosion

Relative motion between the fluid and the metal surface will in general affects the rate of corrosion reaction. Flow can accelerate the corrosion attack by increasing convective mass transfer, i.e., convective transportation of oxidizing species towards the metal surface or the flux of dissolved corrosion products away from this surface [6].

For a given flow geometry, the hydrodynamic boundary layer thickness δ is affected by the flow velocity U and the kinematic viscosity n (i.e, it follows that, for any flow system and constant physical properties, [6]

$$NaU^{a} \qquad (1\text{-}1)$$

Where the velocity exponent (a) attains a value of $\approx 0.5 or \approx 0.9$ for fully developed laminar and turbulent flow respectively.

Velocity primarily affects electrochemical corrosion rate through its influence on the diffusion phenomena. For corrosion processes controlled by activation polarization, velocity has no effect on the corrosion rate. If the corrosion process is under cathodic diffusion control, then the velocity increases the corrosion rate [5]. The corrosion rate would be directly proportional to limiting diffusion current, (i.e., $i_{corr}=i_l$), until the intersection of anodic and cathodic polarization curves at a current less than the limiting diffusion current.

1.5. The aim of scope of the present work

The purpose of the present work is to find a relationship between mass transfer coefficient and shear or friction velocity by using rotating cylinder electrode and to study the effect of the following variables: rotational velocity, concentration, and temperature on limiting current density experimentally and theoretically, i.e., to elaborate on the relationship between, *k*, and shear velocity.

CHAPTER TWO
ROTATING CYLINDER ELECTRODE (RCE)

2.1. Introduction

A rotating cylinder will cause swirling of the fluid because of the surface drag whose extent will depend on the exact geometry. A favored experimental arrangement is one involving the presence of a concentric stationary outer cylinder around the inner rotating cylinder [7].

The rotating cylinder electrode offers an interesting alternative for electrochemical studies in that it has simple construction, reproducible response and reaches turbulent flow conditions at low Reynolds number. Its application in corrosion studies for example, permits the use of samples in the form of tubes, simulating the hydrodynamic conditions in which the material is commonly employed.

The lack of an exact mathematical solution for the turbulent flow case has been responsible for the empirical approach used to describe mass transport to a rotating cylinder electrode surface [8].

2.2 Factors affecting limiting current density

Many factors can affect limiting current density which are classified into four categories:

2.2.1 Oxidizing agents

In some corrosion processes, such as the dissolution of zinc in hydrochloric acid, hydrogen may evolve as a gas. In others such as the relatively slow dissolution of copper in sodium chloride, the removal of hydrogen, which must occur so that corrosion may proceed, is effected by a reaction between hydrogen ion and some oxidizing chemical such as oxygen to form water. Because of the high rates of corrosion that usually accompany hydrogen evolution, metals are rarely used in solution from which they evolve hydrogen at an appreciable rate. Most of the corrosion observed in practice occurs under conditions in which the oxidation of hydrogen to form water is a necessary part of the corrosion process. For this reason, oxidizing agents are often powerful accelerators of corrosion and in many cases the oxidizing power of a solution is most important property in so far as corrosion is concerned.

$$4H^{+} + O_2 + 4e^{-} \rightarrow 2H_2O$$

Oxidizing agents that accelerate the corrosion of some materials may also retard corrosion of other through the formation on their surface of oxides or layers of adsorbed oxygen which make them more resistant to chemical attack. This property of chromium is responsible for the principal corrosion resisting characteristics of the stainless steels. It follows then, oxidizing substances, such as dissolved air, may accelerate the corrosion of one class of materials and retard the corrosion of another class. In the latter case, the behavior of the material usually represents a balance between the power of oxidizing compounds to preserve a protective film and their tendency to accelerate corrosion when the agencies responsible for protective-film breakdown are able to destroy the films[9].

2.2.2 Temperature

As a general rule, increasing temperature increases limiting current. This is due reaction kinetics themselves and the higher diffusion rate of many corrosive agents and reaction products at increased temperatures. This latter action delivers these by products to the surface more efficiently. Occasionally, the limiting current in a system will decrease with increasing temperature. This can occur because of certain solubility considerations. Many gases have lower solubility in open systems at higher temperatures. As temperatures increase, the resulting decrease in solubility of the gas causes corrosion rates to go down [10].

2.2.3 Fluid velocity

Velocity primarily affects electrochemical corrosion rate through its influence on diffusion phenomena. It has no effect on activation controlled processes. The manner in which velocity affects the limiting diffusion current is a marked function of the physical geometry of the system. In addition the diffusion process is affected differently by velocity when the flow conditions are laminar as compared to a situation where turbulence exists. For most conditions the limiting diffusion current can be expressed by the equation:

$$i_{\mathbf{l}} = kU^{n} \tag{2-1}$$

Where k is a constant, u is the velocity of the environment relative to the surface and n is a constant for a particular system. Values of n vary from 0.2 to 1[6]. Fig. 2-1 shows the effect of velocity on the limiting current density. The effect of velocity on corrosion rate, like the effect of oxidizer addition, complex and depends on the characteristics of the metal and the environment to which it is exposed. Fig. 2-2 shows typical observations when agitation or solution velocity is increased [7].

For corrosion processes which are controlled by activation polarization, agitation and velocity have no effect on the corrosion rate as illustrated in curve B in fig. 2-2. If corrosion process is under cathodic control, then agitation or velocity increases the corrosion rate as shown in curve A, section 1. This effect generally occurs when an oxidizer present in very small amounts as in the case of dissolved oxygen in acids or water. If the process is under diffusion control and the metal is readily passivated, then the behavior corresponding to curve A, section 1 and 2, will be observed, curve C shows that at high velocities the passive film is removed [11].

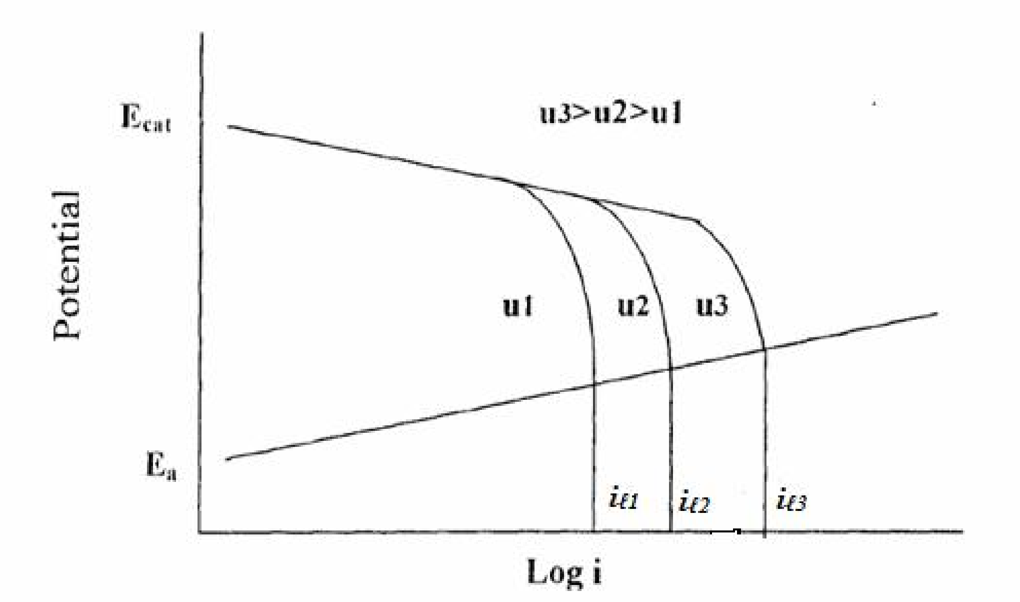

Figure 2-1 Effect of velocity on i_{ℓ}.[12]

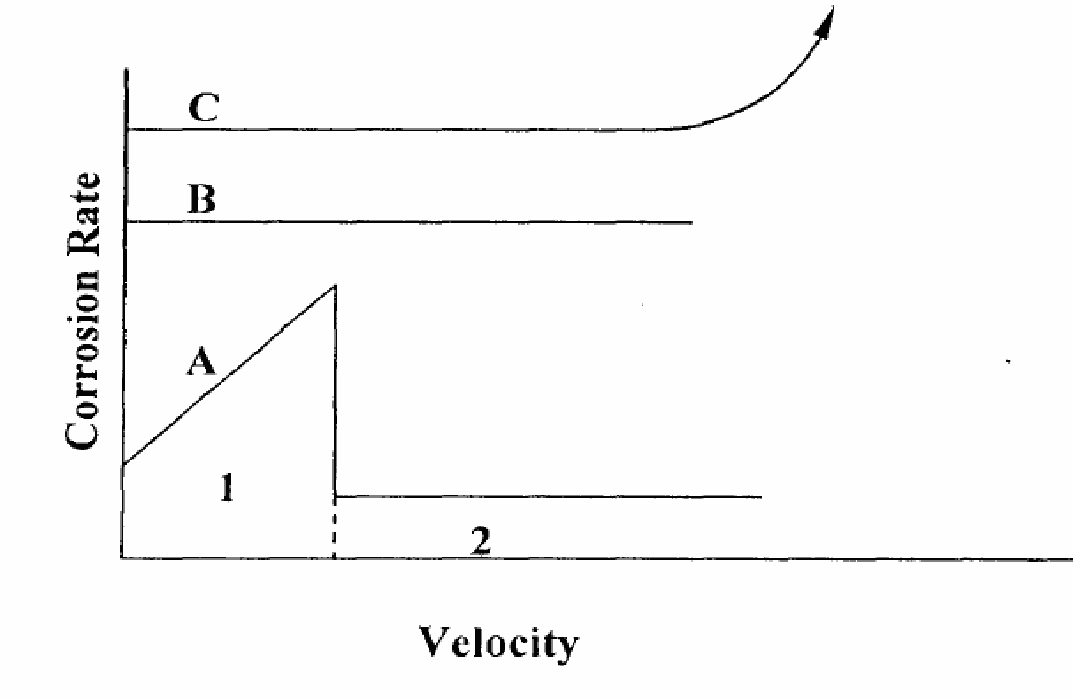

Figure 2-2 Effect of Velocity on the Corrosion Rate. [11]

2.2.4 Effect of Salt Content and Chloride Ion

Chlorides have probably received most consideration in relation to their effect on corrosion. The effect of sodium chloride concentration on the corrosion of iron in air saturated water at room temperature was found to increase the corrosion rate. The corrosion rate in air saturated water at room temperature was found to increase with the increase of sodium chloride solution concentration reaching maximum at about 3% NaCl (seawater concentration), and then decreases, the value falling below that of distilled water when saturation is reached (26 % NaCl). To understand this behavior, oxygen solubility in water decreases continuously with an increase in sodium chloride concentration, explaining the falling off of corrosion rate at higher sodium chloride concentration. The initial rise appears to be related to a change in the protective nature of the barrier rust film that forms on the corroding metal. On the other hand, chlorides increase the electrical conductivity of the water so that the flow of corrosion currents will be facilitated [13, 14].

An increase in suspended solids levels will accelerate corrosion rates. These solids include any inorganic or organic contaminants present in the fluid. Examples of these contaminants include clay, sand, silt or biomass [10].

2.3 The Rotating Cylinder Electrode

The rotating cylinder electrode is operated in the turbulent flow regime at Re > 200 [7], although flow can be complicated with vortexing until much higher Re, where true turbulence develops. A Re > 200 is readily achieved at modest rotation rates and cylinder diameters. Therefore the cylinder can be readily utilized by the corrosion engineer to simulate corrosion conditions in turbulent pipes. For the smooth rotating cylinder electrode, the mass transport correlation is given by Eisenberg [15]. However, surface roughening increases mass transport.

$$Sh = 0.079\,\mathrm{Re}^{0.7}\,Sc^{0.36} \tag{2.2}$$

This correlation is valid within the following range: 1000< Re <100000 and 850 < Sc <11490. Recalling that the limiting current density is given by:

$$i_{\mathrm{l}} = zFk\Delta C \tag{2.3}$$

And that k is given by

$$k = Sh \times \frac{D}{d} \tag{2.4}$$

So that

$$i_l = \frac{zFD\Delta C}{d} Sh \tag{2.5}$$

It is easy to show that the limiting current density can be expressed entirely in terms of very accessible parameters: D, ΔC, d, U, and *v*, again, assuming that C_s =0:

$$i_l = 0.079 zFC_b U^{0.7} D^{0.64} n^{-0.34} d^{-0.3} \tag{2.6}$$

If the characteristic dimension is taken as the radius of the cylinder, r (U=r*w*), throughout the calculation where d=2r we have

$$i_l = 0.064 zFC_b w^{0.7} D^{0.64} n^{-0.34} r^{-0.4} \tag{2.7}$$

Hence if the corrosion rate is determined by the mass transport of cathodic reactant to the cylinder surface, then the corrosion rate will increase as a function of the rotation rate raised to the 0.7 power and linearly with dissolved reactant concentration. Increasing the velocity by a factor of ten increases the corrosion rate by a factor of five. Silverman [16] has shown that the velocity of the rotating cylinder necessary to match the mass transport conditions for pipe flow, assuming the Eisenberg correlation applies, is given by:

$$U_{cyl} = 0.11845 \left(\left(\frac{r}{n} \right)^{0.25} \left(\frac{d_{cyl}^{0.429}}{d_{pipe}^{0.179}} \right) Sc^{-0.857} \right) U_{pipe}^{1.25} \tag{2.8}$$

Useful velocity conversions in order to have equality of mass transport conditions between the rotating cylinder and the annulus and impinging jet are also reported by Silverman[16]. The rotating cylinder electrode utilized a specimen with a fixed diameter. Consequently, all points on the surface are exposed to the same surface velocity (excluding surface roughness effects). The RCE can be used to simulate flowing conditions present in other geometries if flow in those geometries is tangential to the electrode surface by using in the appropriate rotation rate. The surface shear stress for the rotating cylinder is given as [17]:

$$t\left({}^{kg}\!/_{m.s^2} \right) = const.\frac{f}{2} r w^2 r^2 \qquad (2.9)$$

where *f* is the friction factor. The Re number and the surface roughness are important factors in determining the surface shear stress. For a smooth cylinder, *f/2* is equal to $0.079\mathrm{Re}^{-0.3}$ [18]. Substitution of the relationship gives the following expression for shear stress:

$$t = 0.079\,\mathrm{Re}^{-0.3}\, r w^2 r^2 \qquad (2.10)$$

$$= 0.079\left(\frac{2r^2 wr}{m} \right)^{-0.3} r w^2 r^2$$

Rearranging yields

$$t = 0.064 r^{1.4} r^{0.7} w^{1.7} m^{0.3} \qquad (2.11)$$

Where the shear stress is given in terms of the fluid density, ρ, the angular velocity, ω, the fluid viscosity, μ, and the cylinder radius, r. Note that the shear stress will increase as a function of the rotation rate raised to the 1.7 power. In contrast, the limiting current density increases with velocity raised to the 0.7 power for the RCE.

2.4. Literature Review

Eisenberg *et al.* [19] were the first to carry out a detailed investigation on mass transport to rotating cylinder electrode under turbulent flow conditions. From measurement of limiting current densities at a smooth RCE made of Ni using $Fe(CN)_6^{-3} / Fe(CN)_6^{-4}$ redox couple in alkaline medium. They obtained:

$$i_l = kzFC_b d^{-0.3} n^{-0.344} D^{0.644} U^x \qquad (2\text{-}12)$$

Where k = 0.0791 and x = 0.7

Pang and Ritchi [20] minimized the end effects by installing inert ends and obtained the following equation:

$$i_l = kzFC_b d^{-0.299} n^{0.644} U^x \qquad (2\text{-}13)$$

Where k = 0.086 and x = 0.71

Gabe and Walsh [21] obtained the value x=0.74 for cupric ion electro-reduction to metallic copper on a smooth cylinder and observed that x changes to 0.9 as the electrode surface becomes rougher.

Silverman [22] showed that one practical geometry which is useful for studying and predicting electrochemical corrosion under dynamic conditions (turbulent flow), is the rotating cylinder electrode (RCE). He presented an equation that allows rotation rates to be chosen so that mass transfer coefficients for the (RCE) would be those for the modeled geometry of pipes, annuli or jets. These equations allow mass transfer controlled corrosion rates to be predicted exactly for geometries discussed using only one of the geometries for experimentation.

Gabe and Makanjuola [24] stated that

1. Artificial roughness elements located at an electrode surface can be expected to generate high levels of mass transfer improvement in a turbulent regime. However, it is essential that the size of a roughness element be several orders of magnitudes greater than the diffusion sublayer thickness.

2. Mass transfer enhancement was found to be independent of roughness height for geometrically similar roughness elements, i.e. those with similar roughness pitch to roughness height ratios, but its magnitude was a function of roughness type.

3. Roughness elements with three-dimensional character were superior to two-dimensional types, but only at the lower Reynolds number ranges. A maximum enhancement of 275% was recorded with a weave-covered RCE at *Re* = 12700.

4. With the exception of wire-wound electrodes, for which the Reynolds number exponent was consistently higher than 0.7 (as for a smooth RCE), the marginal increment in mass transfer coefficient for all other rough RCEs invariably declined at higher Reynolds number.

Jean *et. al.* [24] found that the equations derived from the steady-state mass balance for dissolved oxygen in a divided RCE constitute only one essential part in the optimization of the reactor. However, the results obtained already suggest interesting avenues for further study. These include the possible requirement of a prior degassing step in the flow sheet, the determination of bubble effects on mass transfer and need of further and more complete data to fully validate the derived equations.

Kalantray *et. al.* [25] suggested that

(1) High speed electrodeposition techniques can be used as a tool for predicting suitable plating conditions for production of compositionally modulated samples.

(2) From the morphological studies, it is apparent that, at high electrode rotation speeds, the crystal structure is more refined and compact.

(3) The composition of zinc-nickel alloy can be controlled by changing current density and electrode rotation speed as follows :

- At high current density ($\geq$50 Adm^{-2}), the composition changes significantly with change in rotation speed.
- At low current density ($\leq$10A dm^{-2}) the composition is almost the same with change in speed.
- At current densities of $\geq$50 Adm^{-2}, the optimum electrode speed for obtaining maximum nickel content in the deposit is at 50 rpm. Above that depending on the current density, the nickel content decreases with increase in rotation speed.

(4) A zinc rich deposit of up to 95% is possible at low current densities (0.5-10 A dm^{-2}). A deposit with a nickel content of up to 3-14% is possible in the current density range of 1-50 A dm^{-2}. A deposit with a nickel content of up to 20-30% is possible in the current density range of 100-130 A dm^{-2}.

(5) A preliminary investigation of the zinc-nickel alloy system has demonstrated that compositionally modulated alloy production is possible.

Gabe and Wilcox [26] The RCE has now established itself as a major tool for studying electrochemical mass transport especially under turbulent conditions. During the 15 years which have elapsed since the subject was last reviewed, over 100 applications have been recorded in a number of Reynolds and the versatility of the RCE has been fully demonstrated.

Quddus and Allam [27] The effect of rotational speed (fluid velocity) on barium sulfate scale in a rotating cylinder electrode system has been investigated at atmospheric pressure and at 60^0 C. The following conclusions can be drawn from the study:

- The scale deposition rate increases with the increasing Reynolds number.
- The analysis of the scale deposition data supports the well-established theoretical prediction of a diffusion controlled process.
- The hydrodynamics of solution plays an important role in the scale deposition process, and, therefore, it must be a part of any scale mitigation and control program.

Maciel and Agostinho [8] studied a rotating cylinder electrode which was constructed and hydrodynamically characterized in turbulent flow using four different electrochemical systems. The empirical relationship between rotation rate and mass transfer was:

$$i_{\mathbf{l}} = 0.082 zFC_b d^{-0.3} n^{-0.344} D^{0.644} U^{0.732} \qquad (2\text{-}14)$$

Within a 95% confidence level. It was verified that a moderate increase in surface roughness did not influence the mass transport process and thus the relation is valid in studies of technological importance such as corrosion and electrodeposition.

Nava *et. al.* [28] A straightforward analysis of the RCE through effectiveness factors using the dimensionless Damk**ö**hler number for an electrochemical interface process, Cu(II)/Cu(0), shows the competition between the intrinsic reaction (charge transfer) and bulk mass transport phenomena. Effectiveness factors indicate that the mass transfer controls this process as it was expected considering the potential imposed during electrolysis.

The technique employed to assess the intrinsic reaction rate constant at the equilibrium was the electrochemical impedance spectroscopy. It was performed within an RCE taking into account that the charge transfer constant at electrolysis potential was assessed considering its exponential variation with the overpotential. The specific mass transfer coefficients were obtained by electrolysis at controlled potential in order to calculate a mean value.

Furthermore, through effectiveness factors, it is possible to determine the Reynolds range at which some vortices and other hydrodynamic phenomena, unfavorable for the current flow through the cell, appear. It is recommended to analyze the effectiveness factors for other electrochemical reactions, since some of them are slow and the mass transport would not be the only step to limit the global process. In addition, it is recommendable to use a methodology analog to the one developed in this paper for other types of electrochemical reactions.

Herbert-Guillou *et. al.* [29] Showed the influence of biofilm development conditions on the mechanical properties. For that, a new electrochemical method is used to follow the elasticity and the flexibility of the biofilm. On one hand, the biofilm is elastic, whatever the development conditions (laminar flow with electrode rotation or turbulent flow in a tube). The thickness is the same before and after the mechanical strain (rotation speed). On the other hand, the deformation depends on the development conditions and the mechanical properties of the biofilm are different. This new approach can be performed to detect and monitor the biofilm formation with a sensor.

Huang and Chuang(2000) [30] The potentiodynamic polarization curve of the solution- annealed Fe–Mn–Al alloy exhibited an active-to passive transition behavior in 3% NaCl solution during the erosion-corrosion process, while no passive region could be found for the age-treated Fe–Mn–Al alloy. During the wear-corrosion process, both the solution annealed and age-treated Fe–Mn–Al alloys had no passive region in 3% NaCl solution. The open circuit potentials of the solution-annealed and age-treated Fe–Mn–Al alloys in 3% NaCl solution increased with increasing rotation speed during the erosion-corrosion process, but decreased with increasing rotation speed and contact load during the wear corrosion process. The weight loss of the solution-annealed Fe–Mn–Al alloy during 90-h wear-corrosion test in 3% NaCl solution was about two times larger than that of the age-treated Fe–Mn–Al alloy with the presence of β-Mn. After potentiodynamic polarization curve measurements during erosion- and wear-corrosion tests, the scanning electron microscope observations showed that the ferrite phase in the solution-annealed Fe–Mn–Al alloy was prone to corrode with respect to the austenite phase. However, for the age-treated Fe–Mn–Al alloy, corrosion preferentially occurred in the austenite phase region where β-Mn precipitated.

Maciel and Agostinho [31] The 90/10 Cu-Ni alloy showed nonselective dissolution in all H_2SO_4 media studied: (a) in the presence of Fe(III) ions with or without BTAH as inhibitor; and (b) in the presence of BTAH with the electrode polarized to an overpotential value corresponding to that attained by the alloy at open circuit, in the presence of Fe(III) ions and BTAH.

A model previously developed for the rotating disc electrode (RDE) was successfully applied to the rotating cylinder electrode (RCE). With the latter model, it was possible to obtain mechanistic information about the alloy dissolution process. It was verified that, while in the absence of Fe(III) ions the anodic process is controlled by diffusion and the cathodic one by charge transfer, in the presence of the Fe(III) ions, the cathodic process is under diffusion control and the anodic one is under charge transfer control.

The inhibitive action of BTAH corresponds to an efficiency of practically 100% for [BTAH] $\geq 1.7 * 10^{-3}$ mol L^{-1}. Inhibition efficiency calculations from weight loss measurements and polarization curves, showed that potentiodynamic anodic curves obtained with the RCE can be used to simulate the effect of the oxidant on the corrosion of the alloy.

Giddy *et. al.* [32] An electrochemical study on stability of oxide films formed on AISI 1020 steel in a 2.75 M NaOH solution at temperature 95^0 C to 175^0 C has been carried out by employing a rotating cylinder electrode apparatus. This work has indicated that at high temperature and turbulent conditions the passivity for steel normally afforded by the magnetite films at lower temperatures can no longer be expected. Only in the passive region at low potential (from -0.6 V to -0.4 V) is a compact, more stable film formed. At high potentials, film formation competes with film dissolution, particularly at higher temperatures. The turbulent conditions of the liquor results in the breakdown of passivity resulting in a situation similar to the one experienced in case of non protective magnetite growth.

Jean L. Stojak *et. al.* [33] The effect of particle loading on the polarization behavior during coelectrodeposition of nanometric diameter alumina with copper with a rotating cylinder electrode from the kinetically-controlled to mass-transfer limitation conditions was studied with an optimal electrolytic bath composition of 0.1 M $CuSO_4$ + 1.2 M H_2SO_4, which was used in coelectrodeposition experiments [35]. In the kinetically-controlled region, the particles in suspension led to a decrease in the current for a given potential value compared without particles in suspension for all particle loading. For mass transfer limiting conditions, alumina particle loadings at or below 120 g/l had no effect. However, a particle loading of 158 g/l was found to increase the limiting conditions by as much as 32%.

2.5. Hydrodynamics of Rotating Cylinder

The description of fluid flow effects on corrosion needs an accurate definition of heat, mass and momentum transfer (due to wall shear stress). Although the three factors are strongly interdependent, the focus in corrosion inhibitor studies has tended to be on wall shear stress. For the rotating cylinder electrode (RCE), the turbulent flow conditions result in reasonably high wall shear stress [35]. The transition from laminar to turbulent flow for a rotating cylinder with diameter d at a peripheral speed U occurs at Reynolds number Re of around 200, where Re = U d / ν . A system with rotation speed of up to 10.000 rpm can yield wall shear stresses as high as 100 Pa. In our jet-cylinder arrangement the gap between the RCE and the outside wall of the electrochemical cell is finite which means that the overall hydrodynamic conditions are a weak axial flow superimposed on the rotational flow.

The transfer of mass, heat, or momentum between a solid phase boundary and a turbulent fluid is encountered in many chemical engineering processes, and the interrelationships between the three have received much study. In 1904, Nernst suggested a model for relating turbulent mass transfer at a boundary to the convective flow. A stagnant layer of thickness (δ_D) was pictured to exist near a boundary and a well mixed region outside this layer. If the concentration of diffusing species is (C_b) in the well mixed region and zero at the wall then the rate of mass transfer per unit area, N, is given as [36].

$$N_A = D\frac{C_b}{d_D} \qquad (2\text{-}15)$$

A number of attempts have been made to offer alternatives to the Nernst diffusion layer concept which recognize that the flow close to the wall is not stagnant. These include surface renewal models and the various eddy models [36].

Analogies applicable to fully developed turbulent flow usually assume that molecular and eddy transport occur in parallel, and employ a rate equation involving a transport coefficient which is the sum of the molecular (D) and eddy (ε_D) diffusion coefficients, i.e.,

$$N_A = \left(D + e_D\right)\frac{dC_A}{dx} \tag{2-16}$$

In measuring the rates of mass transfer by the use of electrochemical reactions, it is better and more usual to make the chemical polarization negligible because the mass transfer coefficients are most easily obtained from the limiting currents when the concentration at the liquid-solid interface can be assumed to be zero ($C_s = 0$) [37].The ions are transferred from the bulk of the solution to the surface of the electrode principally by migration due to the potential field, diffusion due to the concentration gradient, and convection by the flow. The current density at the electrode is expressed as:-

$$N_A = \frac{i}{zF} \tag{2-17}$$

Where

$$N_A = k\left(C_b - C_s\right) \tag{2-18}$$

At the liquid solid interface $C_s = 0$ equation (2-18) becomes:

$$N_A = kC_b \tag{2-19}$$

Mass transfer coefficient (k) is usually determined experimentally by the dissolving wall method, or the electrochemical method (limiting current density technique, LCDT), or by the analogy with heat transfer. In the dissolving wall method, a specimen is made of/or coated with a material that is soluble in the test environment. Results obtained by dissolving surfaces are of uncertain reliability because of surface roughness can develop while the dissolution progressing. Consequently, in recent years the electrochemical method (LCDT) has been of greater favour, and has wide applications. So the limiting current density (LCD) values obtained experimentally for a RCE [15], will be analyzed in this study. Mass transfer coefficient can be measured by substituting eq. (2-19) into (2-17)

$$kC_b = \frac{i_{\mathbf{l}}}{zF} \qquad (2\text{-}20)$$

$$k = \frac{i_{\mathbf{l}}}{zFC_b} \qquad (2\text{-}21)$$

The shear velocity or friction velocity can be calculated from shear stress as follows:

$$U^* = \sqrt{\frac{t}{r}} \qquad (2\text{-}22)$$

Where

$$t = \frac{f}{2} r U^2 \qquad (2\text{-}23)$$

Substituting eq. (2-23) into eq. (2-22)

$$U^* = U \sqrt{\frac{f}{2}} \qquad (2\text{-}24)$$

2.5.1. Nernst Boundary Layer

One of the first approaches to mass transfer in electrode processes was given by Nernst in 1904[38]. He assumed a stationary thin layer of solution in contact with electrode. Within this layer it was postulated that diffusion alone controlled the transfer of substances to the electrode. Outside the layer, diffusion was negligible and concentration of electro-active material was maintained at the value of bulk concentration by convection. This hypothetical layer has become known as "Nernst diffusion layer (δ_D)". Fig. 2-3 gives a schematic diagram of this layer. Nernst assumed that the concentration varied linearly with distance through layer. The thickness of this layer is given by:

$$d_D = \frac{D}{k} \tag{2-25}$$

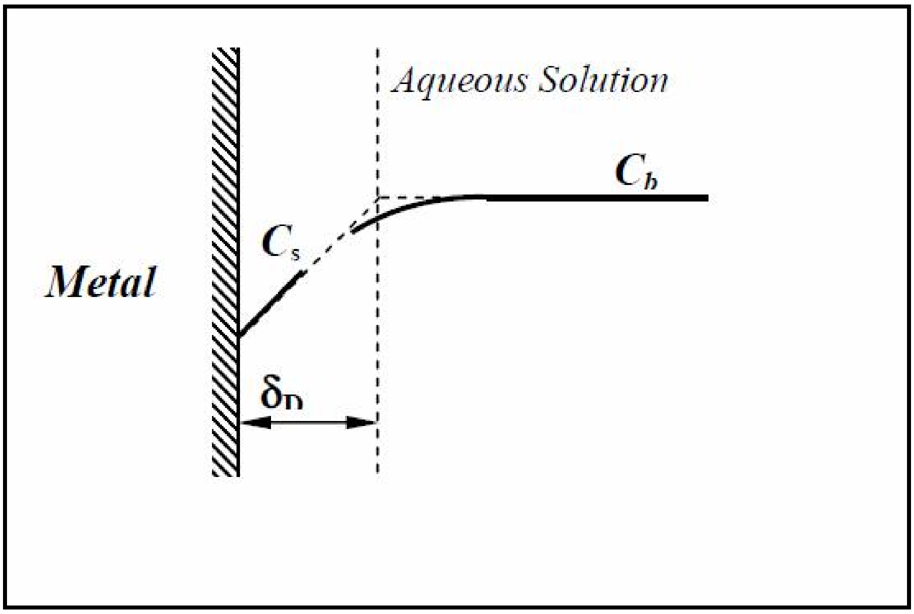

Figure 2-3 Diffusion boundary layer [7].

The diffusion layer thickness is dependent on the velocity of the solution past the electrode surface. As the velocity increases, δ_D decreases and the limiting current density increases [39]. The time interval required to set up the diffusion layer varies with the current density and limiting diffusion rate, but it is usually of the order of 1 second while it is 10-4 second needed to establish the electrical double layer, which makes it possible to distinguish between η_a and η_c experimentally. The diffusion layer may reach a thickness of 100-500 µm, depending upon concentration, agitation (or velocity), and temperature [40].

2.5.2. Hydrodynamic Boundary Layer

When a fluid moves past a stationary, hydraulically smooth surface, there is an implicit assumption that the fluid is stationary at that surface. That assumption is often called "no slip at the wall". In many flow configurations and especially when turbulent flow conditions prevail, the velocity profile shows an increase from 0 at the solid-fluid interface to the free stream value across a relatively short distance into the fluid. Though in the rotating cylinder the surface is moving, the fluid adjacent to that surface moves at the same velocity as the cylinder so, in effect, the fluid is stationary relative to the surface and fulfills the no slip at the wall criterion. The boundary layer thickness is independent of position on the surface meaning that the velocity profile, momentum transfer, and wall shear stress are independent of position. The rotating cylinder electrode as traditionally constructed cannot examine situations where such uniformity does not exist without some modification. Mass transfer requires a concentration gradient between the surface and fluid bulk. Such a gradient implies that the concentration changes across some small distance between the surface and the bulk. This region is called the concentration or mass transfer boundary layer. For large Schmidt Numbers normally encountered in liquids the fully developed mass transfer boundary layer for hydraulically smooth surfaces is much thinner than the fully developed hydrodynamic boundary layer [41]. This relationship is shown in fig. 2-4.

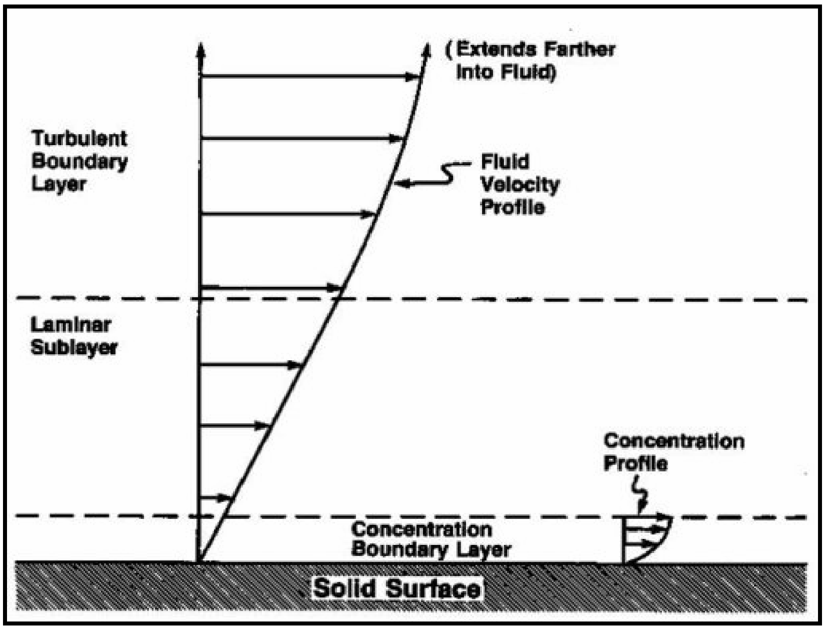

Figure 2-4 Relationship between the hydrodynamic boundary layer and the mass-transfer boundary layer [41].

The hydrodynamic boundary layer is represented as having two sections, a viscous sub layer and a turbulent outer layer and that the fluid is moving relative to a surface. Since the flow is turbulent, the profiles are time-averaged profiles and are not drawn to actual scale. As in the case of the velocity profile, the mass transfer boundary layer thickness is independent of position meaning that the mass transfer rate is independent of position [41].

2.5.3. Application of Hydrodynamics

It is important at the outset to define more closely the effective film thickness δ_D. In any electrolyte solution in contact with a metal surface there is a static layer of solution next to the surface whose thickness will decrease as the solution velocity increases. The way in which this velocity changes the hydrodynamic thickness (δ_H) is complex and depends on such factors as viscosity, geometry, temperature and surface roughness.

It is also necessary to separate laminar flow when a stagnant layer of well defined thickness δ_H is formed, from turbulent flow when values of δ_H, are very low and when flow towards and away from the surface is complex. The analogy of mass transport with heat transfer [42, 43] has led to successful methods of regarding the mass transport interaction with fluid flow, since the behaviour of heat is in many ways similar to mass transport depending as it does on a driving force, i.e. the heat gradient may be regarded as analogous to the concentration gradient.

Relationships between δ_H, and δ_D have been established for certain geometries, e.g. for a rotating disc, Levich [35] has found that for laminar flow $\delta_H \approx 5\delta_D$ The mathematical proofs of these relationships are not appropriate here, but a useful non-mathematical account of the application of hydrodynamic theory to mass transport has been given by King [44]. The most important variables are the main stream solution velocity U, the characteristic length L (diameter in the case of a rotating cylinder) and the kinematic viscosity v (m^2/s). For application to mass transport such as cathodic reduction or anodic dissolution, which are dependent on ion or molecular (dissolved oxygen) transport, the variables are the diffusion coefficient, D, and the activity difference between surface and main solution, ΔC (mol/m^3). Using the mathematical technique of dimensionless group analysis, the rate of mass transport (N) in terms of moles per unit area per unit time can be shown to be a function of these variables, which when grouped together can be related to the rate by a power term. For many systems under laminar flow conditions it has been shown that the following relationship holds:

$$\frac{NL}{D\Delta C} = K\left(\frac{UL}{n}\right)^{x}\left(\frac{n}{D}\right)^{y} \qquad (2\text{-}26)$$

Where K is a constant, and *x* and *y* are exponents that are very often 1/2 and 1/3 respectively. The dimensionless groups in equation (2- 26) are referred to as follows:

$$\begin{aligned}&\frac{UL}{n} = (\mathrm{Re})(\mathrm{Re}\,ynoldsNo.);\ \frac{n}{D} = (Sc)(SchmidtNo.);\\&\frac{kL}{D} = (Sh)(SherwoodNo.);\end{aligned} \qquad (2\text{-}27)$$

Where U is the main stream velocity (m/s), D is the diffusion coefficient (m^2/s), v is the kinematic viscosity (m^2/s) and L is the characteristic length (m). The application of this equation is only useful if:

1. The relationship between δ_H, and δ_D, is known.
2. Concentration has a power exponent of unity, i.e. conforms to a first order reaction.
3. Dissolution is uniform (etching); otherwise, for rough surfaces such as pitting, turbulent flow regimes may occur even at low solution velocities.

The rate N, can be converted to the limiting current density i_ℓ by Faraday's law, so that from physical measurements on the solution it is possible to calculate i_{corr}, since it is of the same order as i_ℓ.

It has not been possible to calculate constant K or exponents x and y directly from theory, except in one case, so that they have to be determined by experiment. The geometry of a system, i.e., flat plates, stirrers, pipes, etc. have a large effect in determining the magnitude of the constants and by using reactions whose parameters are well established for one geometry it has been possible to gather data for many other systems, by using the known reactions in other geometries. In the case of the one system that can be predicted from theory, i.e. the rotating-disc electrode (radius r), this is proving to be a useful tool for understanding the effects of flow on corrosion reactions. The equation can be rearranged to give the limiting current density i_L, and velocity, the characteristic length U/L can be interpreted as the angular velocity ω. The equation developed by Levich [35] by substituting in equation (2- 28) is:

$$i_{\mathbf{l}} = 0.0062zF\left(\frac{U}{L}\right)\left(\frac{UL}{n}\right)^{\frac{1}{2}}\left(\frac{n}{D}\right)^{\frac{1}{3}}D\bar{r}\Delta C \qquad (2\text{-}28)$$

Substituting for *UL* by *ω* and for the limiting case for the cathodic reduction process when $C_s = 0$, the activity term ΔC is then equal to C_b (the concentration of ions in the bulk solution), and then

$$i_{\mathbf{l}} = 0.0062zFw^{\frac{1}{2}}n^{\frac{-1}{6}}D^{\frac{2}{3}}C_b r^{-1} \qquad (2\text{-}29)$$

Kamabra [45] has made specific use of the rotating disc for investigation of the effect of flow on corrosion reactions. This work has shown that it is possible to determine the type of control (activation or concentration polarization) of zinc dissolving in 0.1 N Na_2SO_4, (de-aerated), which followed closely the predicted increase in hydrogen ion reduction as the flow rate increased, and proved that in this example

$$i_{corr} \approx i_{\mathbf{l}} \tag{2-30}$$

2.5.4. Diffusion Boundary Layer

A thin, uniform, and stationary diffusion boundary layer is important in obtaining high-quality electrodeposits. Limiting current depends on thickness of the diffusion boundary layer for a given reactant concentration.

If concentration gradient exists within a fluid flowing on a surface, mass transfer is usually created. The whole concentration gradient of the resistance to mass transfer lies within a thin layer known as diffusion boundary layer in the vicinity of the surface. Outside this layer, the concentration is maintained at its bulk value. According to Nernst, the mass is transferred across this layer by diffusion alone. Following Fick's law of diffusion transfer, the mass transfer rate could be determined using concentration gradient across this layer, species diffusion coefficient and layer thickness as [46]:

$$J = \frac{D}{d_D}\left(C_s - C_b\right) \tag{2-31}$$

2.6. Mass Transfer Of Rotating Cylinder Electrode

Mass transfer of rotating cylinder electrode can be classify into two kinds

2.6.1. Mass Transfer Controlled Electrochemical Reactions

Mass transfer plays a big role in chemical and electrochemical dynamic processes. It is the movement of materials from one location in the solution to another arises from difference in electrical or chemical potential at the two locations or from the movement of a volume element of solution.

The understanding of this process has been enhanced by the application of the basic principle of mass transfer .There are three modes of mass transfer [46]:

Migration

This occurs when charged particles placed in an electric field. Thus a negatively charged ion is attracted towards a position electrode and vice versa. This movement is due to a gradient in the electrical potential [47].

Diffusion

This occurs whenever a species moves from a region of high concentration to one of low concentration, thus it is movement due to concentration gradient [47].

Convection

This occurs from a movement of the fluid by forced means (stirring, for example), or from density gradient within fluid. Generally fluid flow occurs because of natural or forced convection.

Mass transfer to an electrode is governed by the Nernst-Plank equation which may be expressed by [46, 48]:

$$J(Y) = -D_i \frac{\partial C_i(Y)}{\partial Y} - \frac{n_i F}{RT} D_i C_i \frac{\partial \Theta(Y)}{\partial Y} + C_i V(Y) \qquad (2\text{-}32)$$

And the 1St term of equation (2.32) is diffusion term ,2nd is migration term and 3rd is convection term . In many practical cases the cathodic reaction is under diffusion control. In this case the reaction current is governed by Fick's first law which relates flux to the concentration gradient:

$$J_i(y,t) = -D_i \frac{\partial C_i(y,t)}{\partial y} + X_i(J_j + J_i) \tag{2- 33}$$

In flowing systems the convection term is small compared with the diffusion term, the equation (2-33) becomes

$$J_i(y) = -D_i \frac{\partial C_i(y)}{\partial y} \tag{2- 34}$$

The negative sign in equation (2.34) has been omitted as it indicates only that the direction of transfer from a region of high concentration to one of low concentration.

$$J_i = \frac{i}{nF} = -D_i \frac{\partial C_i}{\partial y}\Big|_{y} = 0 \tag{2- 35}$$

Or it is equivalent (for any species) to

$$i = nFD \frac{C_b - C_s}{d_D} \tag{2- 36}$$

At a given current or more exactly, at a given reaction rate, the concentration right at the electrode surface is determined by a mass transfer process. If this current is increased, the reaction rate is increased due to a faster consumption of the reactive species at the electrode, resulting in a lower interfacial concentration C_s . However ,this concentration can not, drop below zero, thus the current at which the interfacial concentration reaches zero is called the limiting current This current is determined by setting C_s equals to zero in equation (2-36) [42] .

$$i_l = nF \frac{D}{d_D} C_b \tag{2- 37}$$

$$i_l = nFkC_b \quad (2\text{- }3)$$

Where: $k = \frac{D}{d_D}$

2.6.2. Limiting current density

The limiting current is defined as the maximum current that can be generated by a given electrochemical reaction, at a given reactant concentration, under well-established hydrodynamic conditions, in the steady state. This definition implies that the limiting rate is determined by the composition and transport properties of electrolytic solution and by the hydrodynamic conditions at the electrode surface.

In the mass transfer boundary layer (or diffusion layer), whose thickness is indicated by (δ_D), the reactant concentration varies from the bulk value to practically zero at the electrode, this is the limiting-current condition. Determination of mass transfer coefficient involves the measuring of limiting currents of the cathodic reaction process.

Measurement of limiting currents is an experimental technique that has been quite widely employed in mass transfer experiments. Its relative simplicity and flexibility make limiting current method a powerful tool in experimental studies of forced and free convection. At the limiting current the rate of transport of reactant to the interface is smaller than the rate at which it can be potentially consumed by the charge transfer reaction; as a result, at the interface the concentration of this species approaches zero [49] . The flux of reacting species is given by:

$$N = \frac{i_l}{zF\left(1 - t_+\right)} \quad (2\text{-}38)$$

When concentration of the reacting species relative to the total ionic concentration of the electrolyte is small, $t_+ << 1$, Eq.(2.38) becomes;

$$N = \frac{i_l}{zF} \qquad (2\text{-}15)$$

From the measured current, a mass transfer coefficient, k, defined by;

$$N = k(C_b - C_s) \qquad (2\text{-}16)$$

May be calculated. Since at the limiting current the concentration is set as C_s = 0, hence

$$k = \frac{i_l}{zF\Delta C} \qquad (2\text{-}21)$$

Eisenberg *et al.* [15] were the first to study the mass transfer to a rotating cylinder electrode comprehensively using both chemical dissolution and limiting current density, and they suggested that in the range of Re from (1000 to 100000) and Sc from (835 to 11,490), the best relationship is within ±8.3%. It is obtained for the *ferri-ferrocyanide* redox reaction in alkaline medium smooth Ni RCE using $Fe(CN)_6^{-3} / Fe(CN)_6^{-4}$:-

$$i_l = 0.0791 zFC_b U^{0.7} d^{-0.3} n^{-0.344} D^{0.644} \qquad (2\text{-}6)$$

Which is expressed in terms of dimensionless numbers as either:-

$$Sh = 0.0791\,\mathrm{Re}^{0.7}\,Sc^{0.356} \qquad (2\text{-}2)$$

Or

$$St = 0.0791\,\mathrm{Re}^{-0.3}\,Sc^{-0.644} \qquad (2\text{-}39)$$

The relationship of Eisenberg *et al.* [15] was effectively confirmed by Robinson and Gabe [50] who obtained the following equation for the cathodic electrodeposition of copper from $CuSO_4$-H_2SO_4 solutions:

$$St = 0.0791\,\mathrm{Re}^{-0.31}\,Sc^{-0.59} \qquad (2\text{-}40)$$

They subsequently pointed out [51] that critical review of the literature reveals some slight variation in the values of the power indices; for example the index for *Re* has been reported as -0.3 [15], -0.31 [50], -0.333 [52] and -0.4 [53], while for *Sc* the values reported include -0.59 [50], -0.644 [15, 54, 55] and -0.666 [53]. These indices can be expressed by equations as follows

Ariva and Carroza [54] measured mass transfer rate for the electrodeposition of copper ions under different rates of stirring. The reaction occurs on the fixed cathode of a cylindrical cell where the anode is the stirring device. They obtained data in quite good agreement with the Eisenberg *et al.* correlation, eq.(2-41), but represented by :-

$$St = 0.0791\,\mathrm{Re}^{-0.3}\,Sc^{-0.644} \qquad (2\text{-}41)$$

Or,

$$St = 0.0791\,\mathrm{Re}^{-0.4}\,Sc^{-0.666} \qquad (2\text{-}42)$$

It may be noted that if such a dependence of *Sc* can be assumed Robinson and Gabe [50] obtained:-

$$Sh = 0.169\,\mathrm{Re}^{0.66}\,Sc^{0.33} \qquad (2\text{-}43)$$

Mass transport to an inner RCE in a turbulent flow system may be described by empirical dimensionless correlations of the general form:

$$Sh = a\,\mathrm{Re}^{b}\,Sc^{c} \qquad (2\text{-}44)$$

Where a and b are empirical constant, c = 0.33, indicating forced convection region [56]. In this study, a forced convection mechanism is obtained which agrees very well with the relationship:-

$$Sh = 0.0791\,\mathrm{Re}^{0.7}\,Sc^{0.356} \qquad (2\text{-}2)$$

Given by Eisenberg *et al.* [57] for mass transfer to a rotating cylinder in turbulent flow system and exponents in all equations denote a highly turbulent flow, which agree with the previous mass transfer during cementation using RCE studies by by Mamdoh *et al*. in aqueous media [58].

$$Sh = 1.581\,\mathrm{Re}^{0.725}\,Sc^{0.33} \qquad (2\text{-}45)$$

Maciel and Agostinhc [8] studied by using 90/10 CuNi alloy rotating cylinder electrode was constructed and hydrodynamically characterized in turbulent flow using three different electrochemical systems:-

- Cu^{+2}/Cu^{0} reduction in 0.1 mol dm^{-3} K_2SO_4 solution with the electrode held at -300, -400 and -500mV vs. SCE.
- Fe^{+3}/Fe^{+2} reduction in 1 mol dm^{-3} HCl solution with the RCE polarized at -350, -400 and -450 mV vs. SCE.
- Fe^{+3}/Fe^{+2} reduction in 1 mol dm^{-3} HCl solution on RCE previously corroded and polarized at -400, -420 and -440 mV vs. SCE. The empirical relationship between rotational rate and mass transport was

$$i_{\mathbf{l}} = 0.082zFC_bU^{0.732}d^{-0.3}n^{-0.344}D^{0.644} \qquad (2\text{-}46)$$

Prandtl found that [59] :-

$$i_{\mathbf{l}} = 0.04zFC_bU^{0.75}d^{-0.25}n^{-0.42}D^{0.67} \qquad (2\text{-}47)$$

Cornet and Kappesser [52] studied by using cathodic electrodeposition of copper from $CuSO_4$-H_2SO_4 solutions.

$$i_{\mathbf{l}} = 0.169zFC_bU^{0.66}d^{-0.34}n^{-0.33}D^{0.67} \qquad (2\text{-}48)$$

Non-faradaic dissolution of benzoic and cinnamic acids was investigated by Eisenberg *et al*. [15] and others [60] and previously Holman and Ashar [61] have attempted to distinguish between reacting and non-reacting dissolution in aqueous alkaline solutions containing glycerol. They obtained correlations of the type

$$Sh = a\,\mathrm{Re}^{b}\,Sc^{c} \qquad (2\text{-}44)$$

For non-reacting dissolution a = 9.3, c = 0.33, b = 0.425 and for reacting dissolution a = 88.2, c = 0.33, b = 0.492.The fact that the values of *a* and *c* depart so markedly from those found previously suggests that the dissolution was not completely diffusion-controlled and that as found elsewhere for alkaline solutions [58] some other mechanism assumes importance perhaps amphoteric complex formation.

Ahmed [58] studied for mass transfer during copper cementation for alcoholic-water mixtures using RCE in turbulent system.

$$i_{\mathbf{l}} = 0.061zFC_bU^{0.833}d^{-0.167}n^{-0.503}D^{0.67} \qquad (2\text{-}49)$$

This equation was approximately agree with experimental results in present work in all concentrations and temperatures for Brass and Carbon Steel this clear in Appendix-E- .

Ariva and Carozza [53] studied by using cathodic electrodeposition of copper from $CuSO_4$-H_2SO_4 solutions.

$$i_{\mathbf{l}} = 0.0791zFC_bU^{0.6}d^{-0.4}n^{-0.27}D^{0.67} \qquad (2\text{-}50)$$

2.6.3. Application to Mass Transfer Measurement

Utilizing the electrochemical method, three mass transfer coefficients at a solid-liquid interface in many different flow systems can be easily measured. If one chooses an electrolytic system in which only one kind of reaction occurs at the electrode to be used as a mass transfer surface, the limiting current is reached provided that the opposite electrode does not limit the rate of the reaction. These conditions are satisfied when the opposite electrode is large enough and when the reaction occurring at the measuring electrode is sufficiently rapid. And then the limiting current is a direct measure of the mass flux of a specific species of ion at the measuring surface [37].If the concentration of this species of ion in the bulk of the solution, C_b, is known, the mass transfer coefficient can be calculated from Eq.(2- 21).

2.7. Shear Stress and Friction Velocity

Shear stress and friction velocity can be classified into three kinds:

2.7.1 Wall shear stress

The shear stress is a force per unit area (= rate of transport of momentum per unit area in positive r direction) is:-

$$t = m\frac{\partial U}{\partial r} - r\overline{Un} \tag{2-51}$$

The viscous part varies from being the sole transporter of momentum at the wall to a negligible fraction of the total stress in the outer part of a turbulent boundary layer.For $r < 0.1\delta$, τ is approximately constant and equal to it's value at the wall:

$$t \approx t_w \qquad (2\text{-}52)$$

This is the constant-stress layer. As τ_w has dimensions of [density]*[velocity]^2, it is possible to define an important velocity scale-the friction, U by

$$t_w = rU^2 \qquad (2\text{-}53)$$

Or

$$U = \sqrt{\frac{t_w}{r}} \qquad (2\text{-}22)$$

The turbulent flow at the RCE induces a wall shear stress on the surface of the cylinder. Again Eisenberg's original reports [15] offer a well accepted equation for the wall stress, τ (g cm^{-1}s^{-2})

$$t = 0.0791r\,\mathrm{Re}^{-0.3}U^2 \qquad (2\text{-}54)$$

2.7.2. Shear Stress Measurements

It is very difficult to measure directly the velocity gradient close to a surface because the boundary layer thickness is so small that any measuring instrument disturbs the flow. However, a diffusion-controlled electrochemical reaction at small cathodes embedded in the wall can be applied to obtain the velocity gradient at the wall [37].

If the test electrode is made quite small in length, the concentration boundary layer is very thin owing to a large value of the Sc. Therefore, the curvature of the surface may be neglected, and it can be assumed that the velocity gradient in the concentration boundary layer is linear. Thus, the electrode is analogous to a constant temperature hot wire anemometer with the characteristics that the surface concentration is constant and the electrical current in the circuit depends on the surface shear stress. Furthermore, several limitation on both measurements are also similar. High frequency velocity fluctuations cannot be measured by either method owing to the thermal inertia of the wire of the anemometer and the capacitance effect of the concentration boundary layer over the electrode. Non linear response is caused in both systems by large turbulent intensities. In addition, if there is non uniform flow over the wire length or the electrode width, it may result in some error [37].

2.7.3.Friction factor

A well know extension of Reynolds analogy is the correlation of Chilton and Colburn [62] in 1934. The correlation based on an empirical modification of equ.(2-55)

$$\frac{1}{St}=\frac{2}{f}\Rightarrow St=\frac{k}{U}=\frac{f}{2} \qquad (2\text{-}55)$$

For the effect of *Sc*, gives

$$St=\frac{f}{2}Sc^{-\frac{2}{3}} \text{ or } Sh=\frac{f}{2}\operatorname{Re}Sc^{\frac{1}{3}} \qquad (2\text{-}56)$$

Sherwood and Pigford [63], in 1952, have shown that equ. (2-55) to be in good agreement with a wide range of experimental data.

One fundamental property of boundary layers of significance is the friction velocity (*U**), which is a measure of the fluid shear at the boundary and is defined by the formula $U^{*}=\sqrt{n\frac{dU}{dr}}$ and has the units of velocity.

$$U^* = U_{av}\sqrt{\frac{f}{2}} \qquad (2\text{-}24)$$

From equ. (2-54) fanning friction factor can be expressed by:-

$$\frac{f}{2} = \frac{Sh}{\mathrm{Re}\, Sc^{0.33}} \text{ and } \frac{f}{2} = \frac{St}{Sc^{-2/3}} \qquad (2\text{-}57)$$

When $Sh = \frac{kd}{D}$ and $k = \frac{i_l}{zFC_b}$ one can estimate friction velocity from limiting current

$$\frac{f}{2} = \frac{i_l d}{zFC_b D\, \mathrm{Re}\, Sc^{0.33}} \qquad (2\text{-}58)$$

Where $\mathrm{Re} = \frac{Ud}{n}$. equ. (2-58) becomes

$$\frac{f}{2} = \frac{i_l n}{zFC_b UDSc^{0.33}} \qquad (2\text{-}59)$$

2.8 Polarization

When the metal is not in equilibrium with a solution of its ions, the electrode potential differs from the equilibrium potential by an amount known as the polarization. Other terms having equivalent meaning are overvoltage and overpotential. The symbol commonly used is **η**. Polarization [14] is an extremely important parameter because it allows useful statements to be made about the rates of corrosion process. In practical situations, polarization sometimes defined as the potential change away from some other arbitrary potential and in mixed potential experiments, this is the free corrosion potential [64, 65, 66].The change in the electrode potential from equilibrium potential depends on the magnitude of the external current and its direction. The direction of potential change always opposes the shift from equilibrium and hence opposes the flow of current or is of galvanic origin. For example, the anode always becomes more cathodic in potential and the cathode becomes more anodic, the difference of potential becoming smaller. Often misnamed (overpotential) is that polarization is the difference between electrode potential (when it is not in equilibrium with its environment) with respect to the Standard electrode potential, the symbol commonly used is η. Polarization can be conveniently divided into three different types [11].

2.8.1 Activation polarization

Activation polarization refers to an electrochemical process which is controlled by the reaction sequence at the metal – electrolyte interface. This is easily illustrated by considering hydrogen – evolution reaction on metal during corrosion in acid solution [11].

Activation polarization refers to electrochemical reactions which are controlled by a slow step in the reaction sequence. The species must first be adsorbed or attached to the surface before the reaction can proceed according to step1. Following this, electron transfer (step2) must occur, resulting in a reduction of the species. As shown in step3, two hydrogen atoms then combine to form a bubble of hydrogen gas (step4) as shown in Fig.2-5.The speed of reduction of the hydrogen ions will be controlled by the slowest of these steps [11].

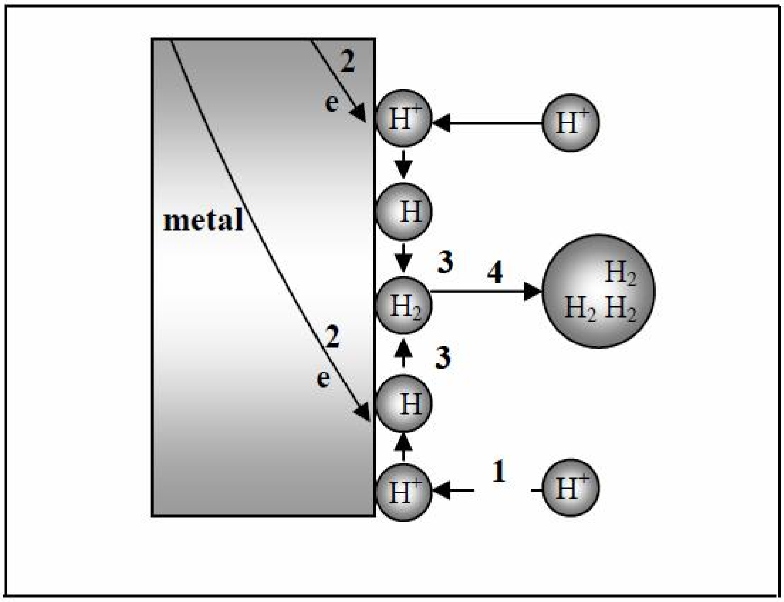

Figure 2-5 Hydrogen-Reduction Reaction Under Activation Control (Simplified)[11]

2.8.2 Concentration Polarization η_c

Concentration polarization refers to electrochemical reactions which are controlled by the diffusion in the electrolyte. It is the slowing down of a reaction due to an insufficiency of the desired species or an excess of the unwanted species at the electrode. This type of polarization occurs at the cathode when reaction rate or the cathode current is so large that the substance being reduced cannot reach the cathode at a sufficiently rapid rate. Since the rate of reaction is determined by the slowest step, the diffusion rate will be the rate determining step. At very high reduction rates, the region adjacent to the electrode surface will become depleted of ions. If the reduction rate is increased further, a limiting rate will be reached which is determined by the diffusion rate of ions to the electrode surface. This limiting rate is the limiting diffusion current density i_ℓ. It represents the maximum rate of reduction possible for a given system; the expressing of this parameter is [11, 67]:

$$i_{\mathbf{l}} = \frac{DzFC_b}{d_D}$$

Where i_L is the limiting diffusion current density, D is the diffusion coefficient of the reacting ions, C_B is the concentration of the reacting ions in the bulk solution, and δ_D is the thickness of the diffusion layer.

By combining the laws governing diffusion with Nernest equation [11]:

$$E = E_o + 2.3\frac{RT}{nF}\log\frac{a_{oxid}}{a_{red}} \qquad (2\text{-}60)$$

The following expression can be developed [11, 67]:

$$E_i - E_{eq} = h_C = \frac{2.303RT}{nF}\log\left[1 - \frac{i}{i_{\mathbf{l}}}\right] \qquad (2\text{- }61)$$

This equation is shown in Fig.2-6. For the case of hydrogen evolution any change in the system which increases the diffusion rate will decrease the effects of concentration polarization and hence increases reaction rate. Thus, increasing the velocity or agitation of the corrosive medium will increase rate only if the cathodic process is controlled by concentration polarization [11] Fig. 2-7.

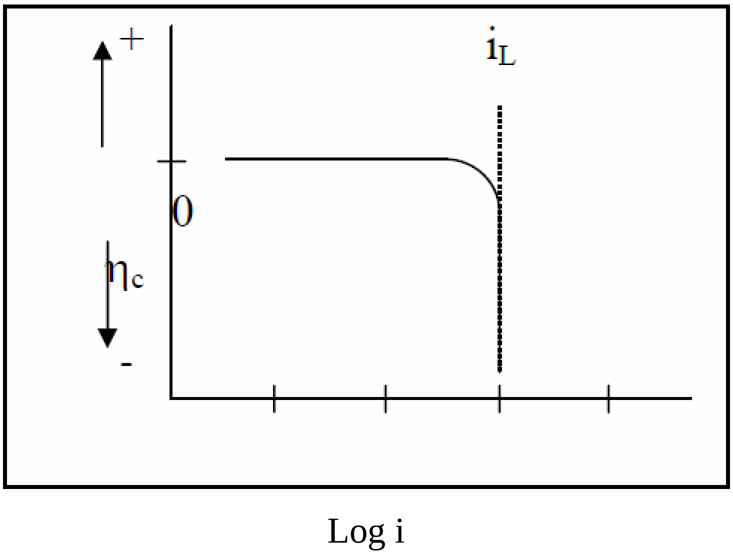

Figure 2-9 Concentration Polarization Curve (Reduction Process)[11].

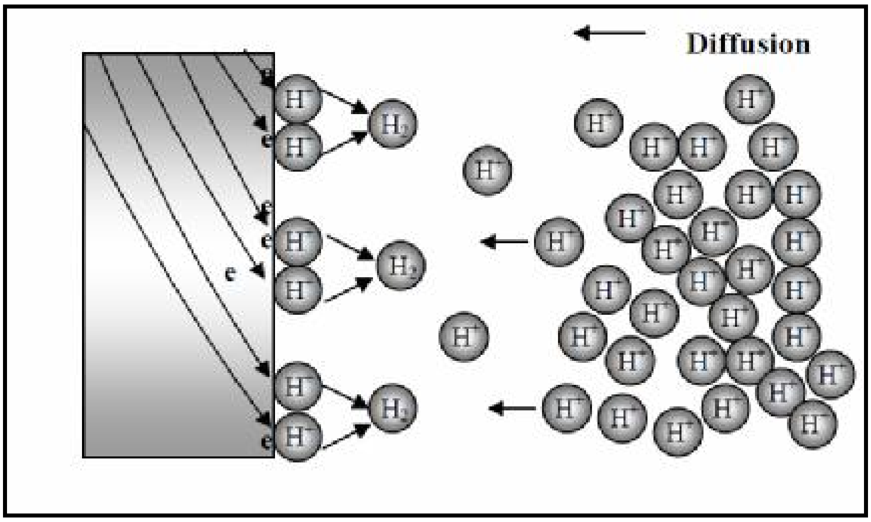

Figure 2-10 Concentration Polarization During Hydrogen Reduction [11].

2.8.3 Combined Polarization

Both activation and concentration polarization usually occur at an electrode. At low reaction rates activation polarization usually controls, while at higher reaction rates concentration polarization becomes controlling. The total polarization of an electrode is the sum of the contribution of activation polarization and concentration polarization [11]:

$$h_t = h_A + h_C \qquad (2\text{-}62)$$

During reduction process such as hydrogen evolution or oxygen reduction, concentration polarization is important as the reduction rate approaches the limiting diffusion current density. The overall reaction for activation process is given by [11]:

$$h_{red} = -b_C \log\frac{i}{i_o} + \frac{2.303RT}{nF}\log\left[1 - \frac{i}{i_l}\right] \qquad (2\text{-}63)$$

This case is shown in Fig.2-8.

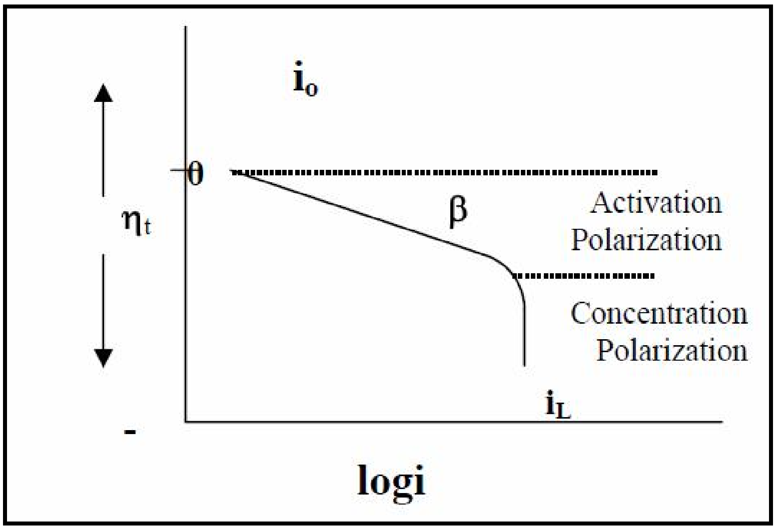

Figure 2-8 Combined Polarization Curve [11].

2.8.4 Resistance Polarization

In corrosion the resistance of the metallic path for charge transfer is negligible. Resistance overpotential η_R is determined by factors associated with the solution or with the metal surface. Resistance polarization η_R is only important at higher current densities or in higher resistance solution. It may be defined as [11]:

$$h_R = I\left(R_{solution} + R_f\right) \qquad (2\text{-}64)$$

Where $R_{slutionn}$ is the electrical resistance of solution, which is dependent on the electrical resistivity (Ω cm) of the solution and the geometry of the corroding system, and R_f is the resistance produced by films or coatings formed on the surface of the sites, which block contact between the metal and the solution, and increase the resistance overpotential.

The total polarization at a metal electrode then becomes as the algebraic sum of the three types described above [11].

$$h = h_A + h_C + h_R \qquad (2\text{-}65)$$

2.9. Applications of the RCE

2.9.1. Electroanalysis

The relation between the RCE and RDE was considered in the introduction but in fact that the RCE has found relatively little use in the field of electroanalysis. Adams has reviewed this field and has emphasized that rotating wire electrodes do have a role. Although initiated by Nernst and Merriam it was later workers who placed the RCE technique on a sound footing using a 0.5 mm platinum wire projecting 5-10 mm from a rotating glass stirring rod. The normal mode is vertical; horizontal electrodes have been used but are less satisfactory because of inconvenience in mounting and poorer stability for convective flow. The importance of a free convective diffusion term has been emphasized by Brown who discussed applications in the determination of D and *z* for a diffusion-controlled electrode reaction.

The vertical platinum wire electrodes has also been used in a vibrating rather than rotating mode and may be powered by the voice coil of a loudspeaker at audio frequencies (20-10000 Hz). Harris and Lindsey have shown that at low frequencies (< 40 Hz) the limiting c.d. is proportional to frequency but at higher values they are virtually independent. The case of a vertical wire electrode vibrating perpendicular to its axis has been considered by Grafov who has attempted a dimensional analysis for this case [68].

2.9.2. Electrodeposition

Early work on electrodeposition has been reviewed by Narasimham and Udupa and is essentially qualitative making use of the motion to increase rates of electrowinning and improve surface finish of protective plated coatings. The use of cathodic copper deposition as a reaction to study mass transfer at the RCE has already been described and some of this work has been extended to a discussion of electrodeposition structure and the incidence of diffusion controlled nodular and dendritic growths. (In this application the presence of uniform current over a large area is of particular importance as extensive microscopical examination is required). This approach is important in the development of high-speed electrodeposition processes and the RCE has been used to simulate continuous strip coating processes and might well also be used for continuous wire coating processes [68].

One application likely to be of considerable importance in the future is the electrowinning of metals from waste effluent and dilute leach or pickle liquors. Surfleet and Crowle have discussed the competitive position of the RCE in relation to other processes such as fluidized bed electrodes, annular and parallel plate electrode configurations, etc., the specific requirement being the ability to recover metal from increasingly dilute solutions. This application may not have been envisaged by Edwards and Wall, nevertheless their considerations of power consumption while using the rotating cylinder cell are of relevance in this context. The electrochemical approach to effluent treatment has obvious attractions but commercial processes are at present limited to zinc, tin, gold and silver with other metals such as nickel and copper likely to be treated similarly in the very near future. One particular problem in this field is the need to electrodeposit at high efficiency from very dilute solutions; that this problem is not insuperable is clear from the commercial success of recovering silver from waste photographic solutions using the RCE (300 such units are reported to be in operation in the U.K. alone at the end of 1973)[68].

2.9.3. Cementation

Agitation can only have a beneficial effect on a cementation-type of reaction when it is controlled by ion diffusion through solution. This has been found for a number of cases and both the RDE and RCE have been used. Much work has been reported for systems where the geometry is irregular and the degree of agitation uncertain and in some cases the RDE has been preferred owing to the independence of diffusion flux and position [69].

2.9.4. Corrosion

Much of the earlier work involving the RCE was carried out for corrosion reactions but because of the marked tendency for chemical reaction to become rate-controlling there is a fair amount of confusion in the literature. At low rotation speeds (<1000 r.p.m.) the rate of corrosion was found to depend upon $\omega^{0.7}$ while at speeds in excess of 500 r.p.m. it was often found to be independent of the speed . At intermediate rotation speeds the power index was found to have values of 0.7-1.0 as partial control was exercised. Other factors were recognized; for example, Roald and Beck found that at low acidity the rate of dissolution of magnesium in hydrochloric acid was proportional to $\omega^{0.71}$ but if the acidity was > 1.4 M then were independent because of interference by the evolution of hydrogen bubbles[67].

The effects of solution flow on rates of corrosion have generally been examined by flow rigs but Heitz has pointed out that disc and cylinders are much more convenient for laboratory testing. On this basis the RCE has been used to investigate effects of dissolved oxygen and chlorides on rates of corrosion, efficacy of inhibitors in controlling corrosion and cathodic protection in flowing conditions . Makrides has attempted to introduce a roughness factor into the mass transport equation pointing out that a surface generally becomes rougher as dissolution takes place where upon the rate becomes directly proportional to rotation speed [67].

More recently the RCE has been used to examine transport behaviour in liquid metals and fused salts. For dissolution of metals in liquid metals the Eisenberg correlation has been used as a criterion for diffusion control in view of the marked departures observed although in the case of carbon steel dissolving into a melt of an essentially similar alloy the departure was relatively small . It is clear that in such applications complex solution chemistry involving solute-solute or solvent-solute interaction are much more likely to be rate-controlling. However, the analytical control of such processes by voltammetry at the RCE may well prove to be feasible as a continuous monitor [67].

CHAPTER THREE

EXPERIMANTAL WORK

Experimental work was carried out to determine the limiting current density of dissolved oxygen on Brass and Carbon Steel specimens under static and flow conditions of rpm = 0, 500, 1000, 1500 and 2000 in NaCl solutions of 0.1, 0.3, 0.5 N at PH equals seven at applied temperatures of 40, 50 and 60 ^{o}C.

3.1. The electrolyte

Electrolyte solution used in this work was NaCl of concentration 0.6, 1.8 and 3% NaCl which has a molecular weight of 58.44 g/gmol. The concentration of NaCl was diluted by distilled water to obtain the required normality of 0.1, 0.3 and 0.5 N NaCl.

3.2. Solvents used

These were used to clean the specimens

- Acetone: CH_3CH_6O of concentration = 99 % supplied by FLUKA.
- Ethanol: C_2H_4O of concentration = 99 % supplied by FLUKA.
- Emery paper range = 600, 400, 300, 250, 200, 150 and 100.

3.3 Apparatus

- Thermometers**:** They are made of glass to measure temperature up to 100^{o}C.

- pH-meter**:** A digital pH-meter, type THERMO, was used to measure and monitor the pH of the working solution during the test run. The pH-meter was calibrated using buffer solutions of pH 4, 7, and 9.
- Water bath**:** Water bath with temperature controller was used, type LABTECH. Voltage=200/20, power = 1000 Watt.
- Electronic Balance**:** High accuracy digital balance with 4 decimal points of type (METTLER AE260). The balance has 0.1 mg accuracy.
- Desiccator**.**
- Motor for rotating the specimens**.**
- Beakers (1and 2 liters)**.**
- Teflon rod**.**
- Nylon rubber washers.
- Resistance box.
- Ammeter.
- Voltmeter.
- Power supply.
- Carbon brush.
- Luggin capillary tube.
- Standard calomel electrode.
- Wires.
- Teflon cup.
- Brass shaft.
- Graphite

3.4. Materials

Carbon Steel (C.S) pipe and Brass were used as a working electrode in a cylindrical shape for limiting current density measurement with a length of 3 cm and 3 cm diameter.

The carbon steel and brass were analyzed by **the Specialized Institute of Engineering Industries** as follows:-

Table 3-1 Composition of used carbon steel specimens.

Element	C	Mn	P	S	Fe
Weight (%)	0.1649	0.5027	0.0020	0.0068	Rest

Table 3-2 Composition of used brass specimens.

Element	Zn	Sn	Cu
Weight (%)	0.3922	0.0052	Rest

3.5. Details of experimental set-up

These are shown in figs. 3-1to 3-4

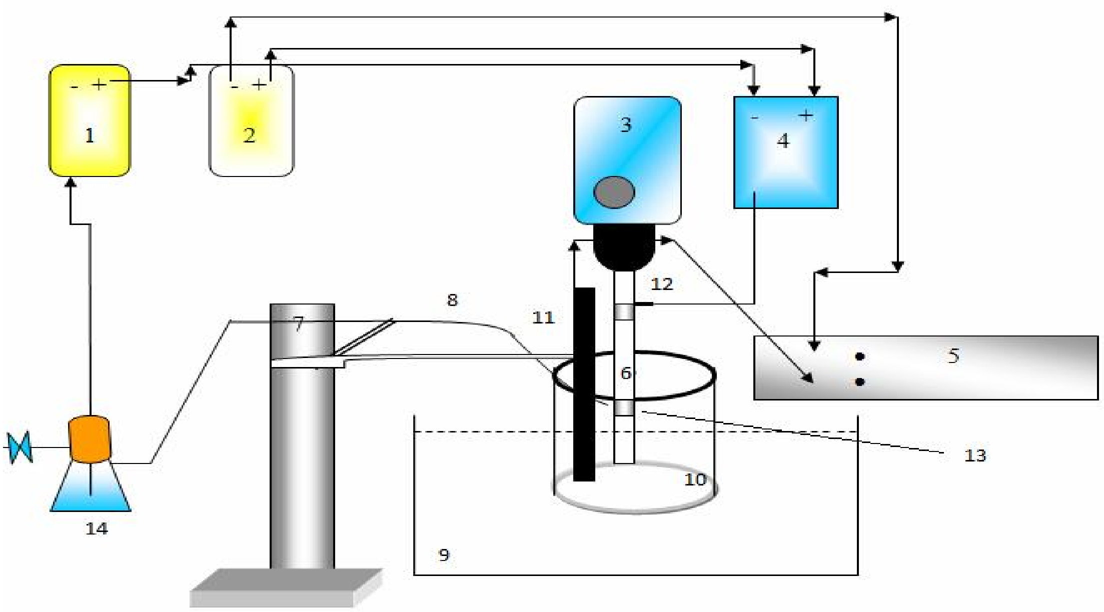

Figure 3-1 Illustrates Rotating Cylinder Electrode

1. Voltmeter
2. Ammeter
3. Rotating motor
4. Power supply
5. Resistance box
6. Rotating shaft
7. Stand
8. Luggin capillary tip
9. Constant temperature water bath
10. Beaker
11. Auxilary carbon electrode
12. Carbon brush
13. Working electrode
14. Reference Saturated Calomel Electrode (SCE) .

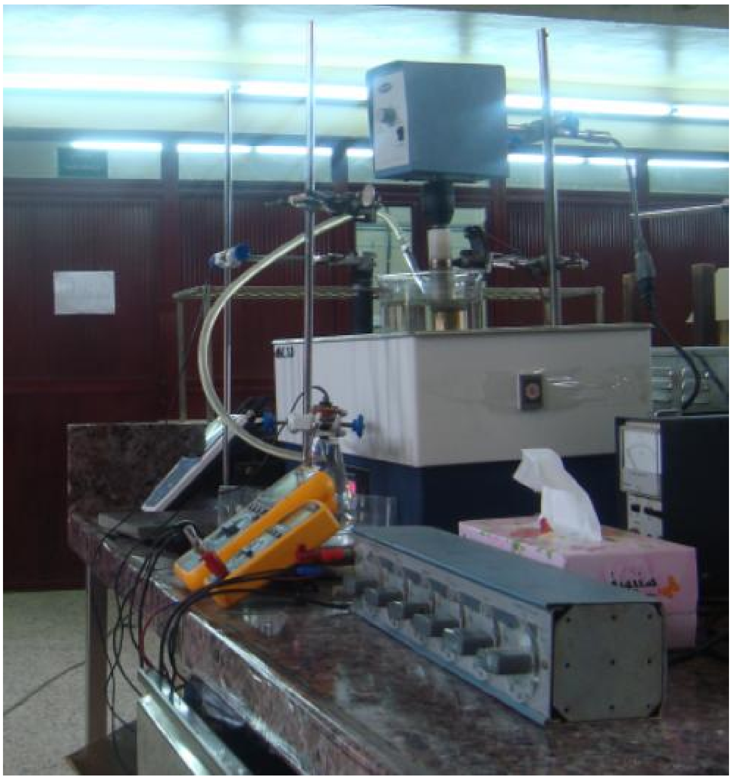

Figure 3-2 Rotating Cylinder Electrode RCE

Figure 3-3 RCE Cell

Figure 3-4 Rotating Electrode Shaft

3.6. Limiting Current Density Measurements

Cylindrical specimens of area $\pi * 3 * 3\ cm^2$ and anode electrode (graphite area $\pi * 2.58 * 10.46\ cm^2$) were immersed in a solution of NaCl of a concentration 0.1, 0.3 and 0.5 N. In order to assess the limiting current density, before each experimental run, the metal specimen was cleaned by emery paper and washed by tap water followed by distilled water, dried with clean tissue, immersed in annalar ethanol for 1 minutes, rinsed with clean acetone and dried with clean tissue. The specimens were then stored in a desiccator over highly active silica gel for overnight before use, and then directly exposed to the solution for cathodic scanning of limiting current [46]. The experimental runs were always performed in duplicate for averaging. They were made thrice or more for checking reproducibility and accuracy when necessary. The total number of runs were 90, i.e., 3 temperatures*5 speeds* 3 solutions* 2 metals.

3.7. Procedure used to measure limiting current

1. Set water bath at 40^o C
2. Place beaker in bath
3. Anode (graphite) and cathode either brass or carbon steel (3cm long and 3cm in diameter) are both immersed in beaker to start the run.
4. Read steady state (i = mA) and (V = volt) after (1 min) of rotating the cylinder
5. Change resistance from resistance box (0 to 10^6 Ohm) to nullify the current, i.e., i =0 mA.
6. Before the two previous steps stated above the PH was adjusted to 7.

CHAPTER FOUR

EXPERIMENTAL RESULTS

Figures 4-1 to 4-18 show experimental results of determining the limiting currents of dissolved oxygen cathodic polarization on brass and carbon steel in 0.1, 0.3 and 0.5 N NaCl solutions at 40, 50 and 60^{0}C respectively. It is clear that the limiting current will be increased with increasing rotational velocity and temperature in NaCl solutions of increasing concentration at the corresponding physical properties of differently varying extents, i.e. viscosity, density, diffusion coefficient, and dissolved oxygen concentration. These properties are presented in Appendix B showing different extents of variation. These results are also presented in Tables A-1 to A-18 in Appendix A.

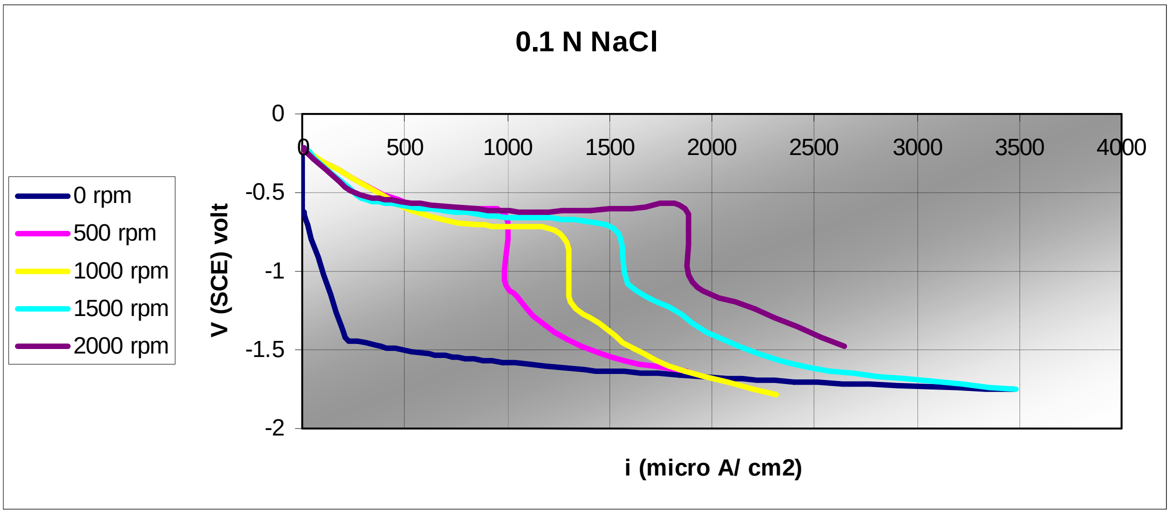

Figure 4-1 Experimental limiting current results of dissolved oxygen cathodic polarization on brass in a solution of 0.1N NaCl at 40^{0}C.

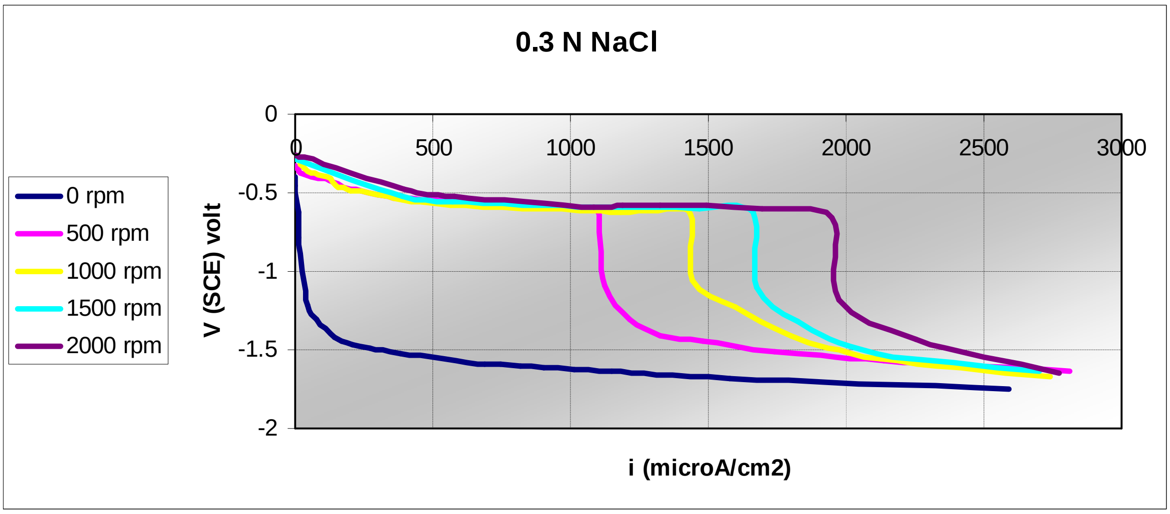

Figure 4-2 Experimental limiting current results of dissolved oxygen cathodic polarization on brass in a solution of 0.3N NaCl at 40^0C.

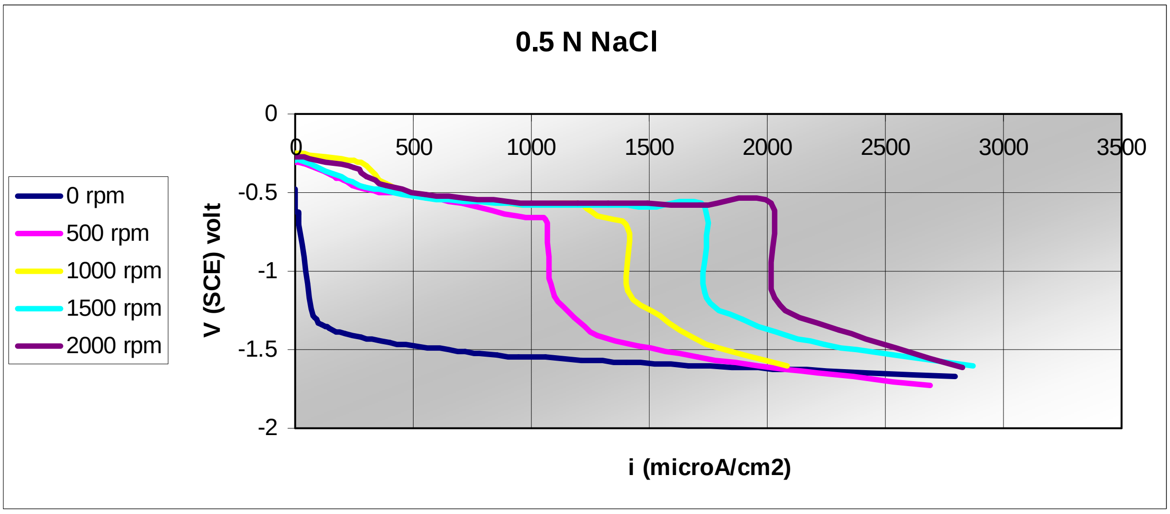

Figure 4-3 Experimental limiting current results of dissolved oxygen cathodic polarization on brass in a solution of 0.5N NaCl at 40^0C.

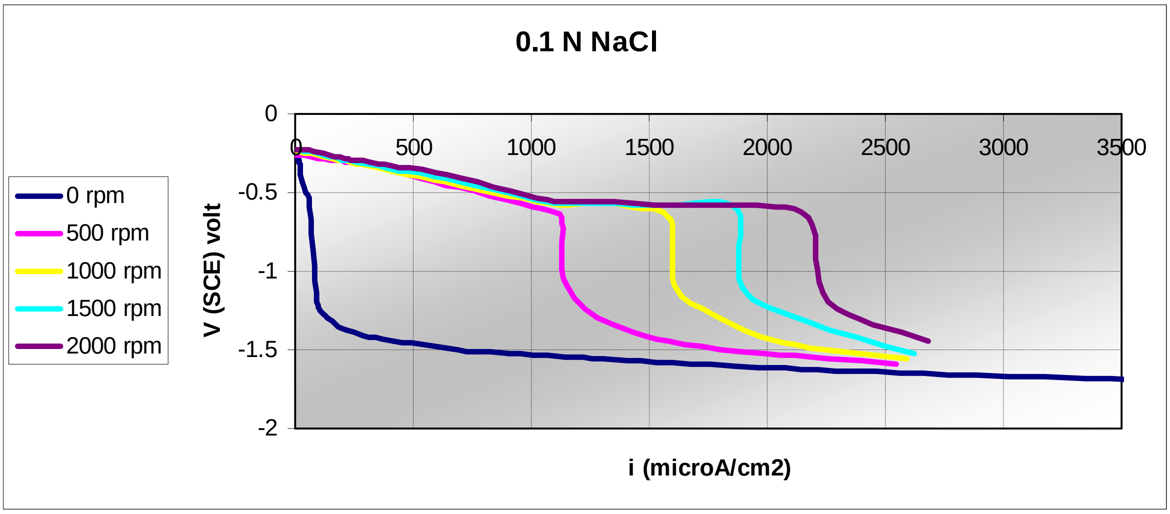

Figure 4-4 Experimental limiting current results of dissolved oxygen cathodic polarization on brass in a solution of 0.1N NaCl at 50^0C.

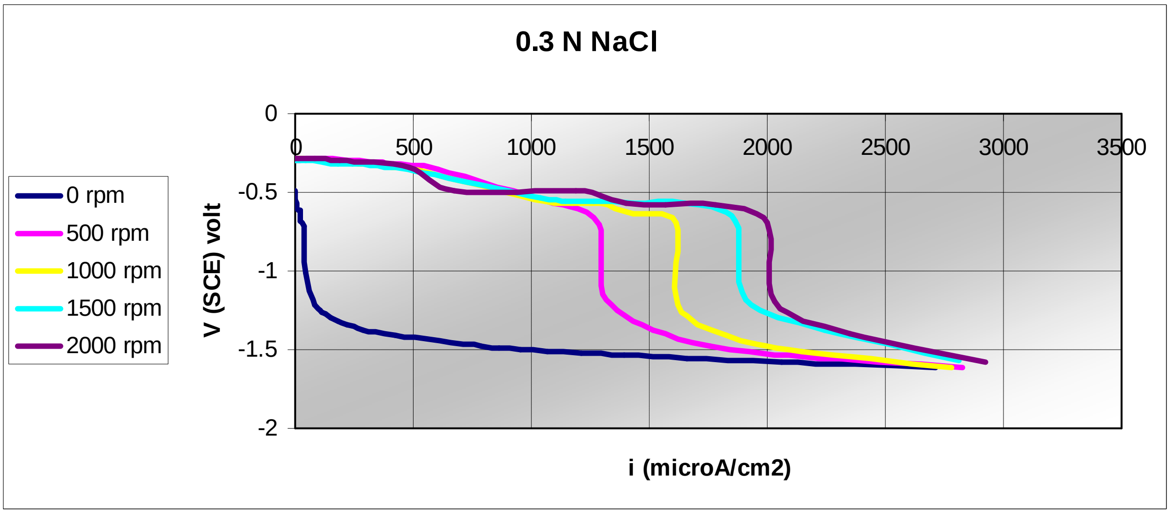

Figure 4-5 Experimental limiting current results of dissolved oxygen cathodic polarization on brass in a solution of 0.3N NaCl at 50^0C.

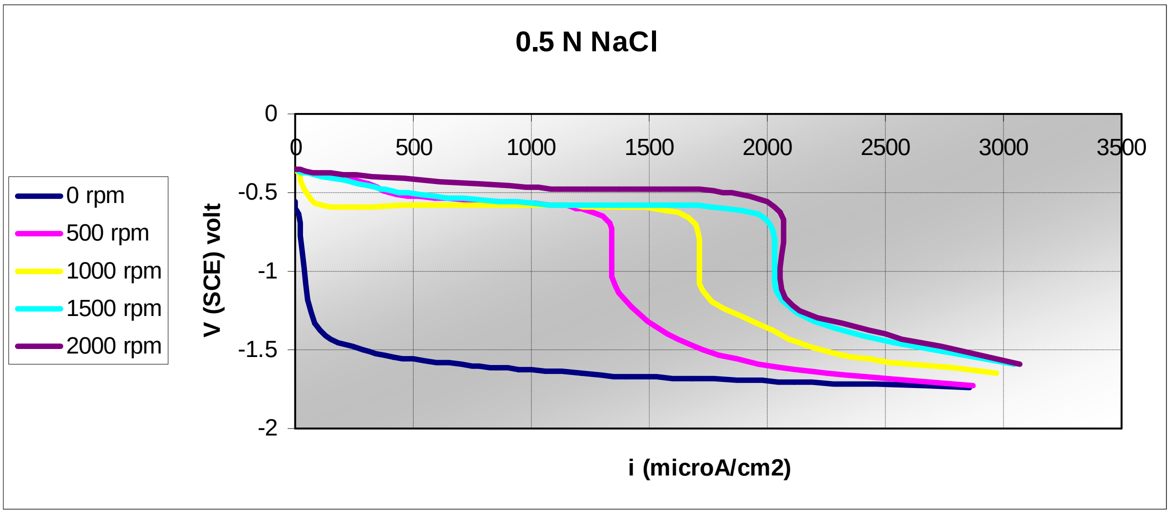

Figure 4-6 Experimental limiting current results of dissolved oxygen cathodic polarization on brass in a solution of 0.5N NaCl at 50^{0}C.

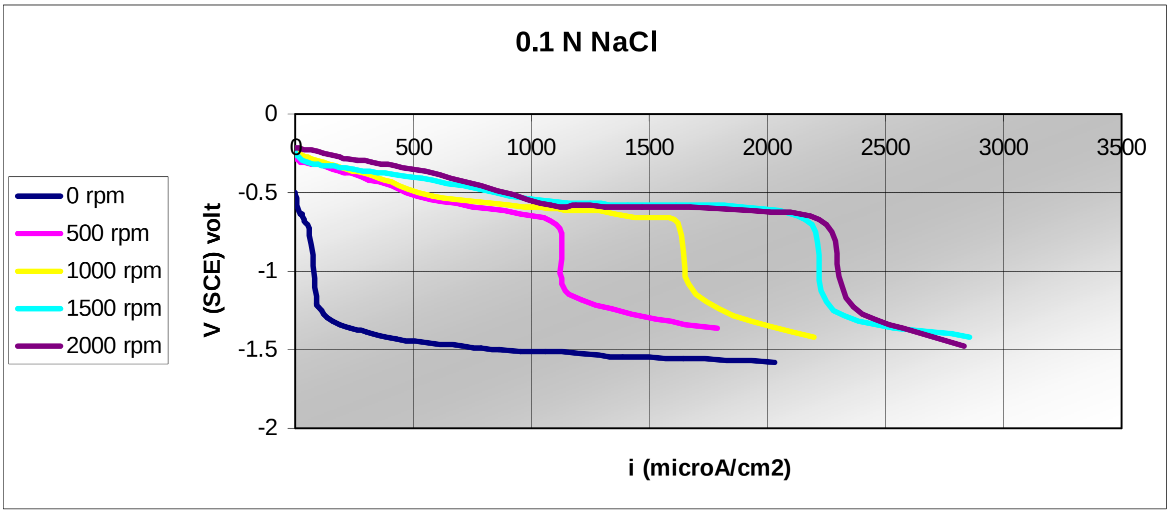

Figure 4-7 Experimental limiting current results of dissolved oxygen cathodic polarization on brass in a solution of 0.1N NaCl at 60^{0}C.

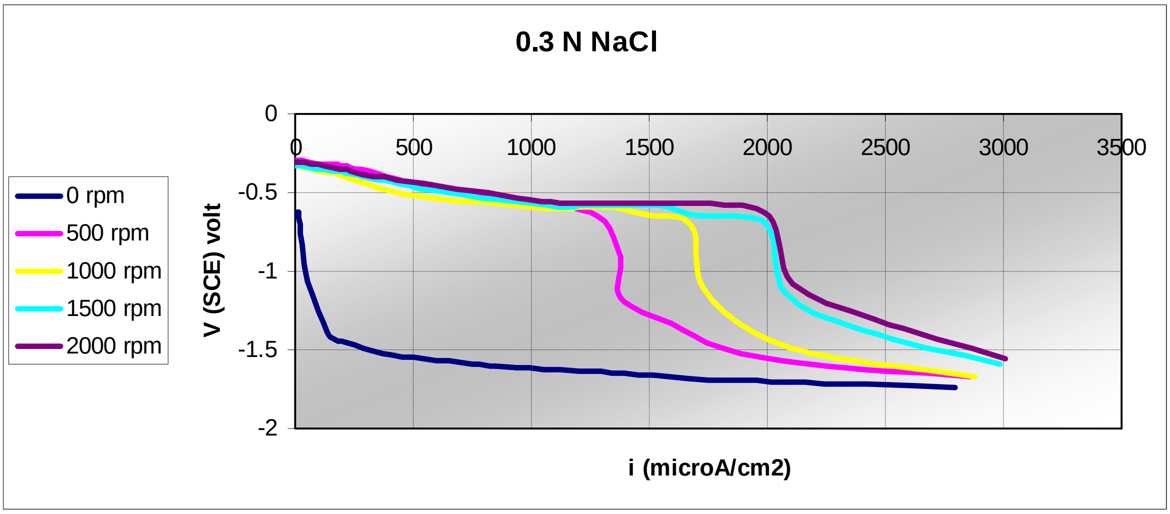

Figure 4-8 Experimental limiting current results of dissolved oxygen cathodic polarization on brass in a solution of 0.3N NaCl at 60^{0}C.

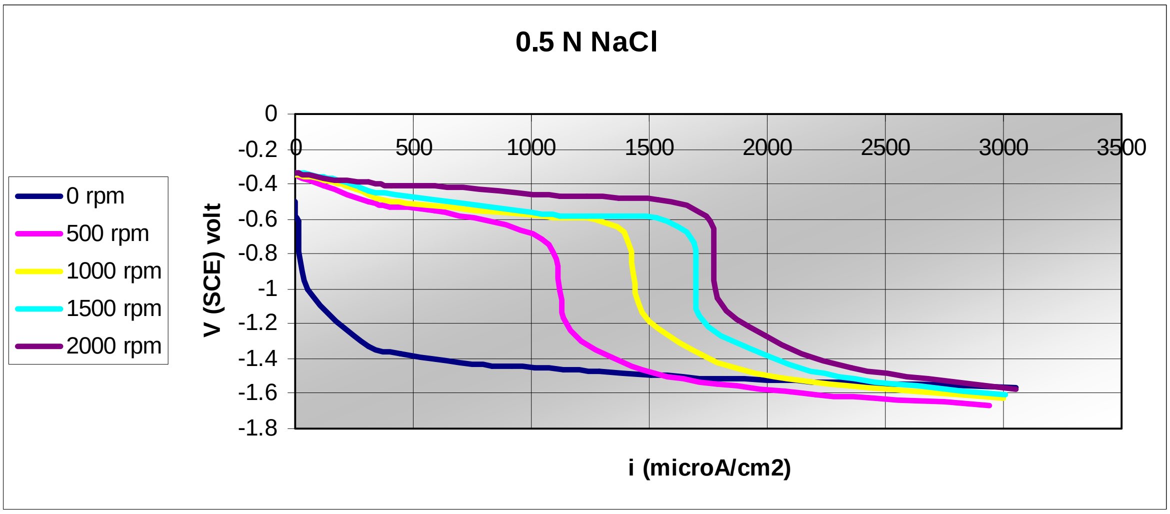

Figure 4-9 Experimental limiting current results of dissolved oxygen cathodic polarization on brass in a solution of 0.5N NaCl at 60^{0}C.

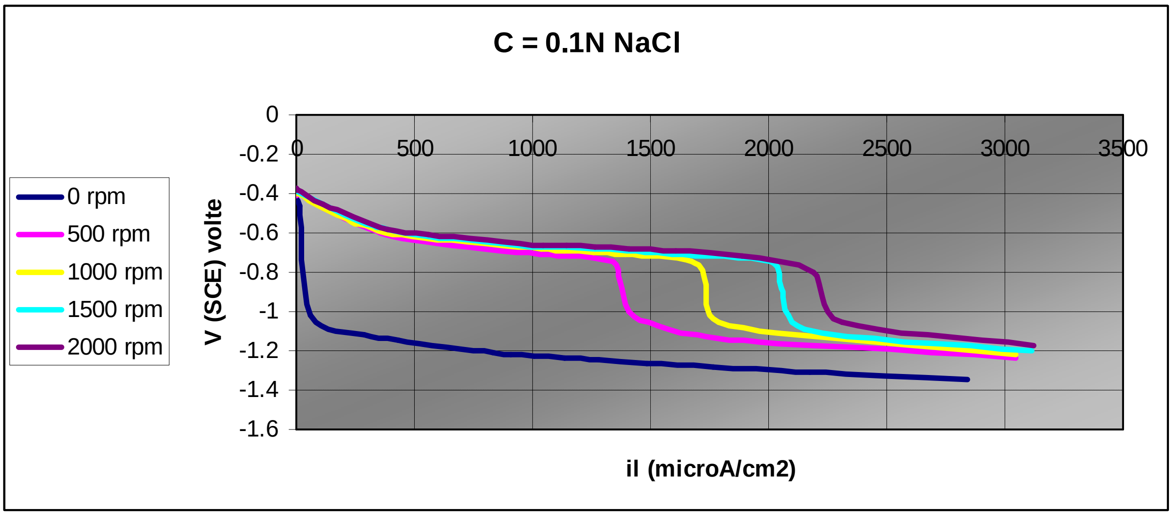

Figure 4-10 Experimental limiting current results of dissolved oxygen cathodic polarization on carbon steel in a solution of 0.1N NaCl at 40^{0}C.

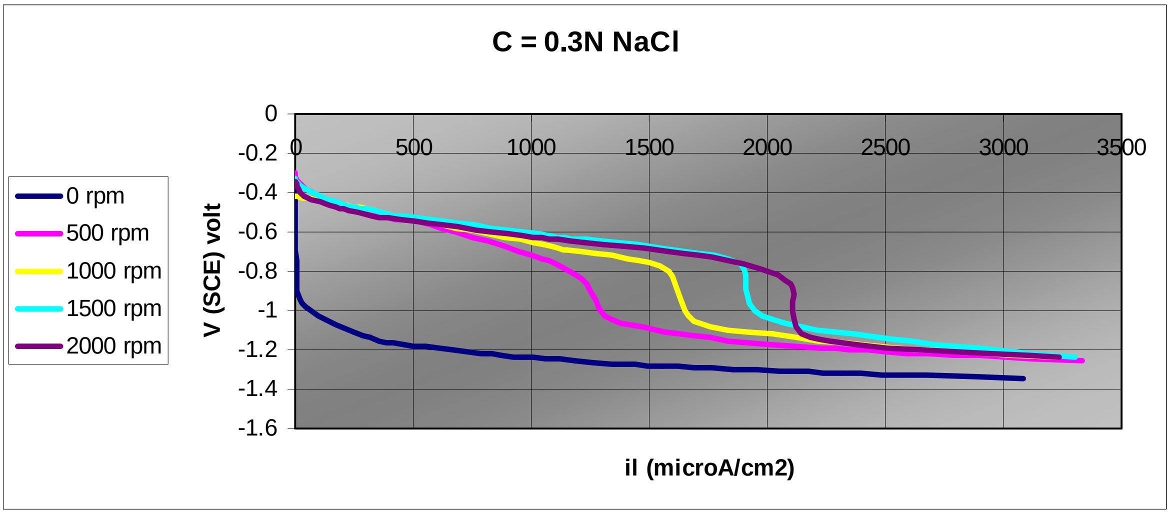

Figure 4-11 Experimental limiting current results of dissolved oxygen cathodic polarization on carbon steel in a solution of 0.3N NaCl at 40^{0}C.

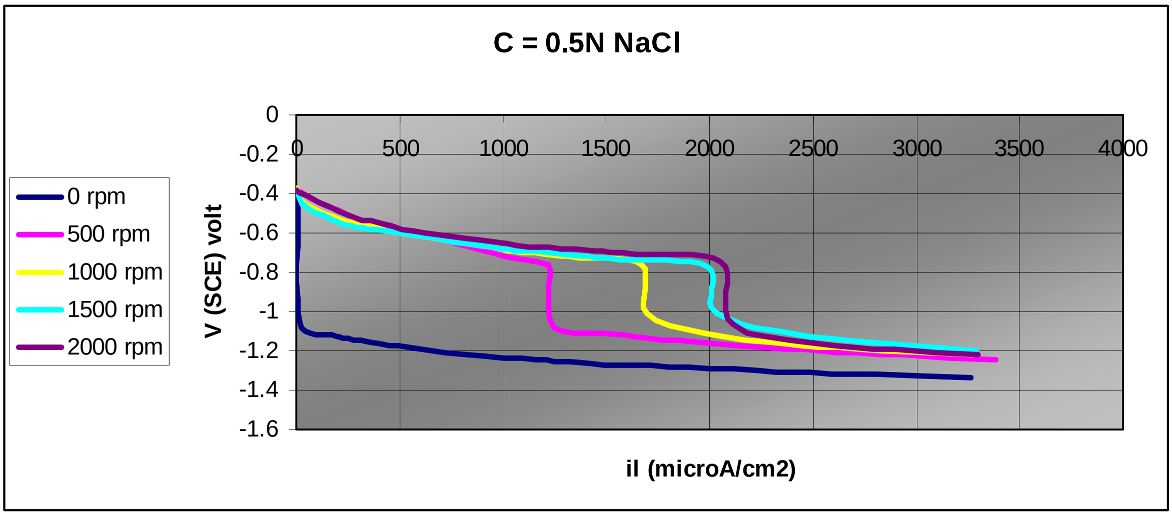

Figure 4-12 Experimental limiting current results of dissolved oxygen cathodic polarization on carbon steel in a solution of 0.5N NaCl at 40^0C.

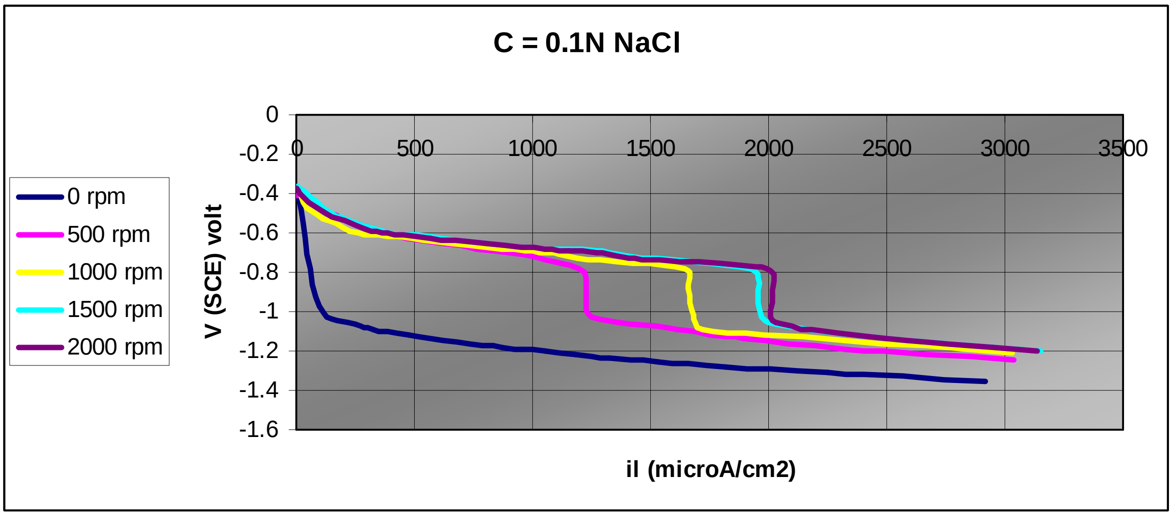

Figure 4-13 Experimental limiting current results of dissolved oxygen cathodic polarization on carbon steel in a solution of 0.1N NaCl at 50^0C.

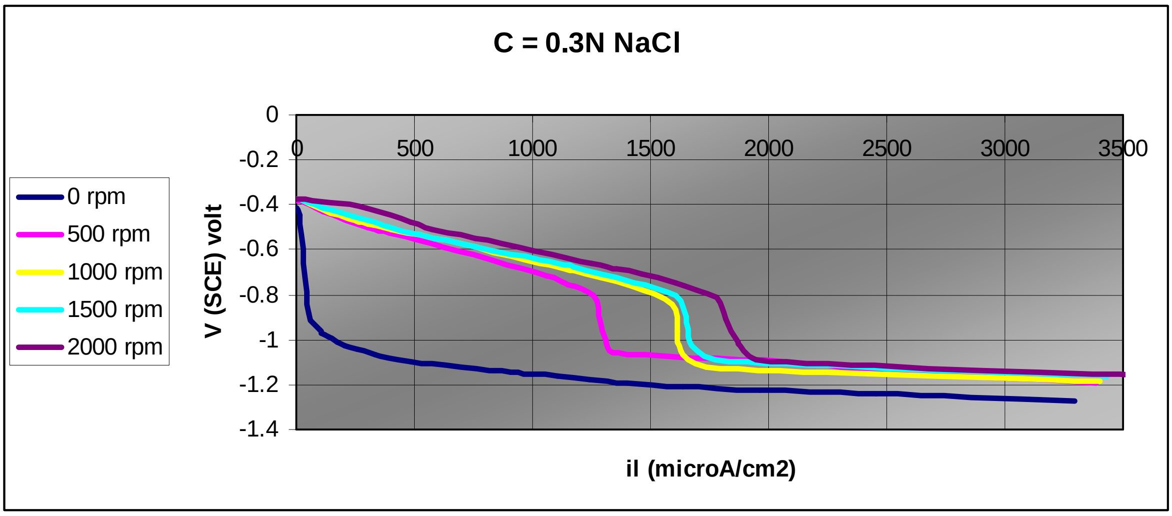

Figure 4-14 Experimental limiting current results of dissolved oxygen cathodic polarization on carbon steel in a solution of 0.3N NaCl at 50^0C.

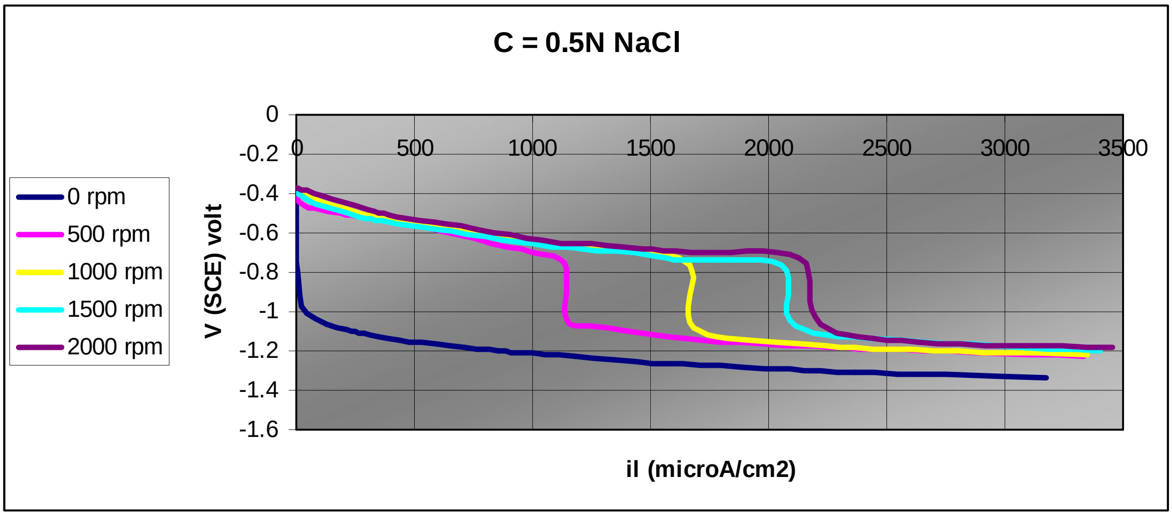

Figure 4-15 Experimental limiting current results of dissolved oxygen cathodic polarization on carbon steel in a solution of 0.5N NaCl at 50^0C.

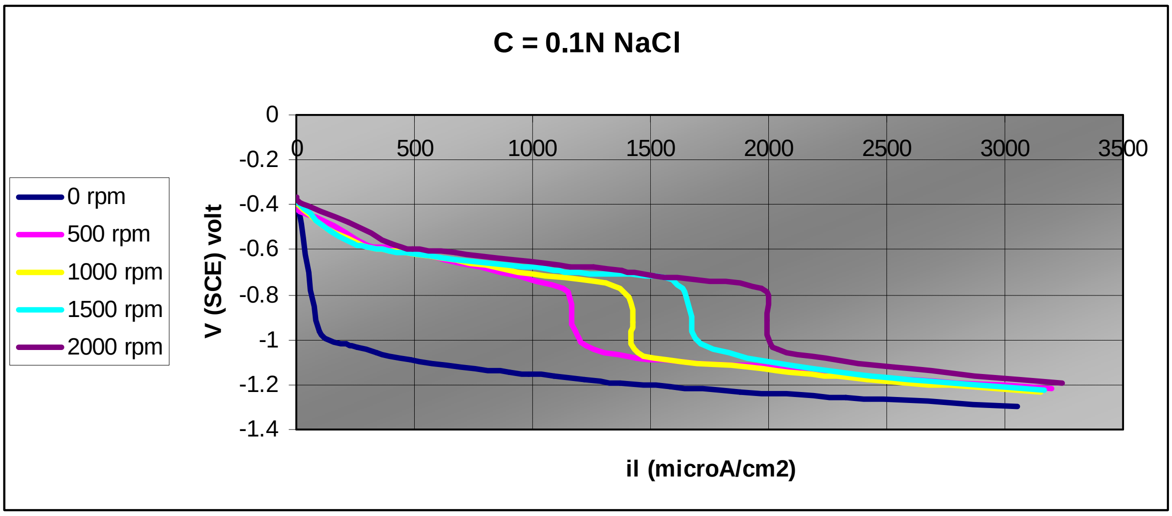

Figure 4-16 Experimental limiting current results of dissolved oxygen cathodic polarization on carbon steel in a solution of 0.1N NaCl at 60^0C.

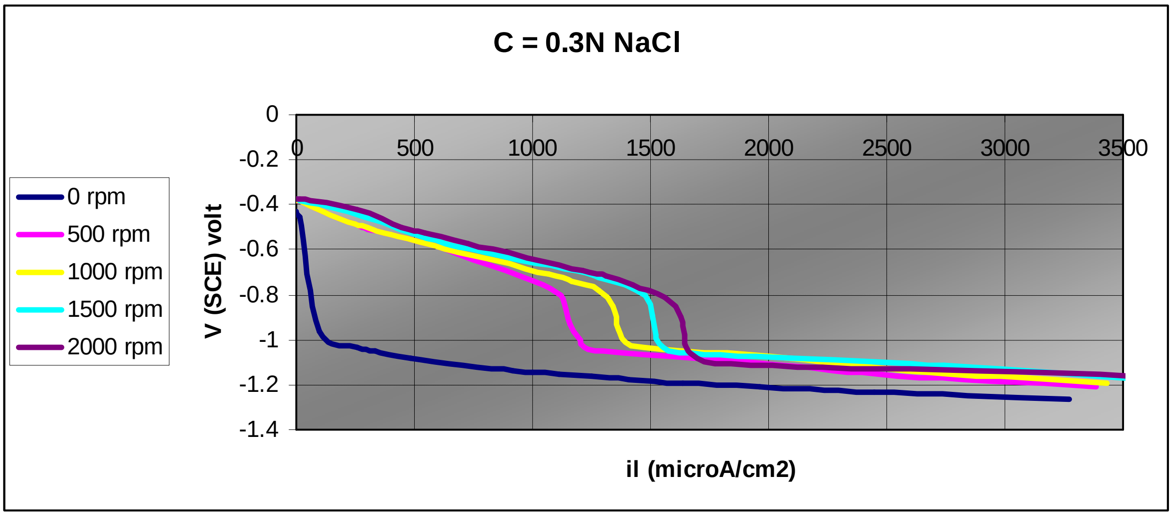

Figure 4-17 Experimental limiting current results of dissolved oxygen cathodic polarization on carbon steel in a solution of 0.3N NaCl at 60^0C.

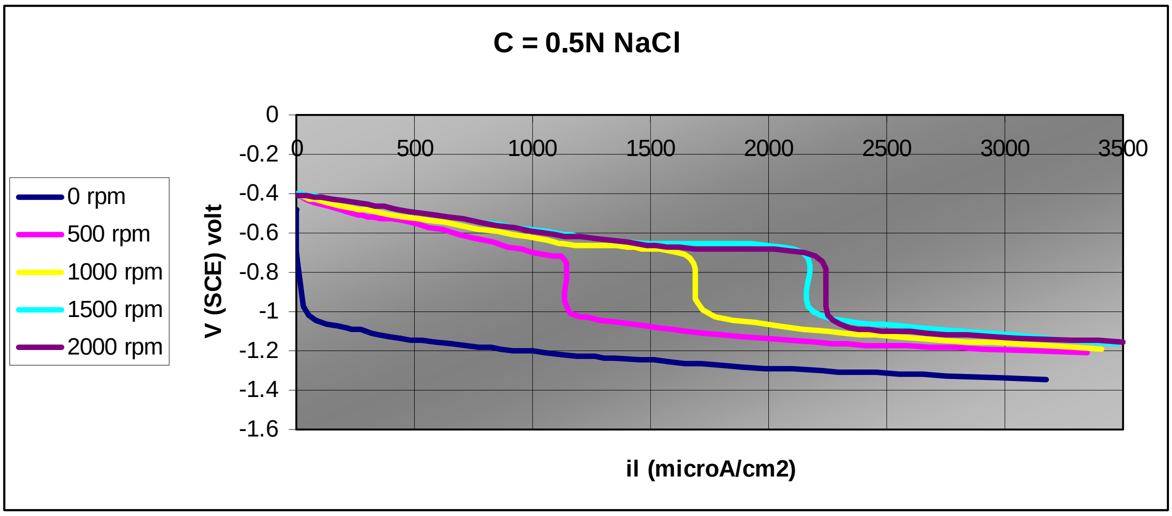

Figure 4-18 Experimental limiting current results of dissolved oxygen cathodic polarization on carbon steel in a solution of 0.5N NaCl at 60^0C.

Tables 4-1to 4-6 show the experimental results of dissolved oxygen mass transfer coefficient (k_{O2}), and oxygen limiting current (i_{O2}) on brass and carbon steel in 0.1, 0.3 and 0.5N NaCl at 40, 50 and 60^0C respectively. From these results it is evident that that increasing of rotational velocity leads to increase the mass transfer coefficient of oxygen which is dependent on the different variations of physical properties due to temperature and NaCl concentration.

Table 4-1 Experimental results on the interaction between mass transfer coefficient and shear friction velocity in 0.1 N NaCl solution on brass.

T (^{0}C)	0.1N NaCl					
	ω (rpm)	$U = \frac{pdU(rpm)}{60}$ (cm/s)	**Re**	**i_1 (A/cm^2)**	$k = i_1 / zFC_b$ **(cm/s)**	$U^* = \sqrt{\frac{kU}{Sc^{-0.67}}}$ **(cm/s)**
40^{0}C	0	0	static	1.13234E-05	0.0001	0
	500	78.5	8823.2	0.001	0.013	9.7992
	1000	157	17646	0.0013	0.0168	15.801
	1500	235.5	26469	0.0016	0.0207	21.469
	2000	314	35293	0.0019	0.0246	27.015
50^{0}C	0	0	static	4.22859E-05	0.0006	0
	500	78.5	10651	0.0013	0.0198	10.755
	1000	157	21302	0.0016	0.0244	16.873
	1500	235.5	31953	0.0019	0.029	22.52
	2000	314	42604	0.0022	0.0335	27.981
60^{0}C	0	0	static	5.73567E-05	0.0011	0
	500	78.5	12602	0.0011	0.0204	9.3021
	1000	157	25205	0.0016	0.0296	15.866
	1500	235.5	37807	0.0021	0.0389	22.262
	2000	314	50410	0.0022	0.0407	26.31

Table 4-2 Experimental results on the interaction between mass transfer coefficient and shear friction velocity in 0.3 N NaCl solution on brass.

T (^{0}C)	0.3N NaCl					
	ω (rpm)	$U=\frac{pdU(rpm)}{60}$ (cm/s)	**Re**	**i_1 (A/cm^2)**	$k=i_1/zFC_b$ **(cm/s)**	$U^*=\sqrt{\frac{kU}{Sc^{-0.67}}}$ **(cm/s)**
40^{0}C	0	0	static	1.43312E-05	0.0002	0
	500	78.5	14786	0.0011	0.015	9.2993
	1000	157	29572	0.0014	0.0191	14.836
	1500	235.5	44358	0.0017	0.0232	20.023
	2000	314	59143	0.0019	0.0259	24.443
50^{0}C	0	0	static	3.64473E-05	0.0006	0
	500	78.5	17841	0.0013	0.021	9.7781
	1000	157	35682	0.0016	0.0259	15.341
	1500	235.5	53523	0.0019	0.0308	20.475
	2000	314	71364	0.002	0.0324	24.256
60^{0}C	0	0	static	3.55626E-05	0.0008	0
	500	78.5	21118	0.0014	0.0302	9.9966
	1000	157	42236	0.0017	0.0367	15.579
	1500	235.5	63353	0.002	0.0432	20.695
	2000	314	84471	0.002	0.0432	23.896

Table 4-3 Experimental results on the interaction between mass transfer coefficient and shear friction velocity in 0.5 N NaCl solution on brass.

T (^{0}C)	0.5N NaCl					
	ω (rpm)	$U = \frac{pdU(rpm)}{60}$ (cm/s)	**Re**	**i_l (A/cm^2)**	$k = i_1 / zFC_b$ **(cm/s)**	$U^* = \sqrt{\frac{kU}{Sc^{-0.67}}}$ **(cm/s)**
40^{0}C	0	0	static	1.61005E-05	0.0002	0
	500	78.5	14908	0.0011	0.015	9.6226
	1000	157	29816	0.0014	0.0191	15.352
	1500	235.5	44724	0.0017	0.0232	20.72
	2000	314	59632	0.002	0.0273	25.95
50^{0}C	0	0	static	0.000011677	0.0002	0
	500	78.5	17987	0.0013	0.0225	10.45
	1000	157	35974	0.0017	0.0294	16.9
	1500	235.5	53962	0.002	0.0345	22.45
	2000	314	71949	0.002	0.0345	25.923
60^{0}C	0	0	static	1.12773E-05	0.0003	0
	500	78.5	21290	0.0011	0.0294	10.199
	1000	157	42581	0.0014	0.0374	16.271
	1500	235.5	63871	0.0017	0.0454	21.96
	2000	314	85162	0.0017	0.0454	25.357

Table 4-4 Experimental results on the interaction between mass transfer coefficient and shear friction velocity in 0.1 N NaCl solution on carbon steel.

T (^{0}C)	0.1N NaCl					
	ω (rpm)	$U = \frac{pdU(rpm)}{60}$ (cm/s)	**Re**	**i_l (A/cm^2)**	$k = i_l / zFC_b$ **(cm/s)**	$U^* = \sqrt{\frac{kU}{Sc^{-0.67}}}$ **(cm/s)**
40^{0}C	0	0	static	1.16773E-05	0.0002	0
	500	78.5	8823.2	0.0014	0.0181	11.595
	1000	157	17646	0.0018	0.0233	18.593
	1500	235.5	26469	0.002	0.0259	24.003
	2000	314	35293	0.0022	0.0285	29.069
50^{0}C	0	0	static	1.20311E-05	0.0002	0
	500	78.5	10651	0.0012	0.0183	10.333
	1000	157	21302	0.0017	0.0259	17.393
	1500	235.5	31953	0.002	0.0305	23.105
	2000	314	42604	0.002	0.0305	26.679
60^{0}C	0	0	static	1.20311E-05	0.0002	0
	500	78.5	12602	0.0012	0.0222	9.7157
	1000	157	25205	0.0014	0.0259	14.841
	1500	235.5	37807	0.0016	0.0296	19.431
	2000	314	50410	0.0019	0.0352	24.451

Table 4-5 Experimental results on the interaction between mass transfer coefficient and shear friction velocity in 0.3 N NaCl solution on carbon steel.

T (^{0}C)	0.3N NaCl					
	ω (rpm)	$U = \frac{pdw}{60}$ (cm/s)	**Re**	**i_l (A/cm^2)**	$k = i_l / zFC_b$ **(cm/s)**	$U^* = \sqrt{\frac{kU}{Sc^{-0.67}}}$ **(cm/s)**
40^{0}C	0	0	static	1.02619E-05	0.0001	0
	500	78.5	14786	0.0012	0.0164	9.7128
	1000	157	29572	0.0016	0.0218	15.861
	1500	235.5	44358	0.0018	0.0245	20.604
	2000	314	59143	0.0023	0.0314	26.893
50^{0}C	0	0	static	1.11465E-05	0.0002	0
	500	78.5	17841	0.0013	0.021	9.7781
	1000	157	35682	0.0017	0.0275	15.813
	1500	235.5	53523	0.0017	0.0275	19.367
	2000	314	71364	0.0017	0.0275	22.363
60^{0}C	0	0	static	1.09696E-05	0.0002	0
	500	78.5	21118	0.0012	0.0259	9.255
	1000	157	42236	0.0014	0.0302	14.137
	1500	235.5	63353	0.0015	0.0324	17.922
	2000	314	84471	0.0016	0.0345	21.374

Table 4-6 Experimental results on the interaction between mass transfer coefficient and shear friction velocity in 0.5 N NaCl solution on carbon steel.

T (^{0}C)	0.5N NaCl					
	ω (rpm)	$U = \frac{pdw}{60}$ (cm/s)	**Re**	**i_1 (A/cm^2)**	$k = i_1 / zFC_b$ **(cm//s)**	$U^* = \sqrt{\frac{kU}{Sc^{-0.67}}}$ **(cm/s)**
40^{0}C	0	0	static	1.13234E-05	0.0002	0
	500	78.5	14908	0.0012	0.0164	10.05
	1000	157	29816	0.0017	0.0232	16.917
	1500	235.5	44724	0.002	0.0273	22.474
	2000	314	59632	0.002	0.0273	25.95
50^{0}C	0	0	static	9.908E-06	0.0002	0
	500	78.5	17987	0.0012	0.0207	10.04
	1000	157	35974	0.0017	0.0294	16.9
	1500	235.5	53962	0.0021	0.0363	23.005
	2000	314	71949	0.0021	0.0363	26.564
60^{0}C	0	0	static	1.02619E-05	0.0003	0
	500	78.5	21290	0.0011	0.0294	10.199
	1000	157	42581	0.0017	0.0454	17.93
	1500	235.5	63871	0.0021	0.0561	24.407
	2000	314	85162	0.0022	0.0588	28.846

CHAPTER FIVE

DISCUSSION

5.1. Introduction

Chapter four introduced the experimental results of dissolved oxygen cathodic polarization on brass and carbon steel in NaCl solution of increasing strength. The variables involved are temperature, concentration, type of metal, and Reynolds number (or velocity as rpm). The influence of these variables on the analysis of results needs to be interpreted and discussed.

In discussing the results, the following manner is followed :- section 5.2 deals with limiting current density as regard the effect of temperature and concentration on limiting current density using brass and carbon steel, section 5.3 deals with mass transfer coefficient regarding the effect of temperature, and concentration employing the two metals individually, and section 5.4 elaborates on friction velocity and the relation between mass transfer coefficient and shear/friction velocity under the influence of temperature and concentration using the two metals separately.

Concentration of NaCl, type of metal, and Reynolds number (or velocity) are the variables in the present work that influence the analysis of results which need to be discussed and interpreted. In discussing the results, the following manner is followed :- section 5.2 deals with limiting current density and the effect of temperature, and concentration on brass(rather soft) and carbon steel(rather hard) on limiting current density, section 5.3 deals with mass transfer coefficient and the effect of temperature and concentration on these two metals, and section 5.4 deals with friction or shear velocity and its relationship with mass transfer coefficient under the effect of temperature and concentration on brass and carbon steel rotating cylinder electrode.

5.2. Limiting Current Density

5.2.1 Effect Of Temperature

I. Brass

Tables A-1 to A-9 in Appendix A are plotted in Figs. 5-1, 5-2 and 5-3 to show the effect of temperature on limiting current density as function of Reynolds No.(Re) and temperature in solutions of 0.1 N, 0.3 N, and 0.5 N NaCl (approximately sea water concentration). It can be seen that when these two variables are increased the limiting current will be increased depending on the variation of physical properties and solubility of oxygen with temperature and NaCl concentration. Increasing temperature leads to change two variables that act in a conflicting way. Firstly, increasing temperature accelerates the reaction rate as dictated by Arrhenius equation. Moreover, diffusion rate of dissolved oxygen is increased by increasing the molecular diffusion coefficient. Secondly, as the temperature increases the oxygen solubility decreases [14, 16 and 66]. Typical examples of the magnitude of this change have been given by Conway et al. [70] who found that for nickel the exchange current increased from approximately 10^{-2} A/m^2 to 1.0 A/m^2 when the temperature changed from 10 to 75 ^{0}C.

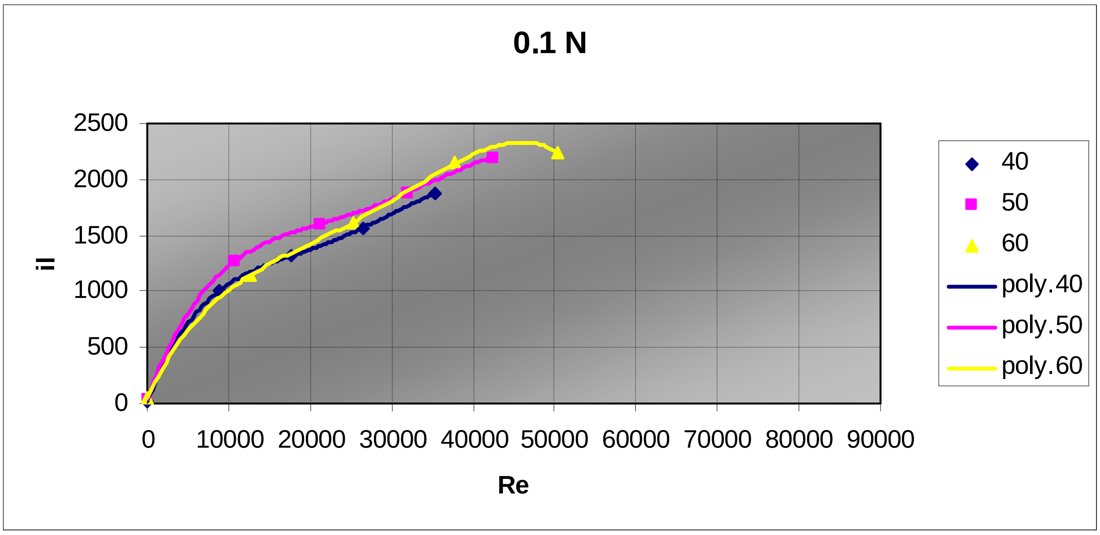

Figure 5-1 Effect of temperature and Re on limiting current of oxygen using brass in 0.1 N NaCl .

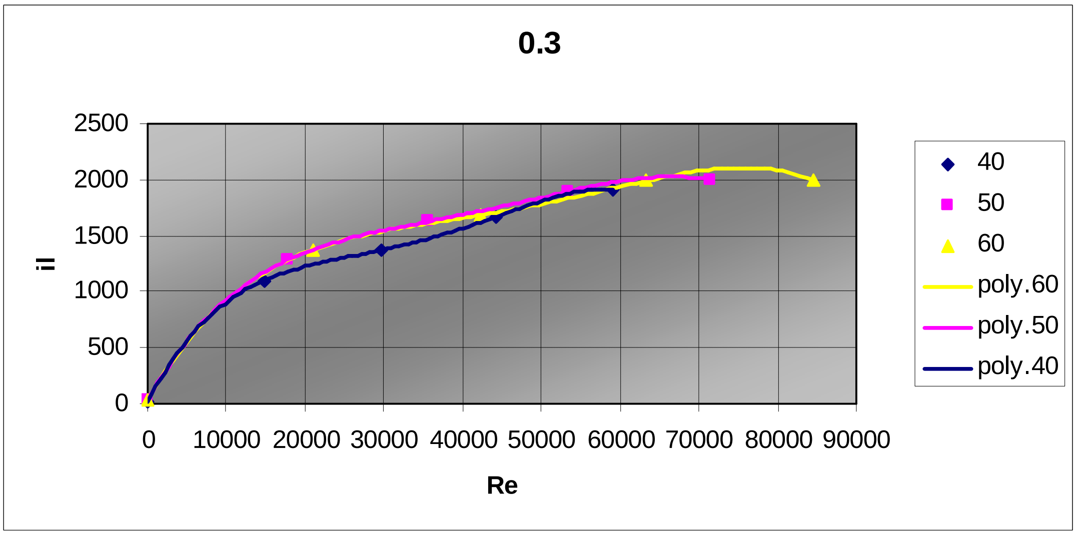

Figure 5-2 Effect of temperature and Re on limiting current of oxygen using brass in 0.3 N NaCl .

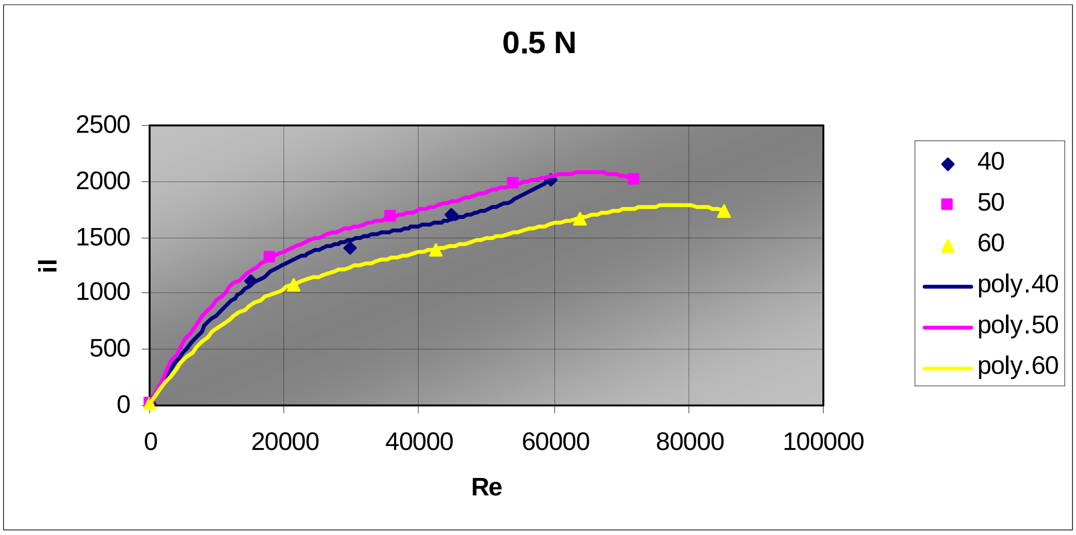

Figure 5-3 Effect of temperature and Re on limiting current of oxygen using brass in 0.5 N NaCl .

II. Carbon Steel

The results of tables A-10 to A-18 are drawn in Figs. 5-4, 5-5 and 5-6 displaying the effect of temperature and Reynolds No. on limiting current. It increases with both variables in NaCl concentration of increasing normality. Carbon steel is a hard metal and very prone to corrosion leading to some hydrogen evolution, and to less extent on brass, in addition to dissolved oxygen cathodic reduction.

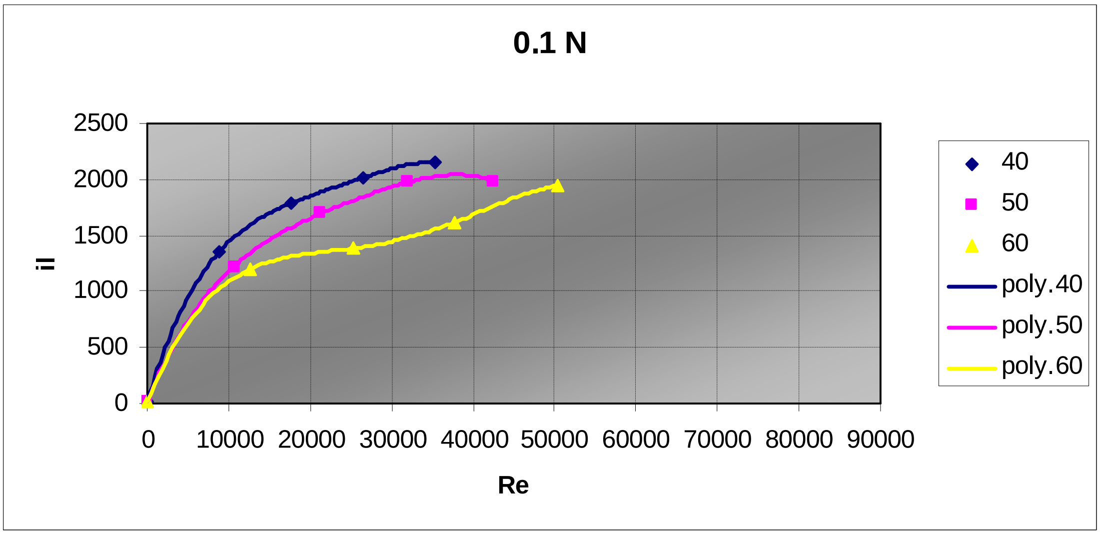

Figure 5-4 Effect of temperature and Re on limiting current of oxygen cathodic reduction on carbon steel in 0.1 N NaCl .

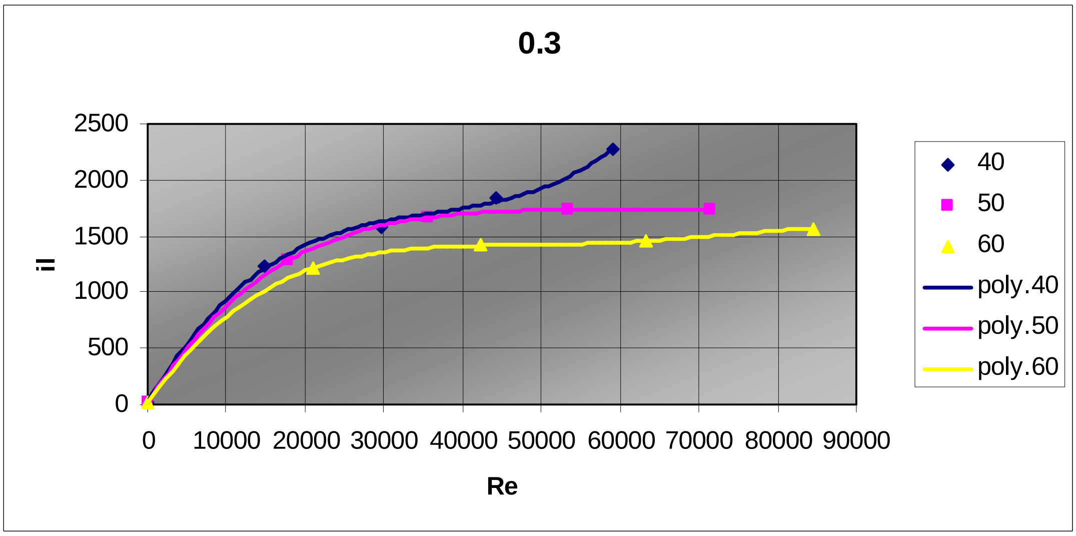

Figure 5-5 Effect of temperature and Re on limiting current of oxygen cathodic reduction on carbon steel in 0.3 N NaCl .

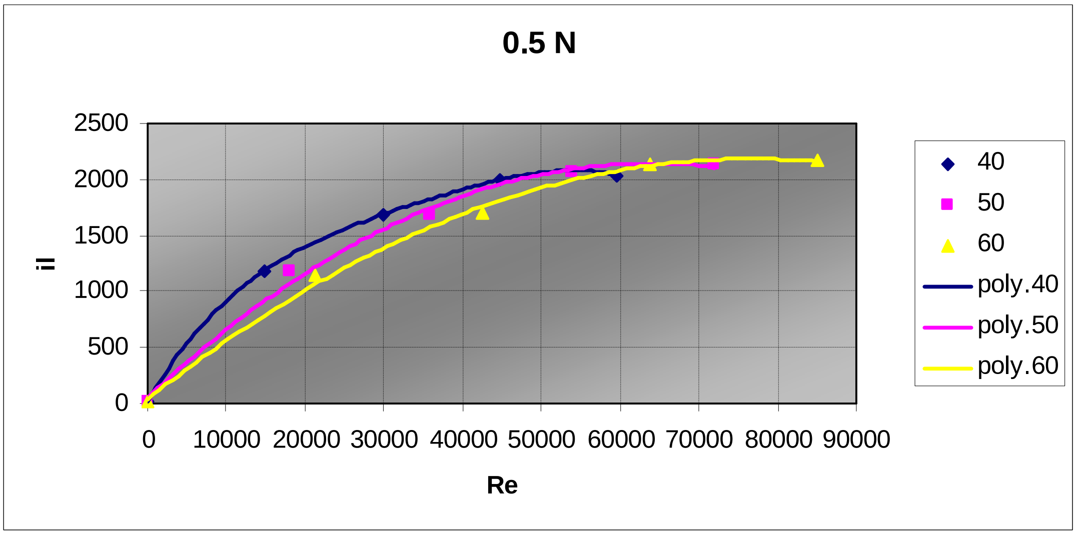

Figure 5-6 Effect of temperature and Re on limiting current of oxygen cathodic reduction on carbon steel in 0.5 N NaCl .

5.2.2. Effect of NaCl concentration

I. Brass and carbon steel

Figures 5-7 to 5-12 demonstrate the effect of concentration change on limiting current on both metals. Generally it increases with Reynolds No. (rpm) with increasing concentration of NaCl salt at all temperatures. The variations noted are as before due to the change in dissolved oxygen concentration and the physical properties with increased temperature and elevated strength of NaCl solutions. It is noticed that the temperature and the salt concentration affect dissolved O_2 concentration and physical properties to different extents as seen next in Appendix B[10, 13, 14].

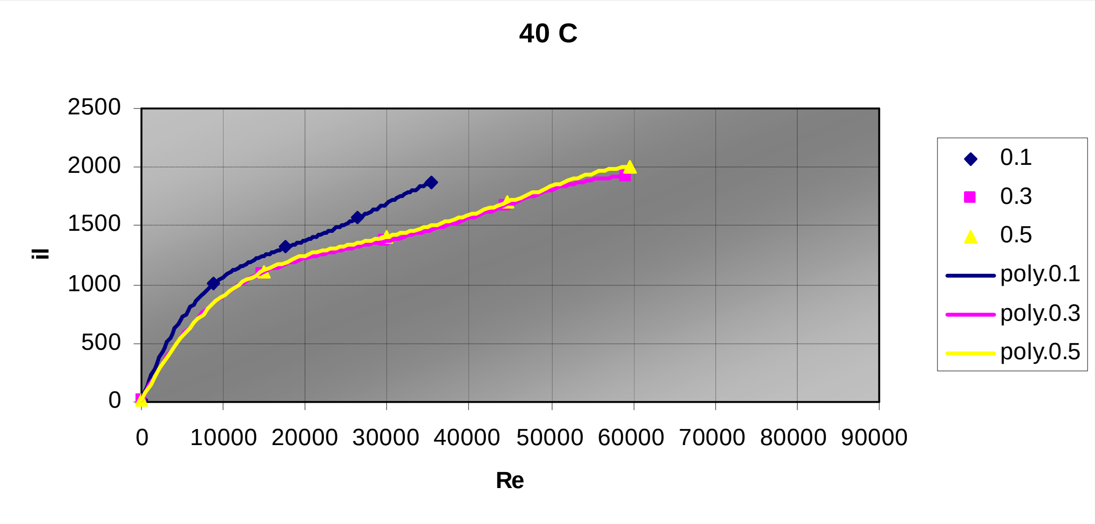

Figure 5-7 Effect of NaCl concentration on O_2 limiting current on brass at 40^0C**.**

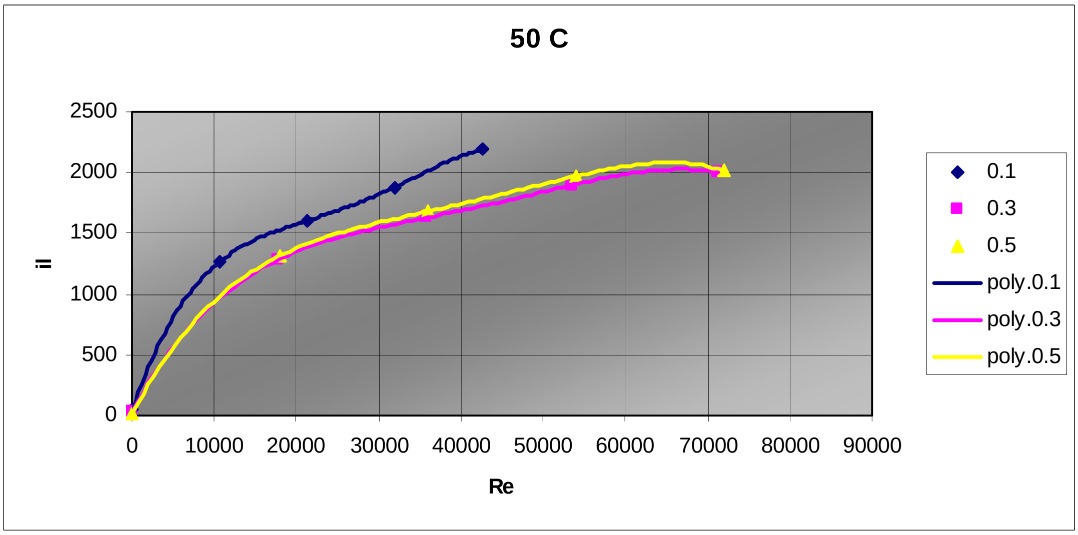

Figure 5-8 Effect of NaCl concentration on O_2 limiting current on brass at 50^0C.

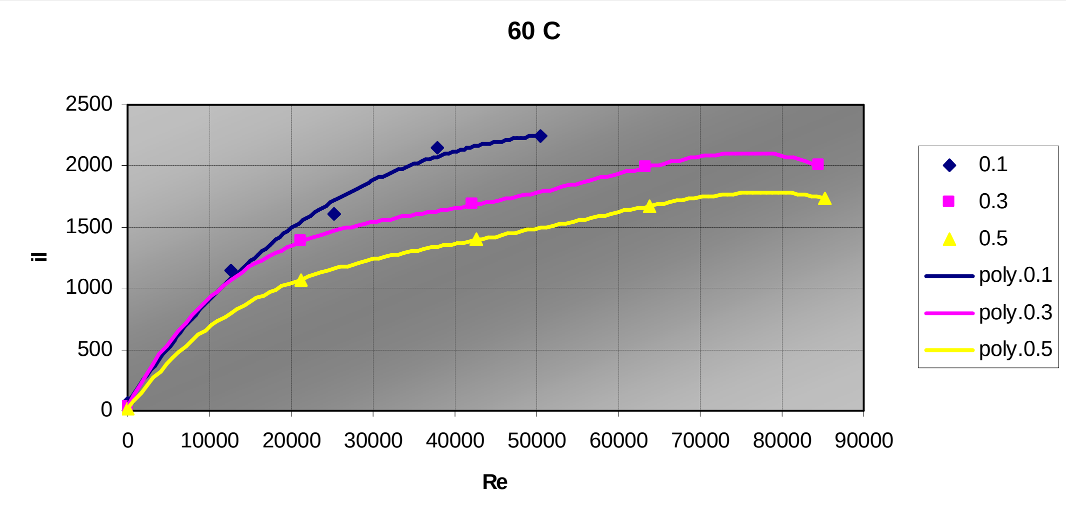

Figure 5-8 Effect of NaCl concentration on O_2 limiting current on brass at 60^0C.

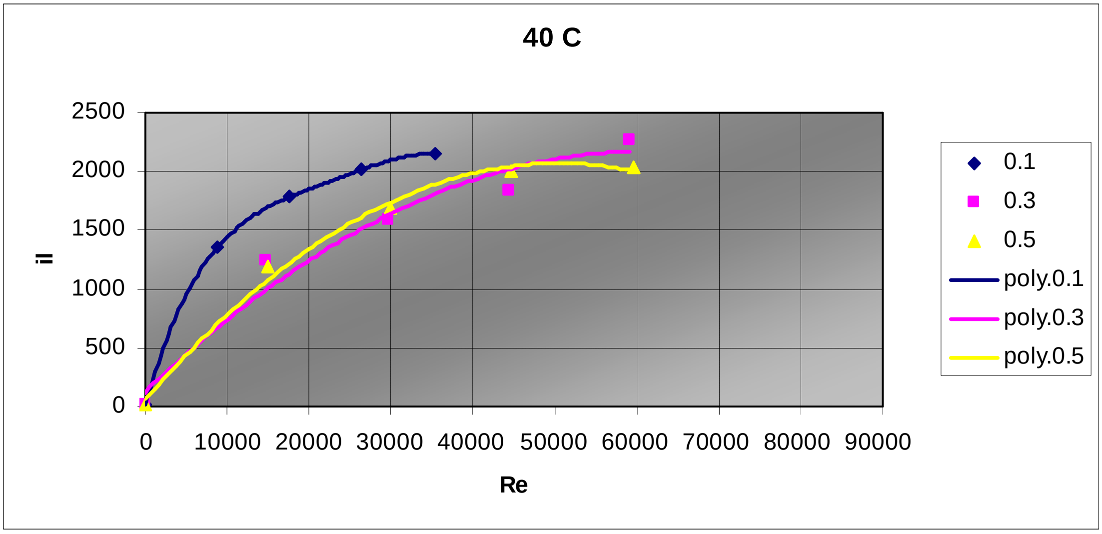

Figure 5-10 Effect of NaCl concentration on O_2 limiting current on carbon steel at 40^oC.

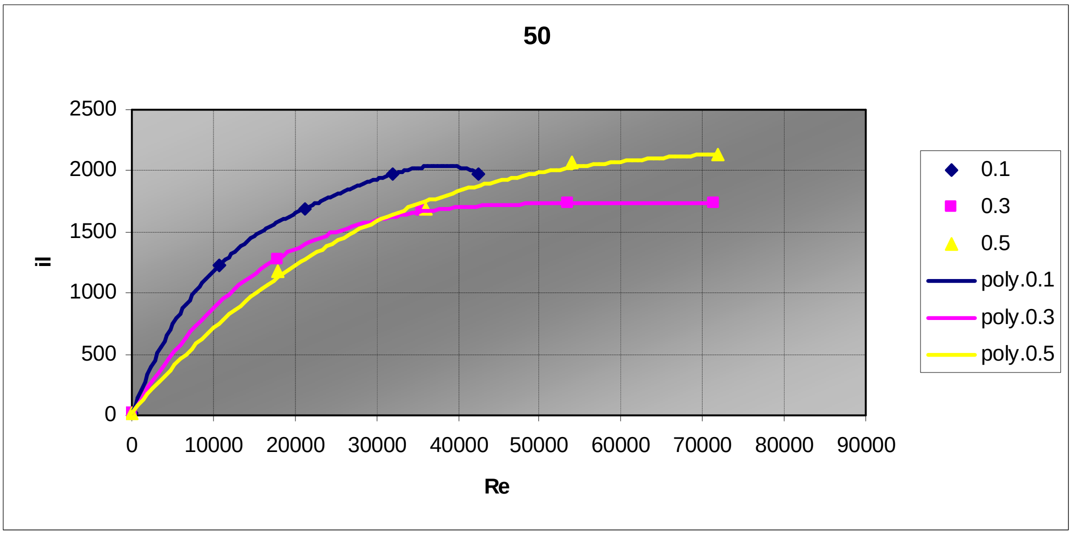

Figure 5-11 Effect of NaCl concentration on O_2 limiting current on carbon steel at 50°C.

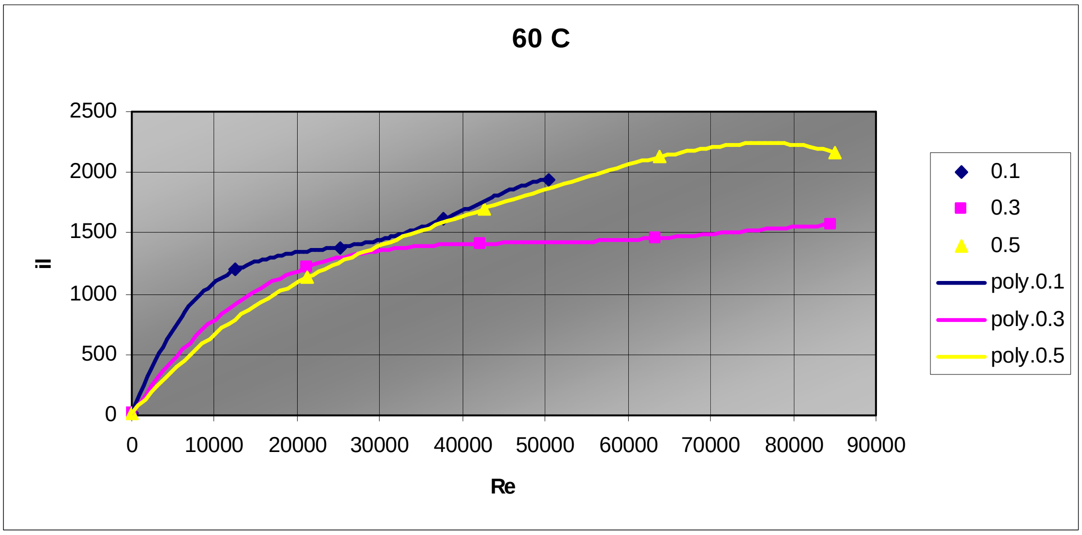

Figure 5-12 Effect of NaCl concentration on O_2 limiting current on carbon steel at 60°C.

5.2.3. Effect Of metal

The mass-transfer controlled limiting currents which are obtained on brass and carbon steel acting as cathodes are nearly similar. It is to be appreciated that the type of metal and surface texture can not be reproduced really similar, i.e., having exactly the same surface characteristics and area, in addition to their different responses as materials to temperature increase. This variation is reflected on the experimentally recorded limiting currents whether on the same metal or the two metals separately. It is also to be stated that the equilibrium potential of hydrogen at pH=7 is -0.654(SCE) and the corrosion potential of brass is less negative than that of carbon steel (see chapter 4). For this reason the limiting current on brass starts at about -0.60 V and that of carbon steel at around -0.80 V. See Figs.4.1 to 4.18 of chapter 4. Such influences of metal type and metal surface texture are presented in Figs. 5.13 to 5.21 as explained above showing no general trend as they are within experimental errors.

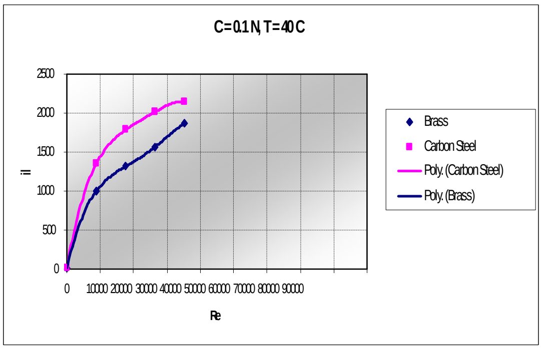

Figure 5-13 Effect of metal type and texture on i_l at $T = 40^0C$, $C_{NaCl} = 0.1$ N NaCl

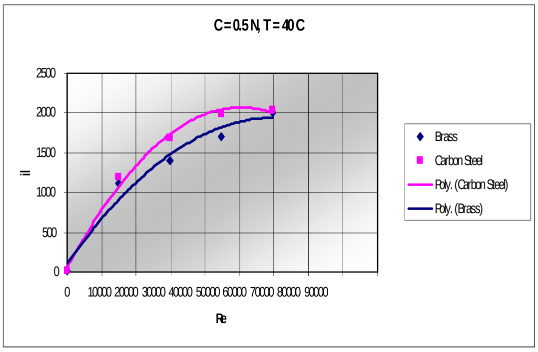

Figure 5-15 Effect of metal type and texture on i_l at $T = 40^0C$, $C_{NaCl} = 0.5$ N NaCl

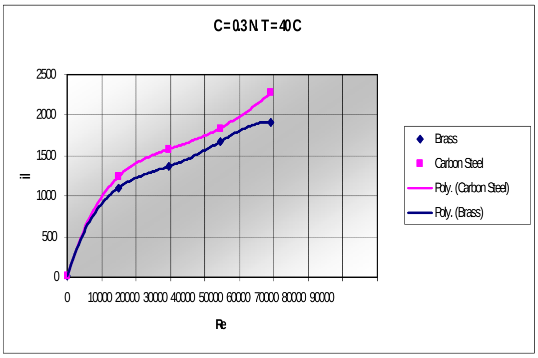

Figure 5-14 Effect of metal type and texture on i_l at $T = 40^0C$, $C_{NaCl} = 0.3$ N NaCl

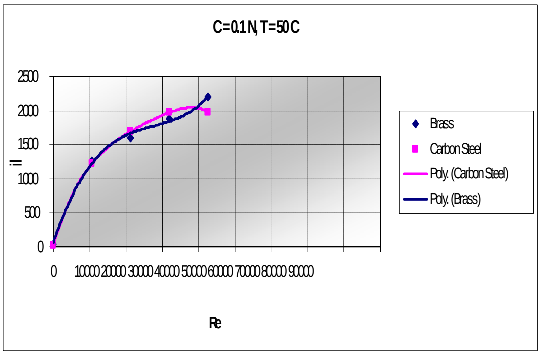

Figure 5-16 Effect of metal type and texture on i_l at $T = 50^0C$, $C_{NaCl} = 0.1$ N NaCl

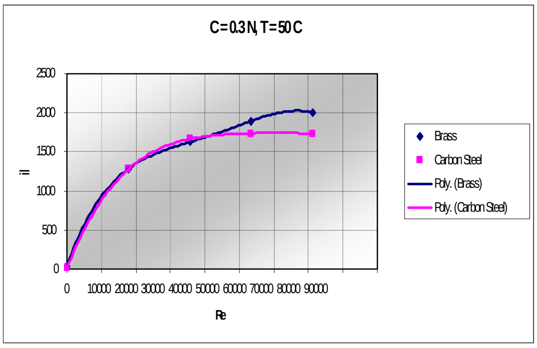

Figure 5-17 Effect of metal type and texture on i_l at T = 50^0C, C_{NaCl} = 0.3 N NaCl

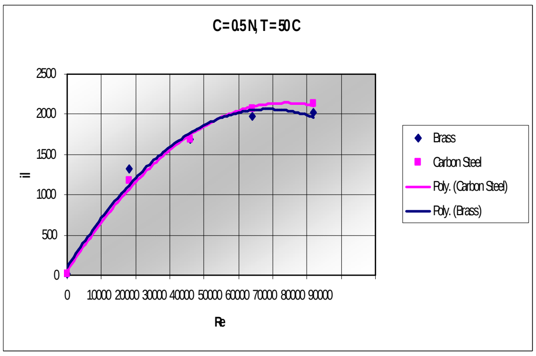

Figure 5-18 Effect of metal type and texture on i_l at T = 50^0C, C_{NaCl} = 0.5 N NaCl

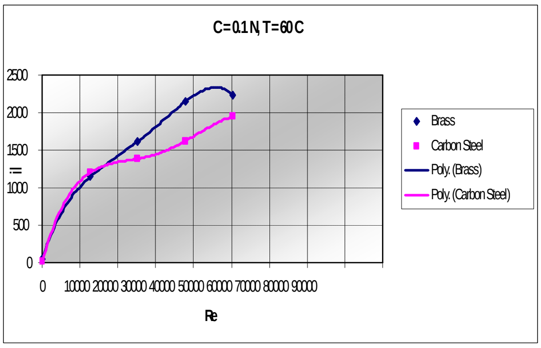

Figure 5-19 Effect of metal type and texture on i_l at T = 60^0C, C_{NaCl} = 0.1 N NaCl

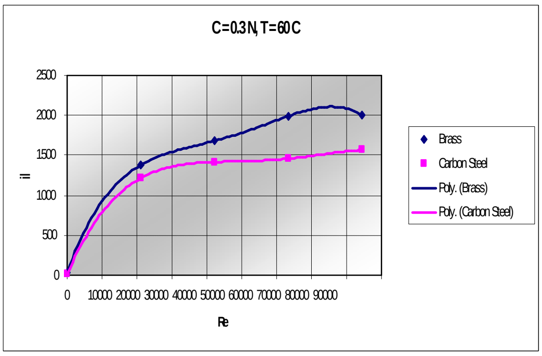

Figure 5-20 Effect of metal type and texture on i_l at T = 60^0C, C_{NaCl} = 0.3 N NaCl

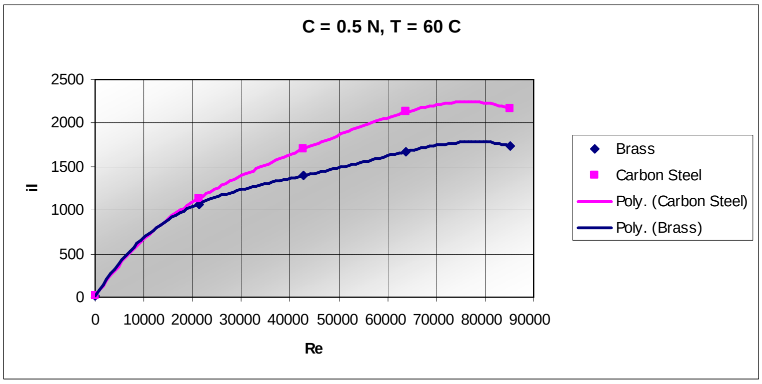

Figure 5-21 Effect of metal type and texture on i_l at T = 60^0C, C_{NaCl} = 0.5 N NaCl

5.3. Mass Transfer Coefficient

5.3.1. Brass

I. Effect of temperature

The results of tables 4-1, 4-2 and 4-3 are plotted in figs. 5-22, 5-23 and 5-24 to show the effect of temperature on mass transfer coefficient as function of friction velocity. It increases with increasing temperature at all concentrations. Although dissolved oxygen decreases with increasing temperature and NaCl concentration as compared with lower temperatures and lower NaCl concentrations used in the present work, this is most likely due to the changing of the physical properties to different extents as pointed above.

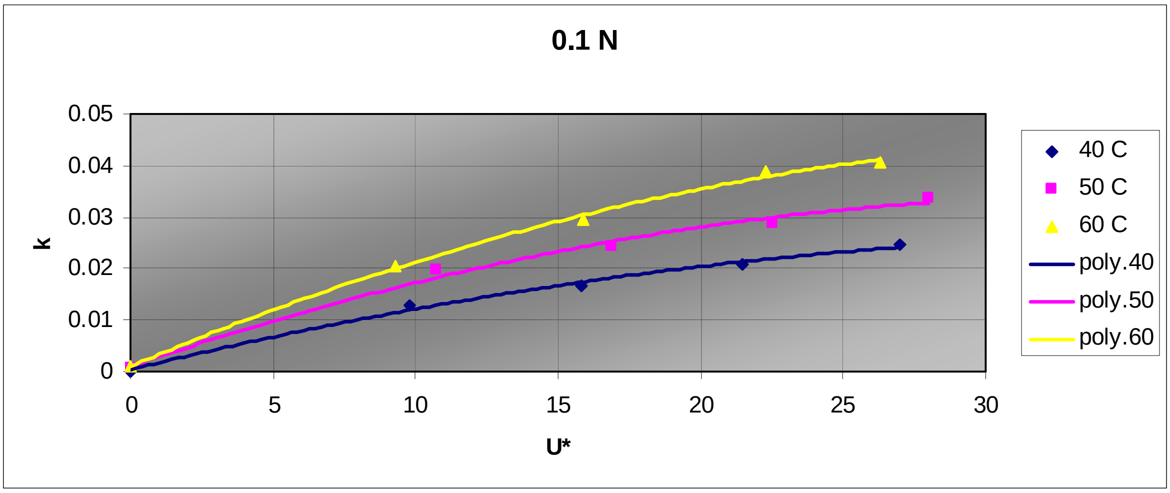

Figure 5-22 Effect of temperature on k in 0.1 N NaCl solution on brass.

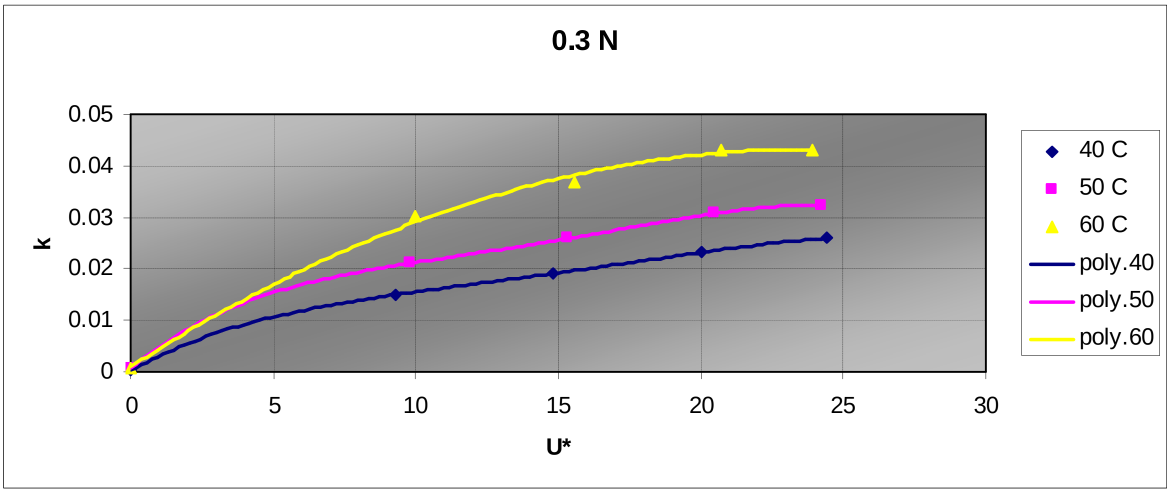

Figure 5-23 Effect of temperature on k in 0.3 N NaCl solution on brass.

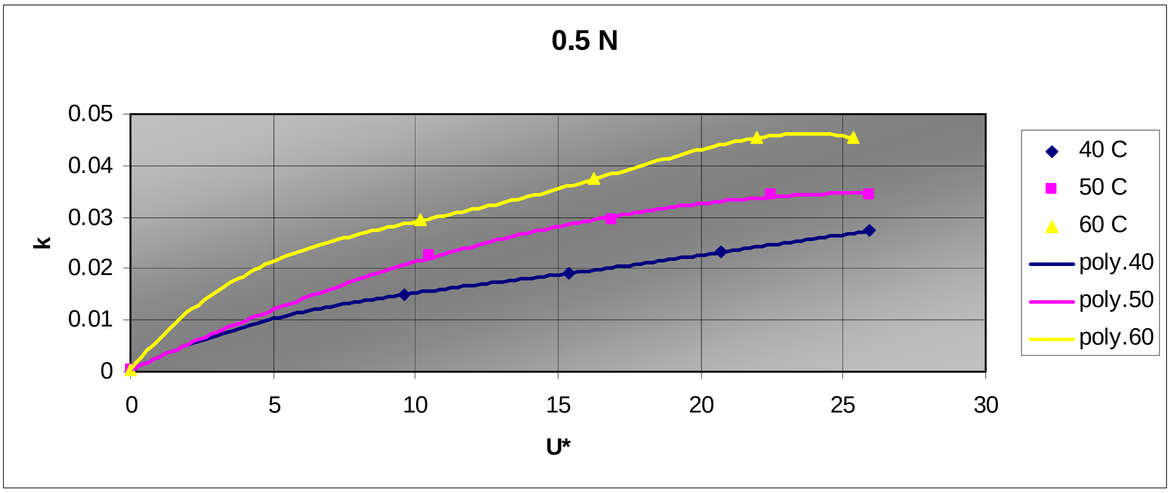

Figure 5-24 Effect of temperature on k in 0.5 N NaCl solution on brass.

II. Effect of NaCl concentration

Figures 5-25, 5-26 and 5-27 display the effect of NaCl concentration on mass transfer coefficient which is less pronounced as compared with temperature. Also it is less influenced at 40^0C. On the other hand at T > 40^0C mass transfer coefficient will increase with increasing concentration of NaCl for the same reasons explained above. In addition to the fact that the physical properties may have a role more effective than dissolved O_2. Also, it is to be noted that the friction velocity depends on shear stress and solution density. See equations (2-22 & 5-1 to 5-4 in page 102).

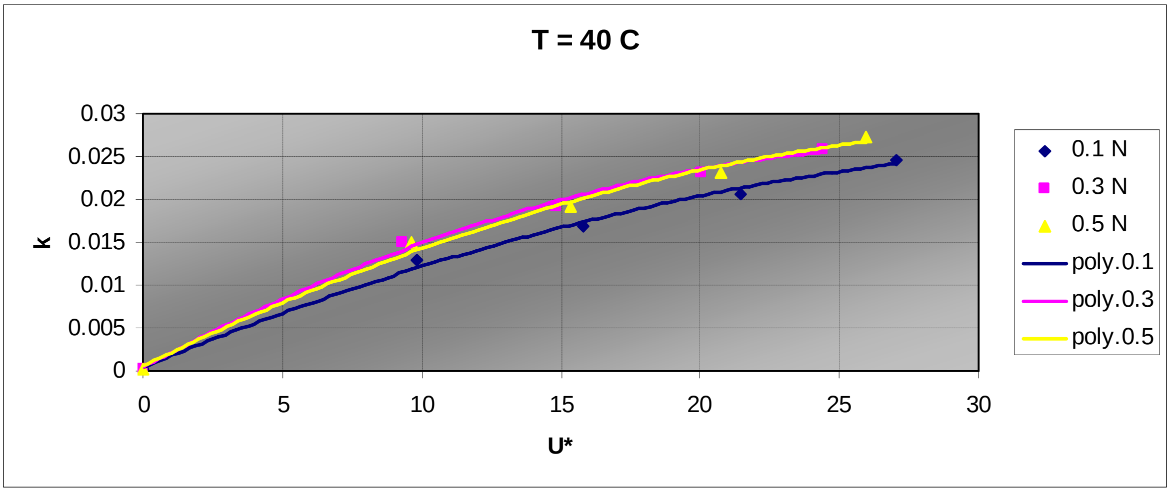

Figure 5-25 Effect of NaCl concentration on k at T = 40^0C on brass.

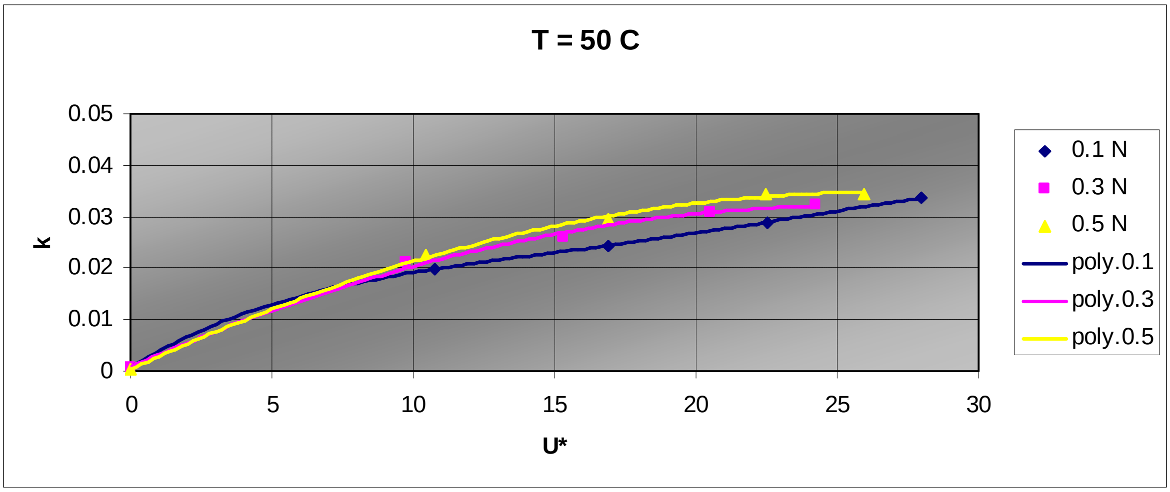

Figure 5-26 Effect of NaCl concentration on k at T = 50^0C on brass.

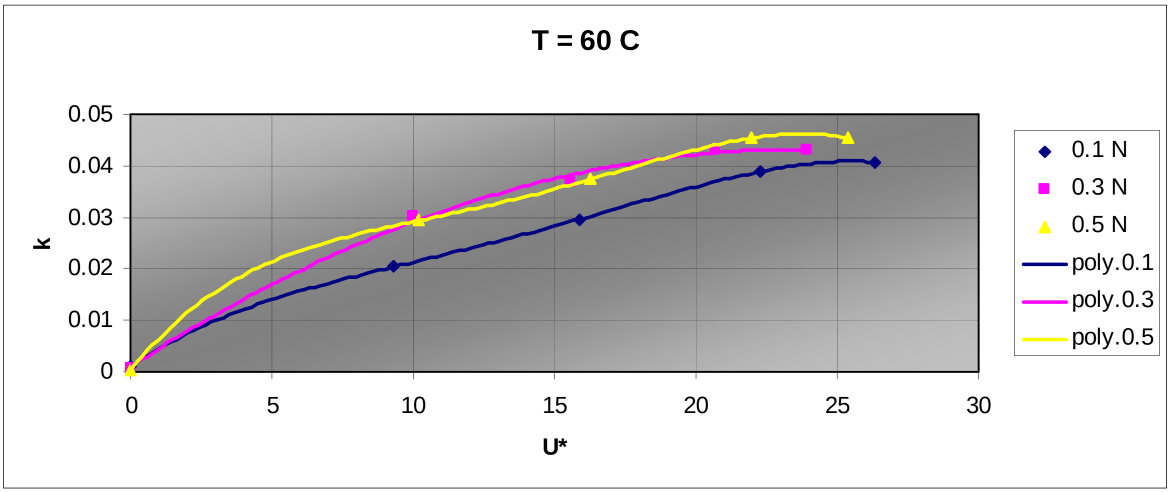

Figure 5-27 Effect of NaCl concentration on k at T = 60^{0}C on brass.

5.3.2.Carbon Steel

I. Effect of temrerature

The results of tables 4-22, 4-23 and 4-24 are drawn in figs. 5-28, 5-29 and 5-30 to show the effect of temperature on mass transfer coefficient which also increases with increasing temperature as function of shear velocity. It will be increased further in 0.5 N NaCl (~sea water) when temperature was increased in spite of less dissolved oxygen revealing the importance of physical properties changes with increasing temperature.

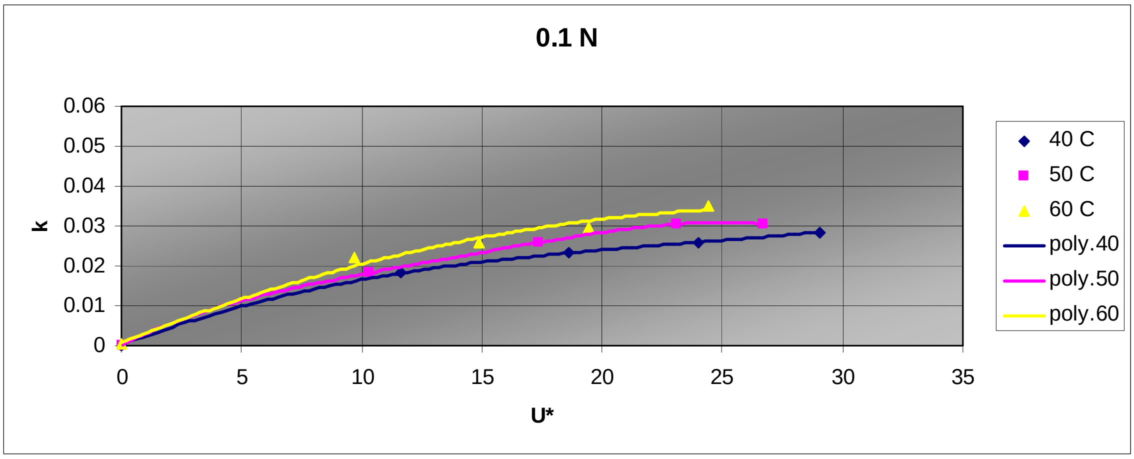

Figure 5-28 Effect of temperature on k in C_{NaCl} = 0.1 N solution on Carbon Steel .

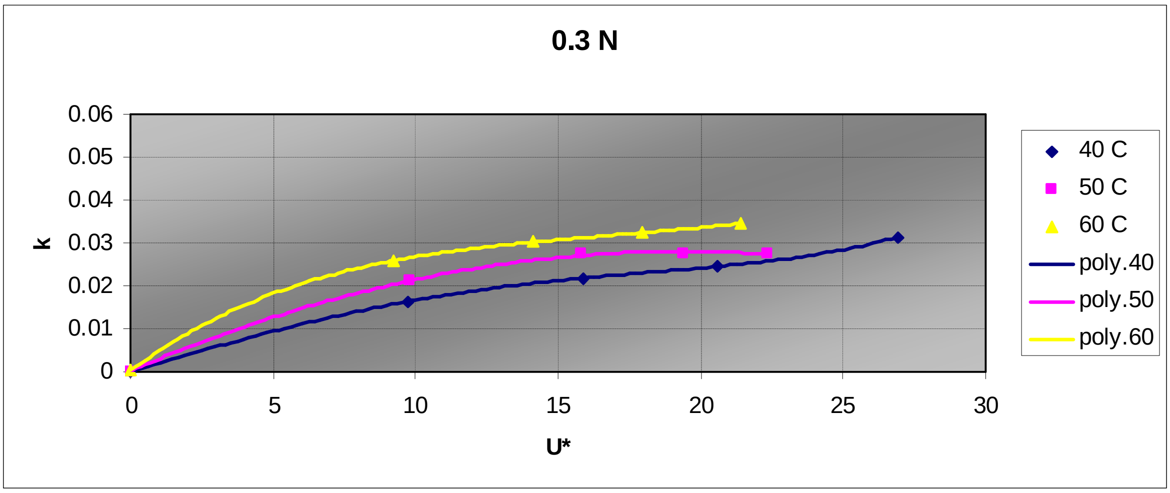

Figure 5-29 Effect of temperature on k in C_{NaCl} = 0.3 Nsolution on Carbon Steel.

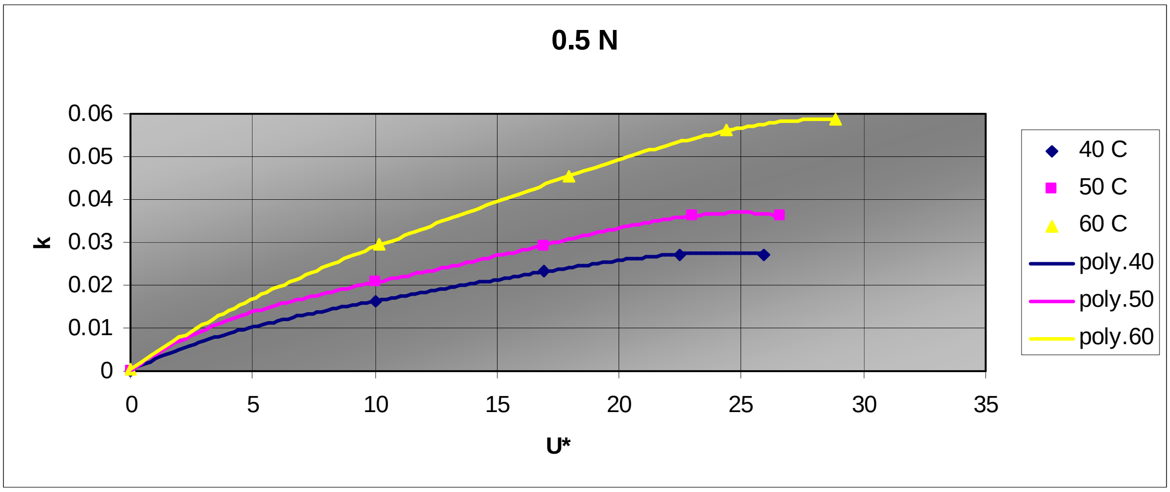

Figure 5-30 Effect of temperature on k in C_{NaCl} = 0.5 Nsolution on Carbon Steel.

II. Effect of concentration

The results of tables 4-22, 4-23 and 4-24 are drawn in Figs. 5-31, 5-32 and 5-33 to show the effect of concentration (also more pronounced in 0.5N solution at 60^0C) on mass transfer coefficient which is of similar behavior to using brass as cathode.

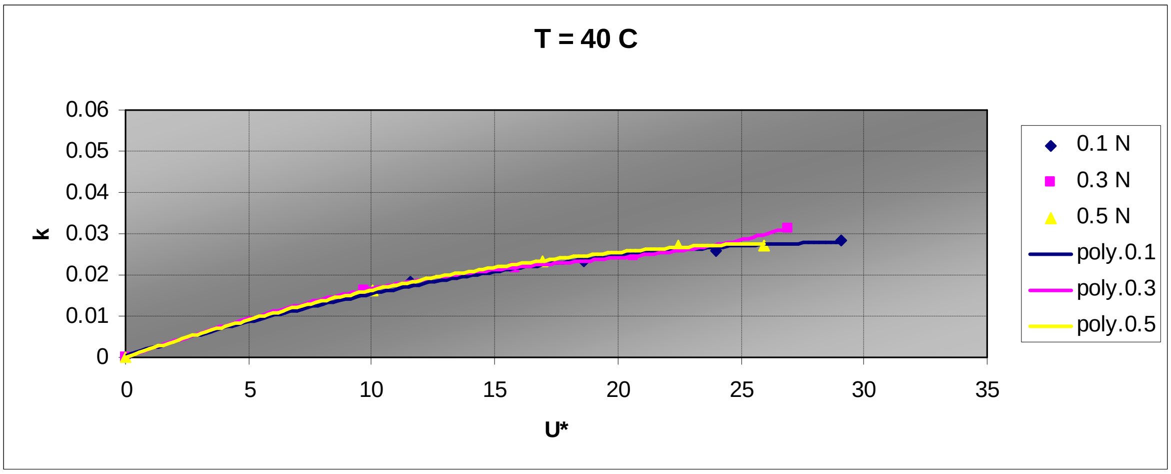

Figure 5-31 Effect of concentration on k at T = 40^0Con Carbon Steel.

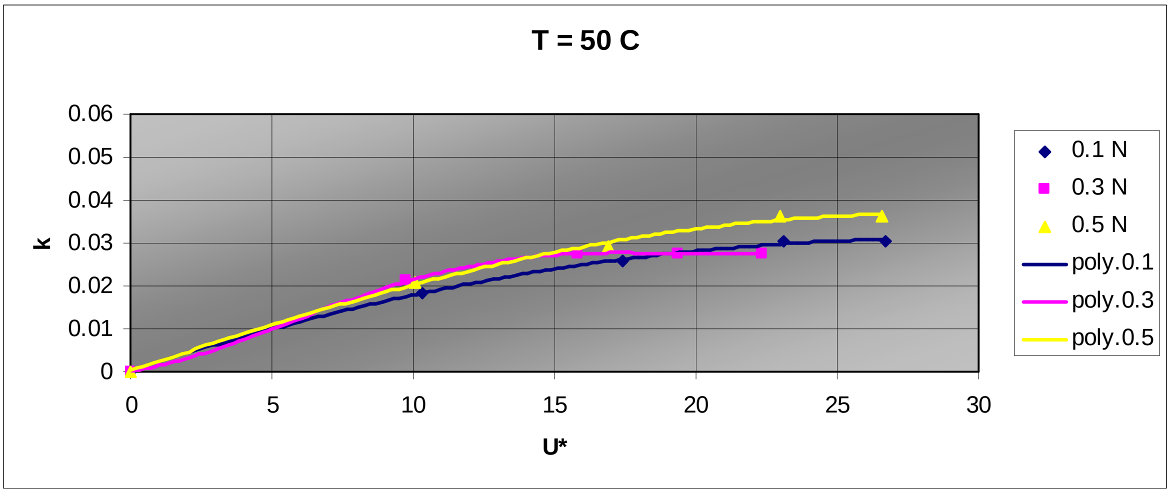

Figure 5-32 Effect of concentration on k at T = 50 °Con Carbon Steel.

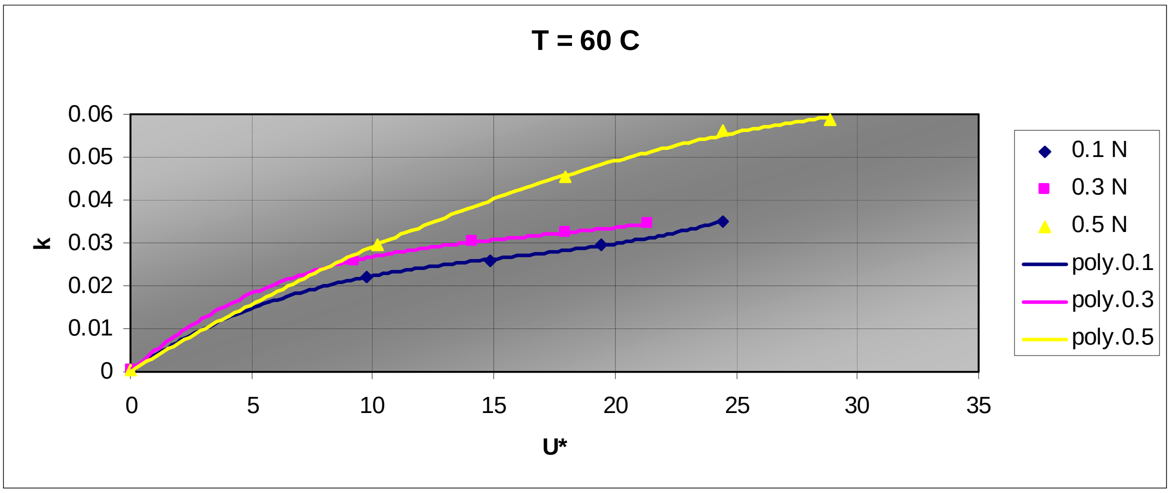

Figure 5-33 Effect of concentration on k at T = 60 °C on Carbon Steel.

5.3.3Effect of metal

The present electrochemical system is mass transfer controlled which is influenced only by metal surface area and texture as explained in section 5.2.3 above. These findings are presented in Figs. 5.34 to 5.42 for brass & carbon steel.

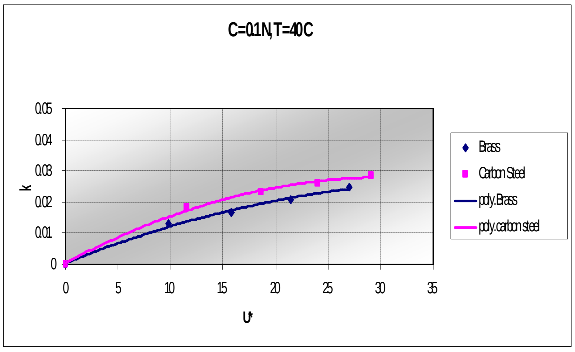

Figure 5-34 Effect of metal on i_l at T = 40^0C in a solution of C_{NaCl} = 0.1 N NaCl

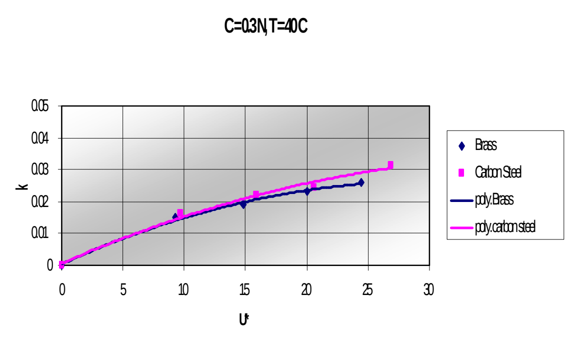

Figure 5-35 Effect of matel on i_l at T = 40 ^{o} C, C_{NaCl} = 0.3 N NaCl

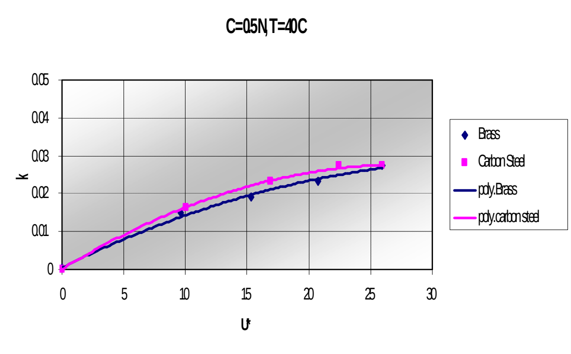

Figure 5-36 Effect of matel on i_l at T = 40 ^{o} C, C_{NaCl} = 0.5 N NaCl

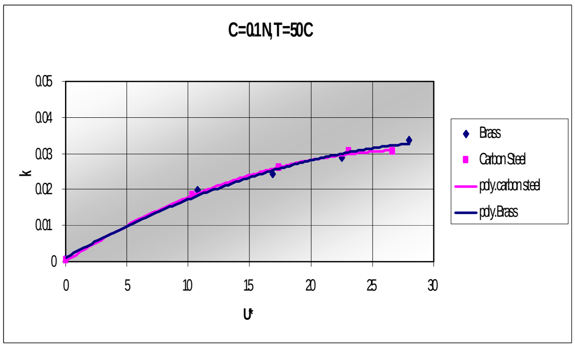

Figure 5-37 Effect of matel on i_l at T = 50 ^{o} C, C_{NaCl} = 0.1 N NaCl

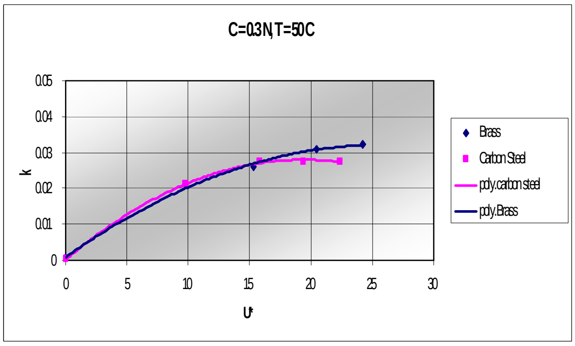

Figure 5-38 Effect of matel on i_l at T = 50 ^{o} C, C_{NaCl} = 0.3 N NaCl

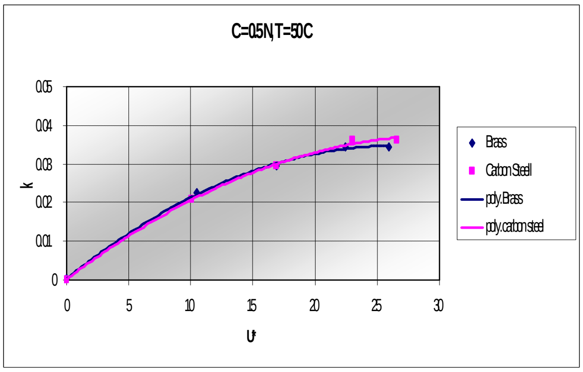

Figure 5-39 Effect of matel on i_l at T = 50 ^{o} C, C_{NaCl} = 0.5 N NaCl

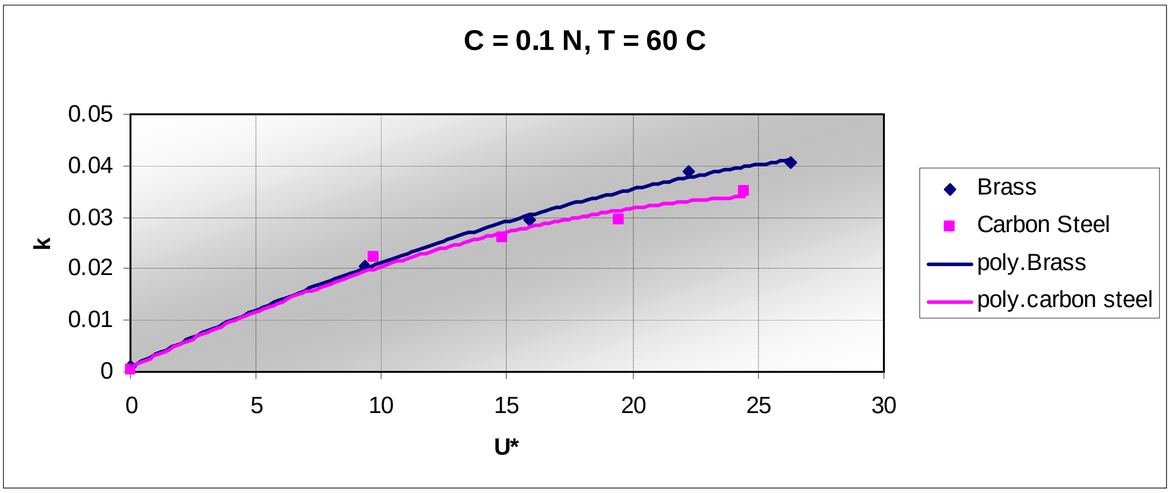

Figure 5-40 Effect of matel on i_l at T = 60°C, C_{NaCl} = 0.1 N NaCl

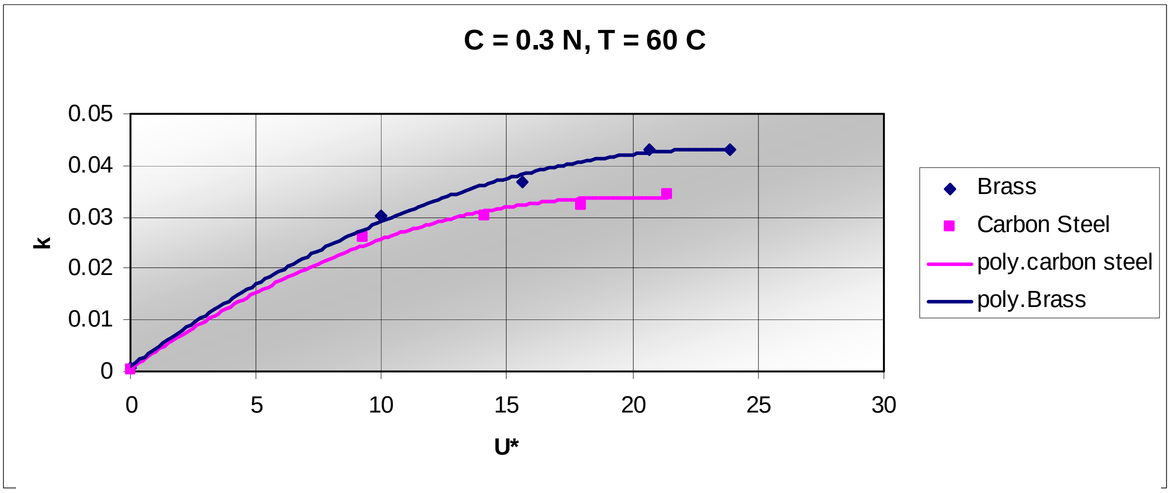

Figure 5-41 Effect of matel on i_l at T = 60°C, C_{NaCl} = 0.3 N NaCl

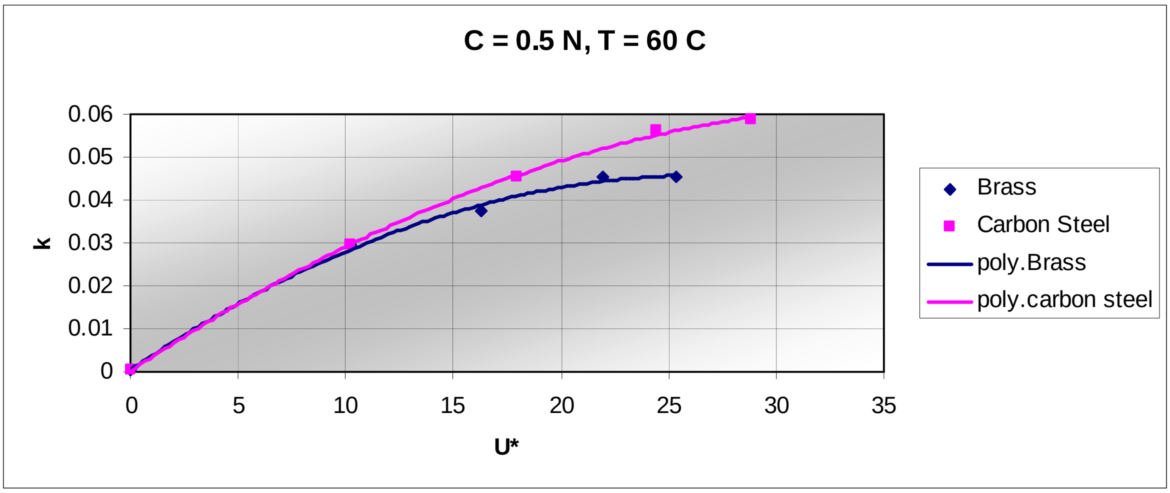

Figure 5-42 Effect of matel on i_l at T = 60°C, C_{NaCl} = 0.5 N NaCl

5.4.Friction or shear velocity

5.4.1. Effect of Tempreature and NaCl concentration

Brass and carbon steel

Figures 5-43 to 5-48 show the effect of temperature which are expressed as limiting current density versus friction or shear velocity due to consequent changes of physical properties with increasing temperature. There is a slight difference between two metals because of surface texture of the two metals. On the other hand, the influence of NaCl concentration is nearly similar to the trend observed due to temperature as illustrated in Figs 5-49 to 5-54.

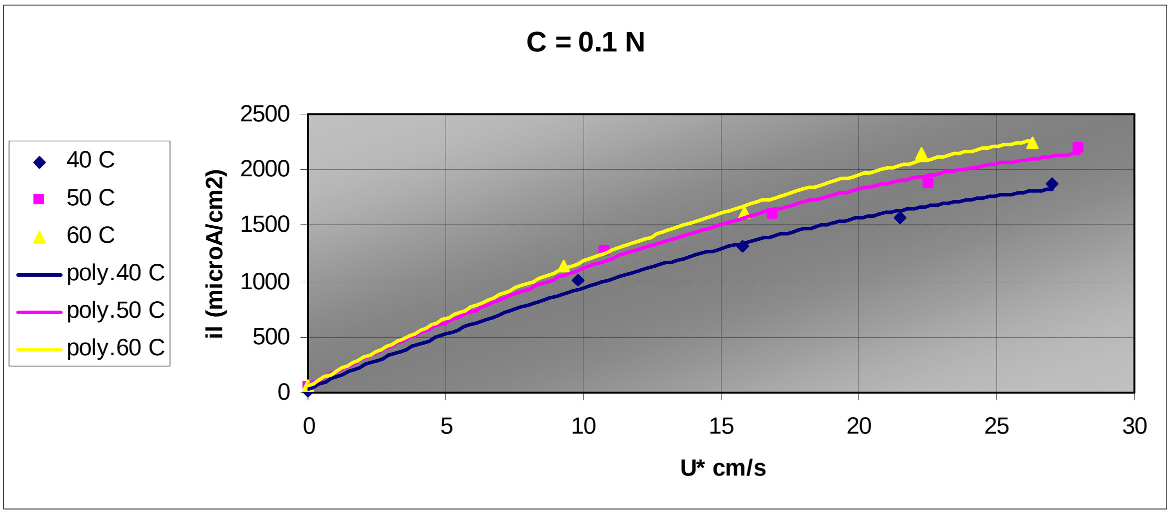

Figure 5-43 Effect of temperature on friction velocity on Brass surface in a solution of 0.1N NaCl.

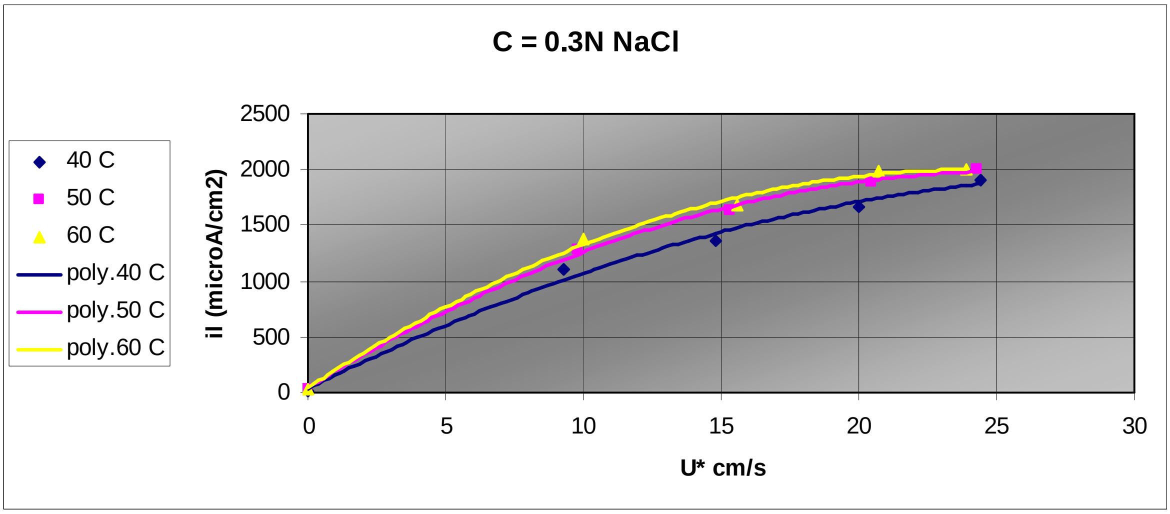

Figure 5-44 Effect of temperature on friction velocity on Brass surface in a solution of 0.3N NaCl.

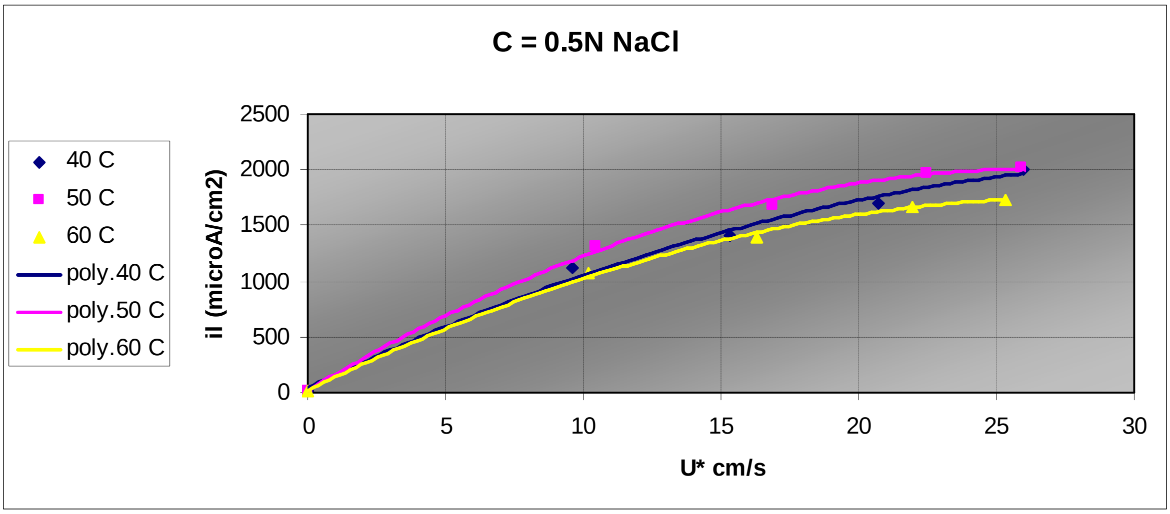

Figure 5-45 Effect of temperature on friction velocity on surface of brass in a solution 0.5N NaCl.

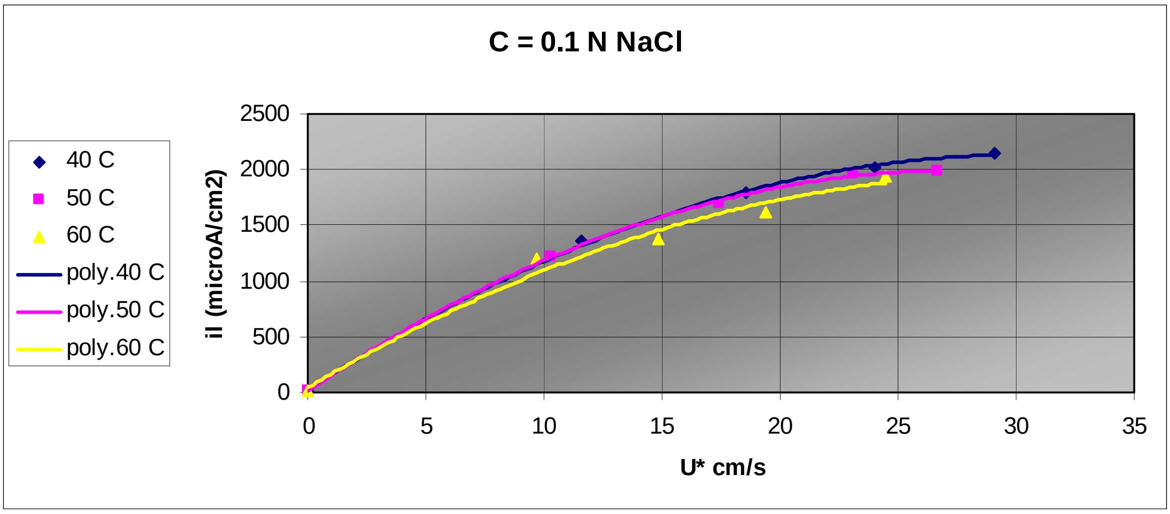

Figure 5-46 Effect of temperature on friction velocity on carbon steel surface in a solution of 0.1N NaCl.

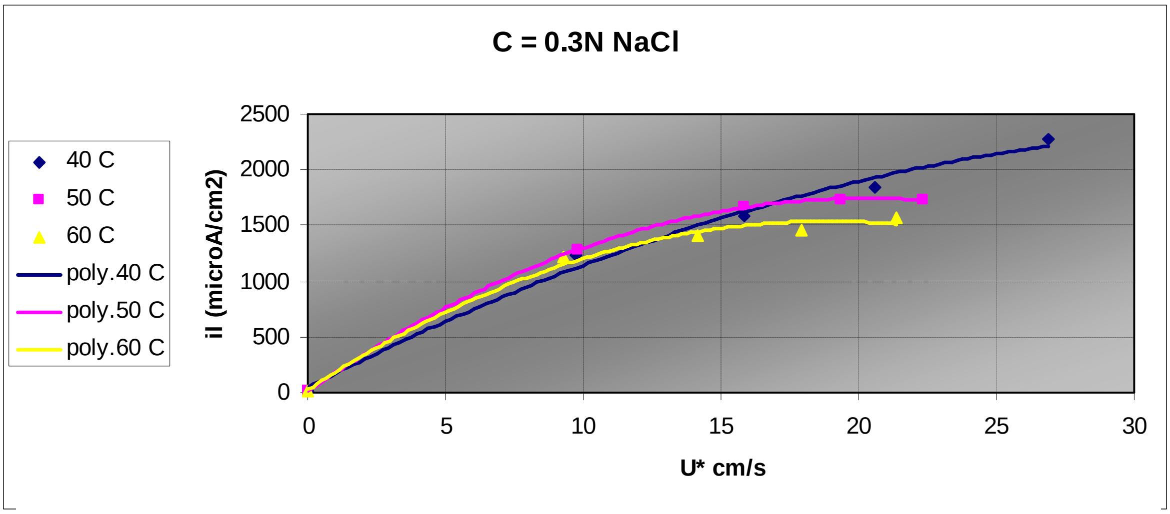

Figure 5-47 Effect of temperature on friction velocity on surface of carbon steel in a solution 0.3N NaCl.

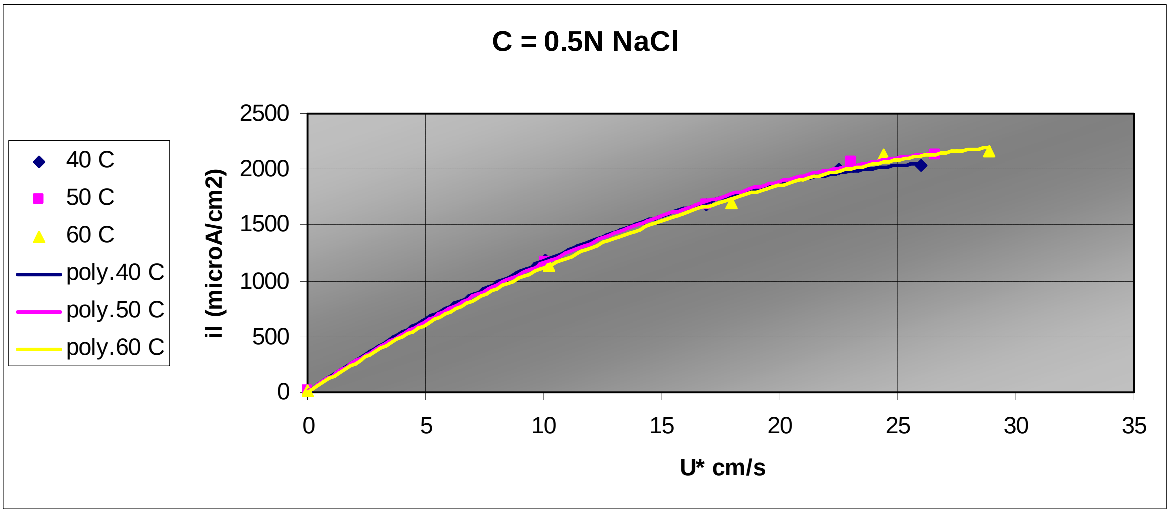

Figure 5-48 Effect of temperature on friction velocity on surface of carbon steel in a solution 0.5N NaCl.

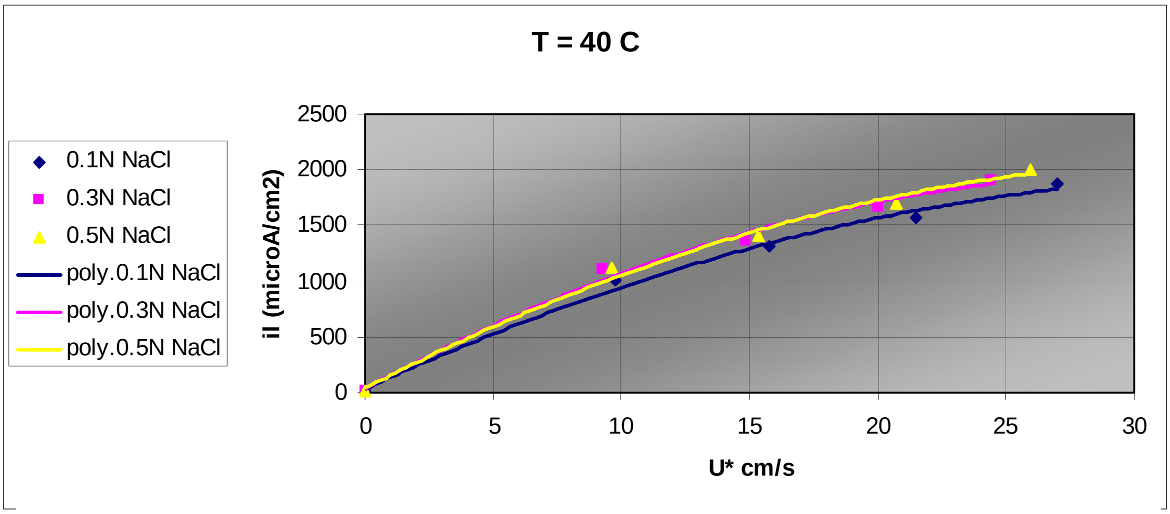

Figure 5-49 Effect of concentration on friction velocity at 40^{0}C on brass surface. .

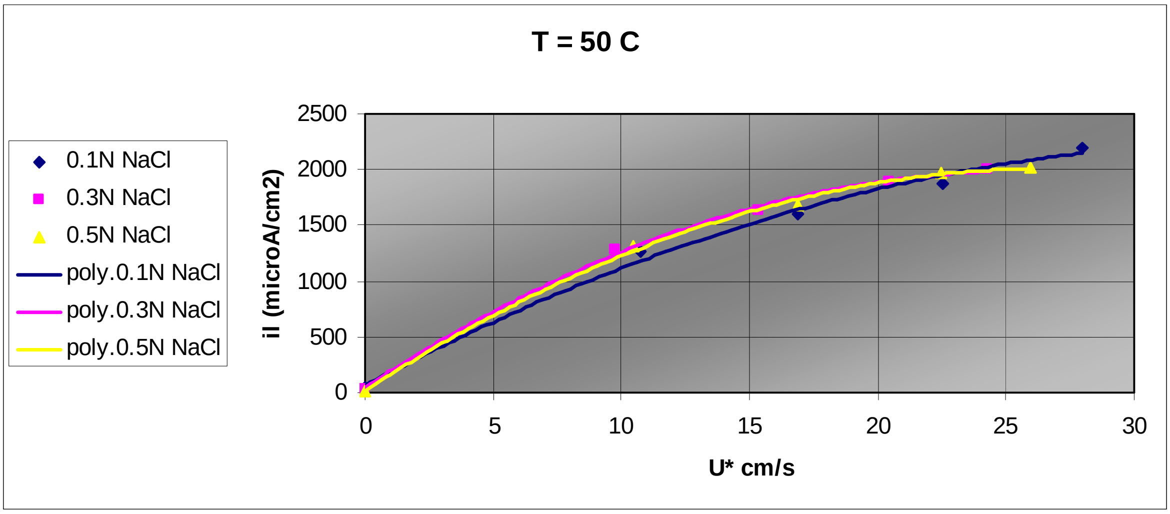

Figure 5-50 Effect of concentration on friction velocity at 50^{0}C on brass surface.

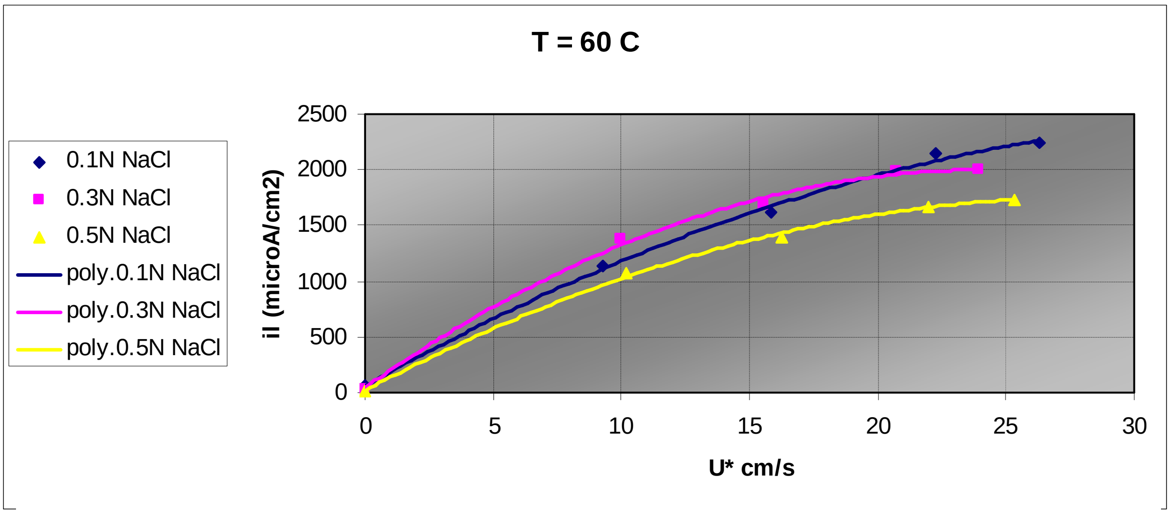

Figure 5-51 Effect of concentration on friction velocity at 60^0C on brass surface.

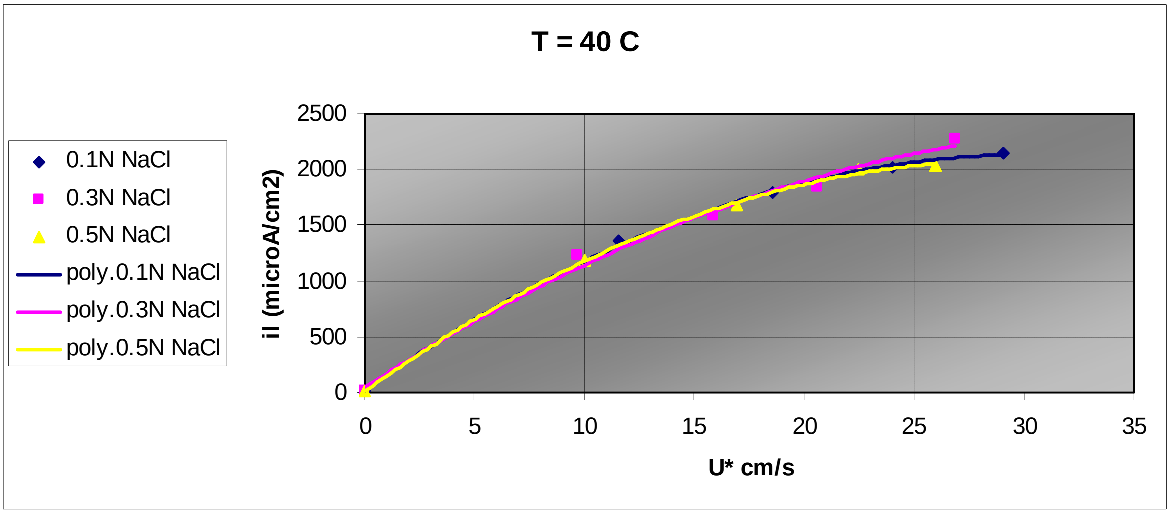

Figure 5-52 Effect of concentration on friction velocity at 40^0C on carbon steel surface .

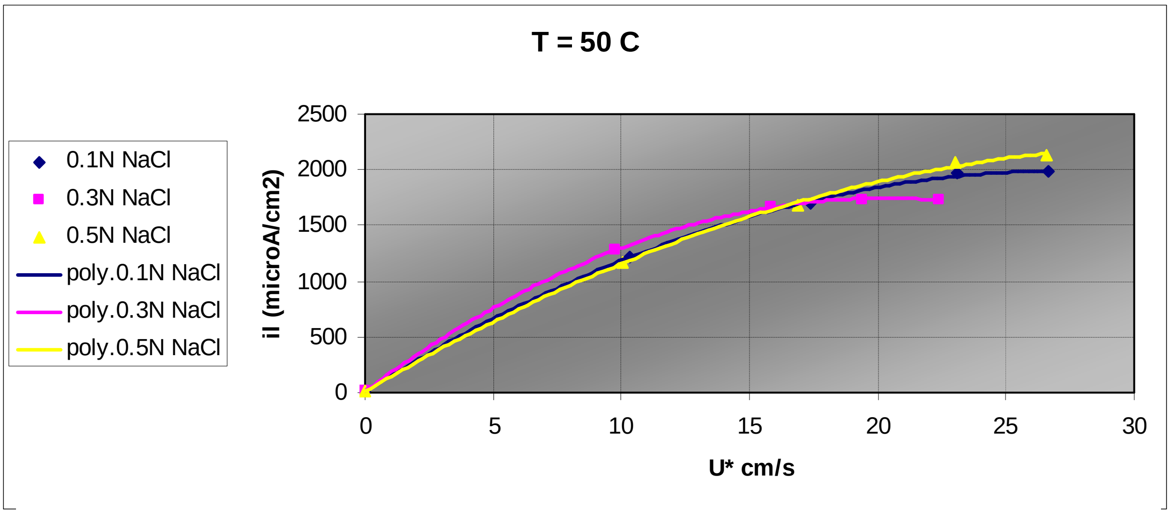

Figure 5-53 Effect of concentration on friction velocity at 50^0C on carbon steel surface .

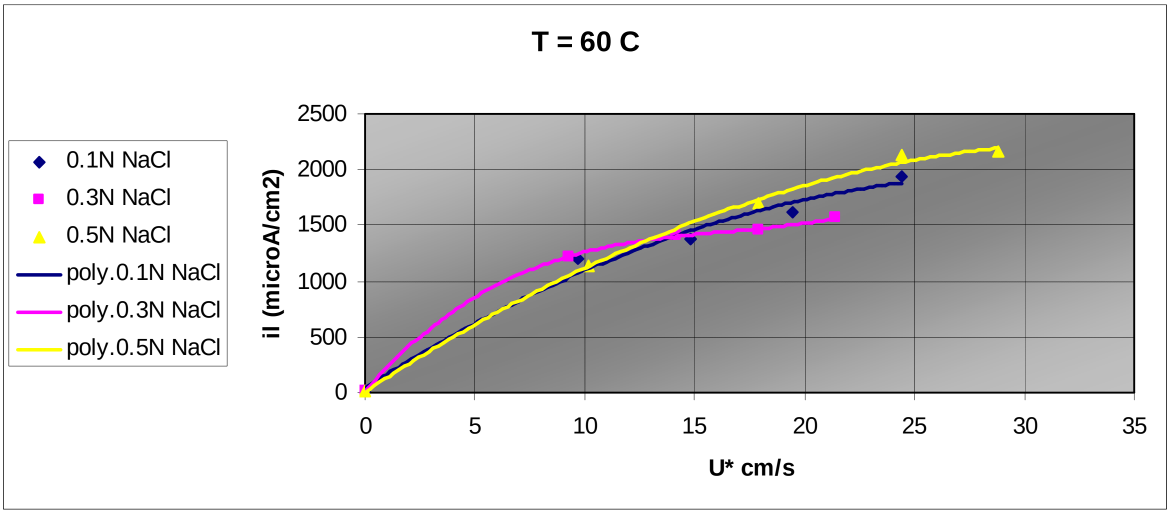

Figure 5-54 Effect of concentration on friction velocity at 60^0C on carbon steel surface .

5.4.2. Effect of metal on friction or shear velocity

It is to be appreciated that friction/shear velocity is determined by the physical properties of the system and the morphology and texture of rotating cylinder electrode surface. These properties are mainly influenced by temperature and concentration of NaCl salt. The small variations are within experimental errors considering the fact that carbon steel is very corrodible metal compared with brass. These findings are presented in Figures 5-55 to 5-63 for all temperatures in all sodium chloride solutions.

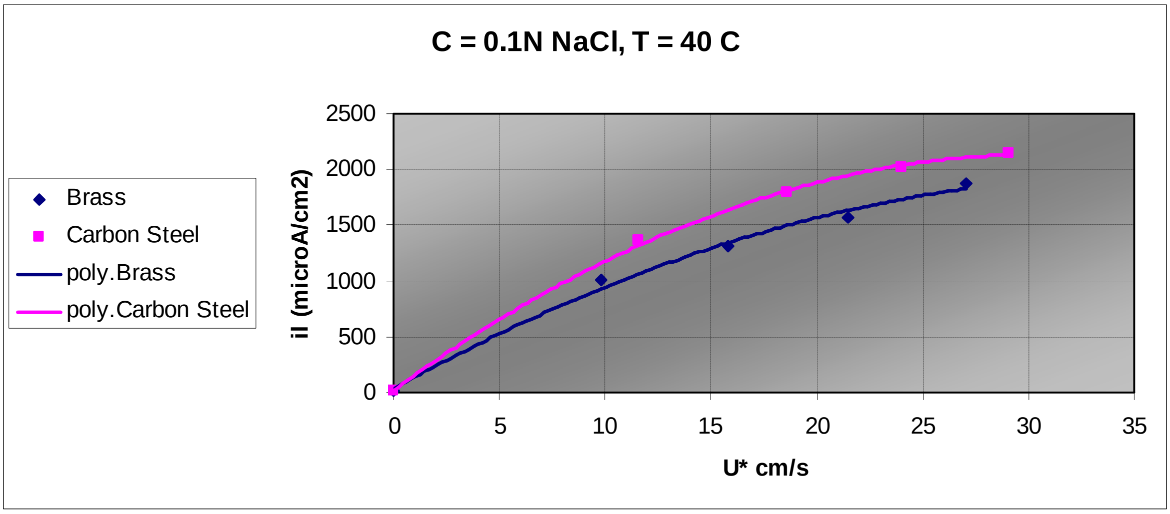

Figure 5-55 Effect of metal type on friction velocity in a solution C_{NaCl} = 0.1N NaCl at T = 40^0C .

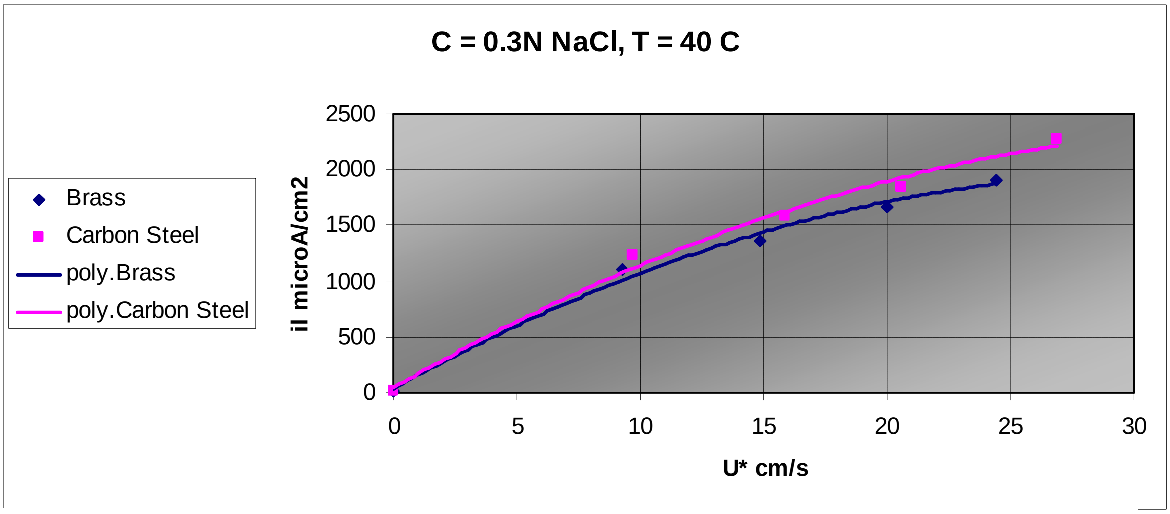

Figure 5-56 Effect of matel type on friction velocity in a solution C_{NaCl} = 0.3N NaCl at T =40^0C .

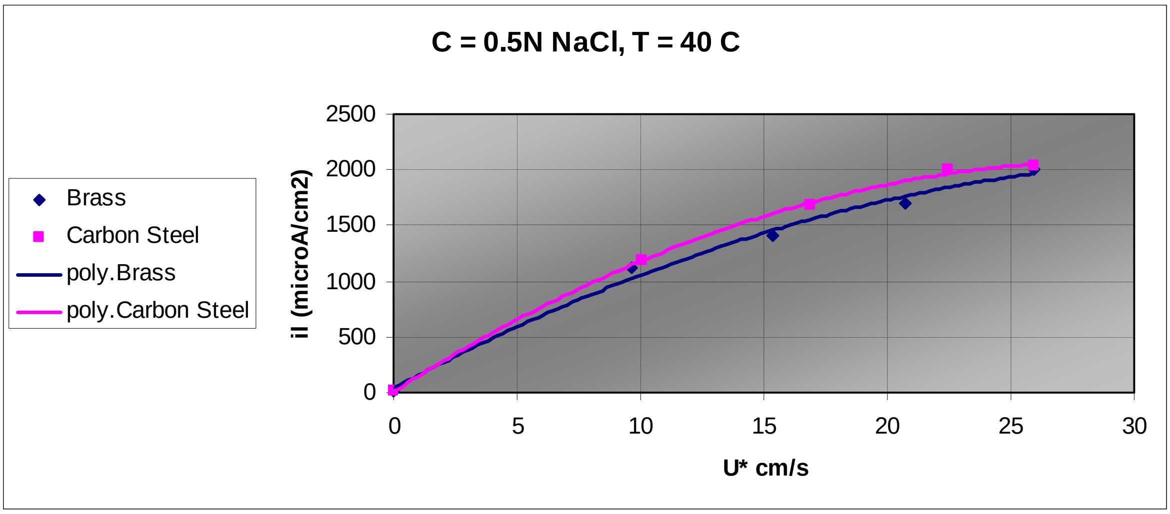

Figure 5-57 Effect of matel type on friction velocity in a solution C_{NaCl} = 0.5N NaCl at T = 40^0C .

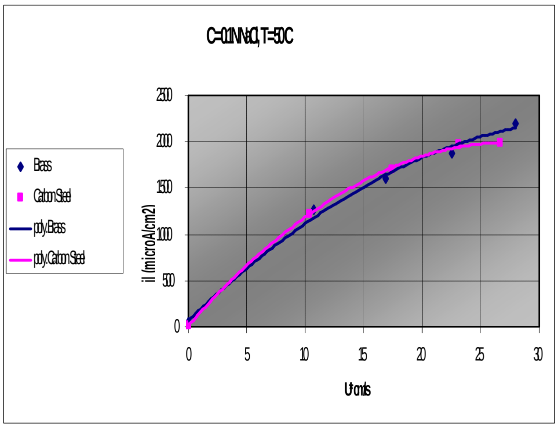

Figure 5-58 Effect of matel type on friction velocity in a solution C_{NaCl} = 0.1N NaCl at T = 50^0C .

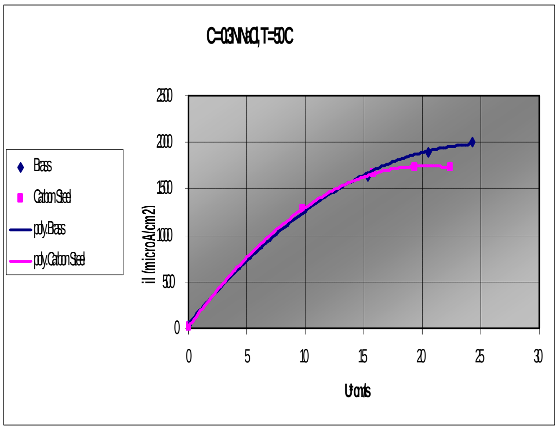

Figure 5-59 Effect of matel type on friction velocity in a solution C_{NaCl} = 0.3N NaCl at T = 50^0C .

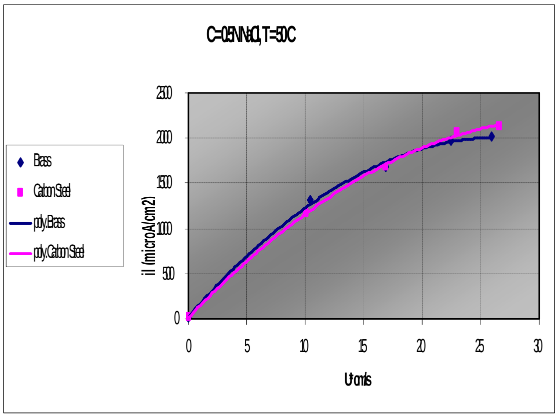

Figure 5-60 Effect of matel type on friction velocity in a solution C_{NaCl} = 0.5N NaCl at T = 50^0C .

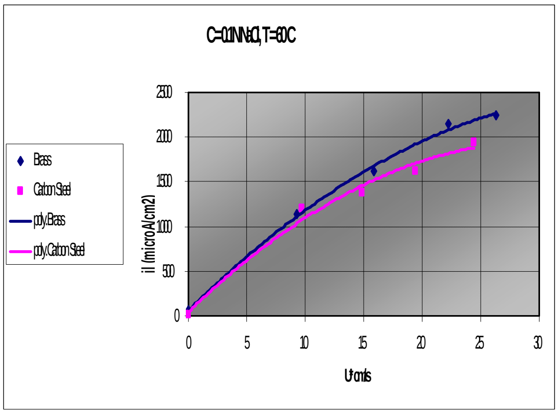

Figure 5-61 Effect of matel type on friction velocit in a solution C_{NaCl} = 0.1N NaCl at T = 60^0C .

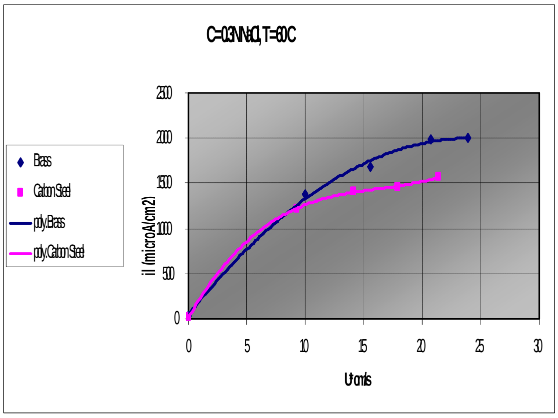

Figure 5-62 Effect of matel type on friction velocity in a solution C_{NaCl} = 0.3N NaCl at T = 60^0C .

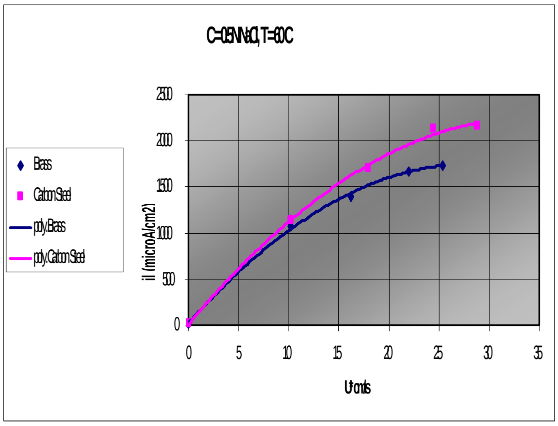

Figure 5-63 Effect of matel type on friction velocity in a solution C_{NaCl} = 0.5N NaCl at T = 60^0C .

From experimental results and theoretical analysis the relationship has been visualized between mass transfer coefficient (k) and shear/friction velocity (U*) as:

$$U^* = \sqrt{\frac{t}{r}} \qquad (2\text{-}22)$$

$$\frac{f}{2} = \frac{t}{rU^2} \Rightarrow \frac{U*^2}{U^2} \qquad (5\text{-}1)$$

From Chilton & Colburn [62] :

$$\frac{f}{2} = \frac{Sh}{\mathrm{Re} \times Sc^{0.33}} \qquad (2\text{-}55)$$

Substitute Equ. (2-55) into (5-1)

$$\frac{U*^2}{U^2} = \frac{Sh}{\mathrm{Re} \times Sc^{0.33}}$$

Or (5-2)

$$\frac{\frac{kd}{D}}{\frac{rUd}{m} Sc^{0.33}} = \left(\frac{U*}{U}\right)^2 \qquad (5\text{-}3)$$

So

$$U* = \sqrt{\frac{kU}{Sc^{-0.67}}} \qquad (5\text{-}4)$$

or

$$U* = Sc^{0.33}\sqrt{kU}$$

5.5.Effect of NaCl concentration on polarization curves

Figures 5-64 and 5-65 show experiments conducted to visualize the effect of NaCl concentration on O_2 cathodic polarization curves. When the concentration of NaCl is increased the limiting current will be increased at co nstant Reynolds number (rotational velocity) and temperature which is in agreement with Fontana and Greene [11]. The effect of oxidizer additions or the presence of oxygen on electrochemical rate depends on both the medium, the different extents of variation of the physical properties, and the metals involved. The rate of (limiting current) may be increased by the addition of oxidizers, oxidizers may have no effect on the corrosion rate, or a very complex behavior may be observed. By knowing the basic characteristics of a metal or alloy and the environment to which it is exposed, it is possible to predict in many instances the effect of oxidizer additions [11].

For diffusion-controlled process, an increase in concentration of the diffusing species in the bulk of the environment increases the concentration gradient at the metal interface. The concentration gradient provides the driving force for the diffusion process. Thus the maximum rate at which oxygen can diffuse to the surface (the limiting diffusion current) would be essentially directly proportional to the concentration in solution. Figs.5.64 and 5.65 are experimental samples of the cathodic polarization diagrams which are operative for this system [12]. For more experimental results see Chapter four.

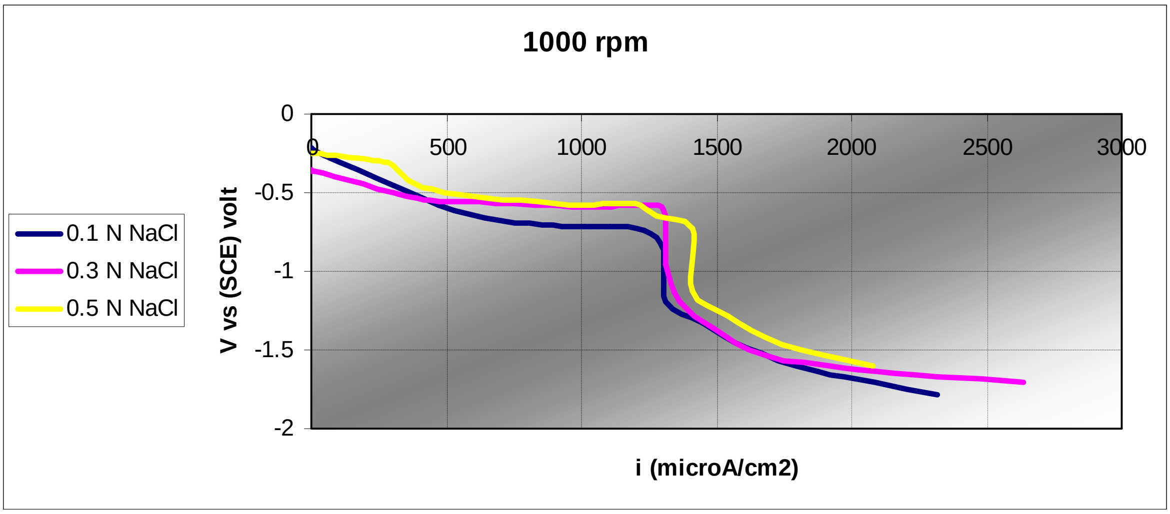

Figure 5-64 Effect of NaCl concentration change on O_2 polarization curves on brass at 40^0C and constant rotational speed (ω = 1000 rpm)

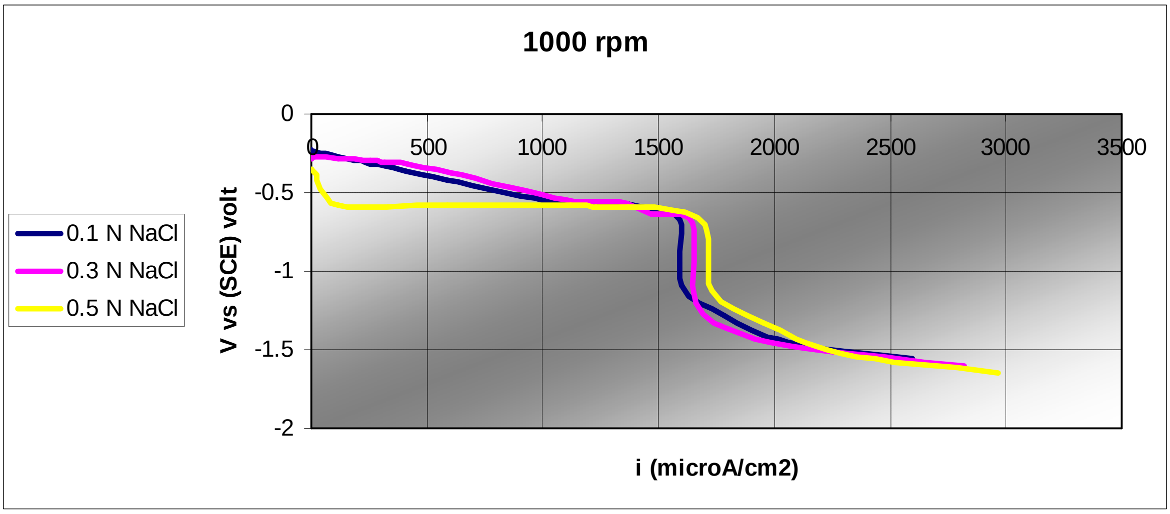

Figure 5-65 Effect of NaCl concentration change on O_2 polarization curves on brass at 50^0C and constant rotational speed (ω = 1000 rpm)

CHAPTER SIX

Conclusions and Recommendations

6.1. Conclusions

The followings are concluded from the experimental results:

1. Temperature and Reynolds No. (Re) in NaCl solutions of increasing normality lead to increase the limiting current on both metals, i.e., brass and carbon steel which is highly corroding metal.
2. NaCl concentration change increases limiting current on both metals (brass and carbon steel) for a given Reynolds No.(Re) with increasing concentration of NaCl salt at all temperatures.
3. The mass-transfer controlled limiting currents which are obtained on brass and carbon steel acting as cathodes are nearly similar. It is to be appreciated that the type of metal and surface texture can not be reproduced exactly similar.
4. Mass transfer coefficient as a function of friction velocity increases with increasing temperature at all concentrations for both metals.

5. From experimental results and theoretical analysis the following relationship has been visualized between mass transfer coefficient (k) and shear/friction velocity(U*):

$$U^* = Sc^{0.335}\sqrt{kU}$$

6.2. Recommendations for future work

The following are recommended for future work:

1. Measuring shear stress (τ) on surface of a rotating cylinder using stress gauges which are not affected by the corrosivity of the solution.
2. Replace working electrode by almost non-corroding electrode, e.g., stainless steel to extend limiting current potential range and to eliminate the intrusion of other reactions.
3. Experimental work using potentiostatic mode of operation.
4. Execution of present work in presence of corrosion inhibitors.

REFERENCE

1. Ellison B. T. and Schmea W. R. , J. Electrochem. Soc., Vol. 125, pp. 524 (1978).
2. Mahato B. K., Cha C. Y. and Shemilt L. W., corros Sci., Vol. 20, (1980). pp. 421
3. Efird K. D., corrosion, Vol. 33, No. 1, (1977). pp. 3.
4. Banerjee S. N., "An Introduction to Science of Corrosion and it's Inhibitor", Oxonian press pvt. LTD., 1985. pp.10
5. Fontana M.G., and Green N.D., "Corrosion Engineering", Mc.Graw-Hill, 2nd. Edition, (1978). pp.2, 20, 21
6. Ross T. K. and Johnes D. H., J. App. Chem., Vol. 12,(1962) pp.314.
7. Poulson B.Corrosion Sci., Vol. 23, 1983, pp. 23.
8. Macial J. M. and Agostinto S.M.L."J. applied of Electra", 1999. pp. 900
9. Perry R.H, and Green D.W, Perry Chemical Engineers Handbook, 7th ed, M.C. Graw-Hill, United States, 1997. pp. 625
10. Corrosion test. Article given on the intrnet at the web site **http://www.gc3.com**.
11. Fontana M.G., and Green N.D., "Corrosion Engineering", 2nd. Edition, Londan (1984). pp. 30
12. Stern M., Corrosion-NACE, Vol. 13, (1957). pp.97,
13. Shereir L.L.,"Corrosion Handbook", Newnes – Butter, London, 2nd Edition, Vol. 1,(2000). pp. 685
14. Uhlig H. H.,"Corrosion and Corrosion Control", 3rd Edition, Wiley-Interscience publication, New Yourk, (1985). pp. 100

15. Eisenberg M, Tobias C.W and Wilke C.R. J. Electrochem. Soc. 101, 1954. pp. 101- 115
16. Sliverman D., Corrosion J. Vol. 44. (1988). pp. 42-49
17. Sliverman D.,"Rotating Cylinder electrode for velocity Sensitivity testing", corrosion, NACE, Houston, Tx (1983). pp . 258
18. Cameron G. R, Chiu-A.S. "Electrochemical techniques for corrosion inhibitor studies", NACE (1986). pp. 183-189
19. Eisenberg M. Tobias C.W. and Wilke C.R. J. Electrochem. Soc. 106, 1954. pp. 130-135
20. Pang J. and Ritchi I.M, Electrochem. Acta, Vol. 26, 1981.pp. 1345
21. Gabe D. R and Walsh F.C, J,Appl. Electrochem. Vol. 14, No. 555 (1984). pp. 200- 225
22. Sliverman D., Corrosion J. Vol. 40. (1984). pp 220
23. Gabe and P.A. Maken Jvola, J. App. Electrochem. No.17. (1987). pp. 384
24. Jeanst-Pierre, Normand Mass and Mario Bergeron, Electrochem. Acta, Vol. 40,No. 8, (1994). pp. 1024
25. Kalamtary M.R., Wilcox G.D. and Gabe D.R., Electrochem.Vol. 40. No. 11, (1995). pp .1615
26. Gabe D.R. and Wilcox G.D., J. Appl. Electrochem. Vol. 28. (1998) pp . 778.
27. Quddus A., Allam I.M., Desalination No. 127. (2000). pp.224.
28. Joseluis Nava, Sosa E, Carlos ponce deleón, M.T. Oropeza, chem..Enginee. since 56(2001). pp. 2701.
29. Herbert-Guillon D, Tribollet B, Festy D, Bioelectrochemistry, No.53. (2000). pp. 125

30. Her-Hsing Huang, Tung-Han chang, materials sci-and Eng, A-292, (2000). pp. 94.

31. Maciel J.M., Agosinho S.M.L., J-appl. Electrochem. No. 30. (2000), pp. 984-985.

32. Giddy S., Cherry B., F. Lawson, M. Forsyth, corrosion sci. No. 43, (2001). pp. 1516.

33. Jean L. Stojak, Jan B. Tablot, J.Appl. electrochem. No.31.(2001). pp. 563.

34. Gibbons D.W, Muller R.H. and Tobias C.W., J. Electrochem. Soc. 138 (1991). pp. 3255.

35. Levich V. G., Physicochemical Hydrodynamic, Prentice Hall, N. J., (1962). pp. 10, 15

36. Campbell J.A. and Hanratty T.J., Turbulent shear flows 3, (1981). pp. 73.

37. Mizushina, T., Advances in Heat Transfer, Irvine, T.F. and J.P. Hartnett (Ed.), Vol.7,Academic press, N.Y.,(1971). pp. 85

38.Adam R.N., "Electrochemistry of solid electrodes", morcel Dekken, Inc.,1969. pp. 2, 4

39. Fundamentals of electrochemical corrosion, ASM international (2000), **http://www. Asminternational. Org.**

40. West J.M., Electrode Deposition and corrosion processed, 1976. pp. 2

41. Hydrodynamic of a smooth cylinder from the site :
http://www. Argentum solutions. Com.

42.Walker G.D., Journal of Biomedical Materials Research (Symposium), Vol.5.(1974). pp.11-26 .

43. Jacobson B., and Webster J.B., Chapter10. Surgery, in Medicine and Clinical Engineering, (Eds.) Jacobson and Webster prentice-Hell Inc. New Jersey (1977). pp. 525-532

44. King C.V. and Hillner E., ibid., Vol. 101, (1954), pp -79.

45. Kambara T., Tsukamoto T. and Tachi I., 3". Electrochem. Soe. Jap. 18 (1950) 356, 386; 19 (1951) pp. 199, 297.

46. Koichi Asano "Mass Transfer From Fundamentals to Modern Industrial Applications", Wiley-Vch verlag Gmbh & Co. KGaA, (2006). pp. 325

47. Bagotsky V.S.,"Fundemental of Electrochemist", 2nd , Wiley Interscience Publication, (2006). pp. 410

48. Perez N.,"Electrochemistry and Corrosion Science", New York, (2004).

49. Selman J.R.,"AICHE", Vol.77, No.204. (1981).pp. 88.

50. Gabe D. R. and Robinson D.J., Electrochem, Acta, Vol.17. (1972). pp.1129.

51. Gabe D. R. and Robinson D.J., Trans. Inst. Met Fin. Vol.49. (1971) . pp. 17.

52. Corent I. and Kappesser R., Trans. Inst. Chem.. Eng, Vol.47. (1969) . pp. 194.

53. Ariva A.J., Carozza J.S.W. and Marchian S.L., Electrochem. Acta, Vol.9.(1964). pp. 1483.

54. Ariva A.J. and Carrozza J.S.W., Electrochim. Acta., Vol.7.(1962) . pp. 65.

55. Sherwood T.K. and Ryan J.M., chem. Eng. Sci., Vol.11 (1959). pp. 81.

56. Gabe D.R., Walsh F.C., J.Appl. Electrochem. Vol.13. (1983). pp. 3.

57. Eisenberg M., Tobias C.W.,and Wilke C.R., J. Electrochem. Soc. 102(1955). pp. 415.

58. Abdel-Rahman H. A., " Kinetic Studies of Cementation of Copper On Rotating Zinc Cylinder in Aqueous and Mixed Solvents", Ph. D. Thesis submitted for faculty of science, Alexandaria University, Egypt. (1998). as

quoted in Soliman H. M. A., Abdel-Rahman H. H., Electrochemical; Vol. 24, (2006). pp. 415-440.

59. Sideman, S. and Pinczewski W.V., Topics in Transport Phenomena, [Edited by C. Gultfinger], John Wiley and Sons, (1975). pp. 55

60. Bennett J. A. R. and Lewis J.B., J.Amer. Inst. Chem.Eng., Vol.4. (1958). pp. 485.

61. Holman K.L. and S.T.Ashar, chem.. Eng. Sci., Vol.26. (1971). pp. 1817.

62. Chilton, T.H., and A.P. Colburn, Ind. Eng. Chem., Vol.26, (1934). pp.1183.

63. Sherwood, T.K., and R.L. Pigford, Absorption and Extraction, 2nd . ed., Mc.Graw-Hill, N.Y., (1952). pp. 140

64. Trethewey K.R., and Chamberlain J., Corrosion for Science and Engineering, 2nd edition, (1996). pp. 75

65. Steiger Wald R.F, corrosion, NACH, P.L,January, (1968). pp. 555

66. Fage A. and Townend H.C., Proc, Soc., London, Vol.354, (1932). pp.646.

67. Uhlig H.H., Corrosion Handbook. John Wiley and Sons, Inc, (1976). pp. 565

68.Gabe D.R., Electrochemical; Vol. 4, (1974). pp. 91-108.

69. Strickland P.H. and Lawson F., Proc. Austral. Inst. Min. Met., Vol. 236,(1970). pp. 25.

70. Conway B. E., Beatty E. M. and DeMaine P. A. D., Electo. Chem. Acta., Vol. 7, (1962) pp. 39.

71. Ming GENG, Zhenhao DUAN, Geochimica et. Cosmochimica Acta. Vol. 74. (2010). pp. 5631-5640.

72. Audin A. and John L., J. "chem.. Eng. Data", Vol.17, No.3,(1972). pp. 789.

الخلاصة

تهدف الدراسة الحالية إلى وضع علاقة رياضية بين انتقال الكتلة وسرعة القص جراء الاحتكاك (Friction Velocity) عند العمل بالقطب الاسطواني الدوار (RCE) وبطريقة تقنية التيار المحدد (Limiting Current Density Technique) كطريقة لقياس كثافة التيار (LCD) تحت ظروف الجريان الاضطرابي (Turbulent Flow) وعند ثلاث درجات حرارية وهي (40, 50, 60) ^{0}C كما تهدف أيضا إلى معرفة تأثير تغيير تركيز كلوريد الصوديوم NaCl في هذه الدرجات الحرارية باستخدام معدنين أحدهما شديد التآكل (الفولاذ الكربوني) لتحديد كثافة التيار المحدد ومعاملات انتقال الكتلة Mass Transfer Coefficient (k) وسرعة القص والاحتكاك (C^*). والآخر ضعيف المقاومة للتآكل (البراص الأصفر).

بينت التجارب أن زيادة درجة الحرارة بثبوت التركيز تؤدي إلى زيادة كثافة التيار المحدد على سطحي سبيكة البراص الأصفر (Brass) والفولاذ الكربوني (Carbon Steel) وبالتالي تؤدي إلى زيادة معاملات انتقال الكتلة بينما عند زيادة تركيز الملح (NaCl) بثبوت درجة الحرارة فإن كثافة التيار المحدد يزداد على سطح كل من سبيكة البراص الأصفر والفولاذ الكربوني ومن ثم يقل بصورة طفيفة نتيجة اختلاف النسيج السطحي لكلا القطبين بالإضافة إلى كون الفولاذ شديد التآكل مقارنة مع سبيكة البراص الأصفر. وعليه فإن زيادة كثافة التيار المحدد يؤدي بالتبعية إلى زيادة في انتقال الكتلة.

نستنتج من البحث إلى أن معامل انتقال الكتلة تعتمد بشكل أساسي على السرعة بثبوت درجة الحرارة والتركيز أي عند زيادة السرعة اى زيادة (Reynolds Number) تزداد كثافة التيار المحدد وبالتالي يزداد معامل انتقال الكتلة.

وكذلك تم صياغة علاقة رياضية لحساب كثافة التيار المحدد وعلاقتها بانتقال الكتلة وسرعة القص/الاحتكاك ومن خلال التجارب العملية والحسابات النظرية تم التوصل إلى علاقة بين انتقال الكتلة وسرعة الاحتكاك كما يلي :-

$$U^* = Sc^{0.335}\sqrt{kU}$$

العلاقة بين معامل انتقال الكتلة وسرعة الاحتكاك

رسالة
مقدمة إلى كلية الهندسة في جامعة النهرين
وهي جزء من متطلبات نيل درجة ماجستير علوم
في الهندسة الكيمياوية

من قبل

هالة محمد حسين
(بكالوريوس علوم في الهندسة الكيمياوية 2009)

ربيع الثاني 1433
أذار 2012

شكر و تقدير

الحمد لله رب العالمين والصلاة والسلام على أشرف الخلق محمد وعلى آله وصحبه أجمعين ..

أقف عاجزاً عن التعبير حين أقدم شكري وامتناني الذي أهديه إلى الأستاذ الفاضل المشرف الأستاذ الدكتور قاسم جبار سليمان لما بذله من جهود وعناء لإخراج هذا النتاج العلمي بهذا [illegible].

وأتقدم بالشكر الجزيل إلى [illegible] الدكتور [illegible] [illegible] الكيمياوية [illegible] في مساعدتي لانجاز هذا العمل.

وأتقدم بالشكر الجزيل إلى [illegible] الكيمياوية [illegible] في مساعدتي لإنجاز هذا العمل.

كما أتقدم [illegible] (رحمه الله) [illegible] المتواضع.

كما أتقدم [illegible] شكر والتقدير.

أقدم شكري وتقديري واحترامي إلى جميع من ساهم في مساعدتي بطريقة أو بأخرى لإنجاز هذا العمل.

هالة محمد حسين

2012 آذار